의학박사 학위논문

PPARγ와 NEDD8의 결합에 의한 지방세포 분화 조절기전의 연구 및 이를 표적으로 하는 새로운 비만 치료제의 발굴

Regulation of adipogenesis via NEDDylation of PPARγ and discovery of a novel anti-obesity agent to target this mechanism

2015년 2월

서울대학교 대학원

의과학과 의과학 전공

박 형 숙

PPARγ와 NEDD8의 결합에 의한 지방세포 분화 조절기전의 연구 및 이를 표적으로 하는 새로운 비만 치료제의 발굴

지도 교수 전 양 숙

이 논문을 의학박사 학위논문으로 제출함

2014 년 12 월

서울대학교 대학원

의과학과 의과학 전공

박 형 숙

박형숙의 의학박사 학위논문을 인준함

2014 년 12 월

위 원 장_____

부위원장_____

위 원_____

위 원_____

위 원_____

Regulation of adipogenesis via NEDDylation of PPARγ and discovery of a novel anti-obesity agent to target this mechanism

by

Hyoung Sook Park

A thesis submitted to the Department of Biomedical science in partial fulfillment of the requirements for the degree of Doctor of Philosophy in Biomedical science at Seoul National University College of Medicine

December, 2014

Approved by Thesis Committee:

Professor _____ Chairman

Professor _____ Vice Chairman

Professor _____

Professor _____

Professor _____

Abstract

Neural precursor cell expressed developmentally down-regulated 8 (NEDD8), an ubiquitin-like protein, regulates the activity, stability, and subcellular localization of target proteins. NEDD8 is covalently conjugated to lysine residues of substrates though E1-E2-E3 enzyme cascades, which is called NEDDylation. Here, I characterized the prominent role of NEDDylation for adipogenesis. The depletion of NEDD8 decreased the expression of adipogenic genes, thereby inhibiting adipogenic differentiation. In particular, the expression of peroxisome proliferator-activated receptor gamma (PPARγ), a master regulator of adipogenesis, was reduced by knocking down NEDD8, and was enhanced by over-expressing NEDD8 in 3T3-L1 cells. Moreover, PPARγ covalently conjugated with NEDD8 during adipogenesis, as shown by Ni^{2+} pull-down assay with His-NEDD8-overexpressed 3T3-L1 cells. In addition, the stability of PPARγ protein was sustained due to decreased ubiquitination during adipogenesis. Notably, mouse double minute 2 (MDM2) was found to be a specific E3 ligase of PPARγ NEDDylation. Based on these results, I tested whether a NEDD8-activating enzyme inhibitor, MLN4924, had an anti-obesity effect. The results showed that MLN4924 can inhibit both adipocyte differentiation and fat accumulation in both 3T3-L1 cells and human adipocyte-derived stem cells (H-ADSCs). Consistently, MLN4924 treatment in diet-induced-obesity (DIO) mice model diminished weight gain, accompanied with recovered lipid metabolism to a normal range. Furthermore, MLN4924 treatment in DIO mice recovered glucose tolerance, insulin sensitivity, body weight, leptin level, and the expression of inflammatory cytokine genes. Taken together, these results suggest

that NEDD8 leads to crucial post-translational modification to regulate the stability of PPARγ proteins in adipogenesis. Accordingly, I report that MLN4924 could be developed as a therapeutic agent for obesity.

Key words: adipocyte differentiation, PPARγ, NEDDylation, MDM2, MLN4924, obesity.

Student Number: 2010-30610

CONTENTS

Page

LIST OF FIGURES

LIST OF ABBREVIATIONS

NEDD8: Neural precursor cell-expressed developmentally down-regulated 8

PPARγ: Peroxisome proliferator-activated receptor gamma

C/EBPs: CCAAT/enhancer binding proteins

MDM2: Mouse double minute 2

LPL: Lipoprotein lipase

FABP4: Fatty acid binding protein 4

CD36: Cluster of differentiation 36

Fasn: Fatty acid synthase

PTM: Post-translational modifications

TZDs: Thiazolidinediones

NCD: Normal chow diet

HFD: High fat diet

DIO: Diet induced obesity

INTRODUCTION

Globally, obesity remains a serious unsolved medical problem, and is a critical contributor to type 2 diabetes mellitus, hypertension, hyperlipidemia (high triglycerides and low high-density lipoproteins), atherosclerosis, cardiovascular disease, cancer, and nonalcoholic fatty liver (Kahn et al., 2006; Hofbauer and Nicholson, 2006; Van Gaal et al., 2006; LeRoith et al., 2008; Fabbrini et Al., 2010). Obesity is also related with abnormal adipokine secretion, macrophage infiltration, and inflammatory cytokine secretion (Bourlier et al., 2008, Henegar et al., 2008). Previously, it was suggested that overfeeding increases adipocyte size, but creates no changes in cell number (Sanlans et al., 1971). However, hyperplasia is correlated strongly with obesity severity, and is most marked in severely obese individuals (Hirsch and Batchelor, 1976). Especially, increasing adipocyte number is an important cause of juvenile obesity, and an increased adipocyte number in the juvenile period persists throughout the lifetime. An increase in adipocyte number may contribute to obesity severity by prolonging periods of weight gain in adulthood. Recent studies have proposed that adipocyte turnover is very dynamic, and approximately 10% of fat cells are renewed annually at all adult ages (Spalding et al., 2008). Lipoaspirates of fat tissues contain a high proportion of mesenchymal stem cells (MSC), which can differentiate into adipocytes, which strongly supports that new fat cells constantly arise from undifferentiated progenitor cells or

preadipocytes, even in adults (Drolet et al., 2008). Therefore, adipogenesis is critical for maintaining adipocyte number in obesity, and high adipogenic potential could be an important therapeutic target for pharmacological intervention in obesity.

Adipocytes are derived from multipotent mesenchymal stem cells that have the ability to develop into adipocytes, chondrocytes, myocytes, and osteocytes. Adipogenesis and adipocyte differentiation are determined by the activation of transcriptional factors, including the nuclear hormone receptor family peroxisome proliferator-activated receptor gamma (PPARγ) and CCAAT/enhancer binding protein alpha, beta, and delta (C/EBPα, β, δ) (Cao et al., 1991). These transcription factors are highly expressed in WAT, and they regulate glucose, lipid metabolism, and adipokine secretion (Rosen and MacDougald, 2006). As a master regulator, PPARγ expressed in the middle stage of adipocyte differentiation is required for the terminal differentiation of preadipocytes toward adipocytes (Chandra et al., 2008). C/EBPβ requires binding C/EBPδ to promote the expression of PPARγ and C/EBPα (Steger et al., 2010). Indeed, PPARγ-deficient mice exhibit an increased expression of leptin, which is reduced in high fat diet–induced fatty liver, and were protected from adipocyte hypertrophy, obesity, and insulin resistance (Lowell, 1999; Yamauchi et al., 2001). Many reports have shown that adipogenic transcription factors play an important role in adipogenesis.

Post-translational modifications (PTM) of transcription factors can regulate protein stability, cellular localization, or function. Phosphorylations of PPARγ were

stimulated by UV, stress, cytokines, growth factor, and a high fat diet (HFD), and affect transcriptional activity. General transcription factor IIH phosphorylates PPARγ at Ser112, inhibits its recruitment of transcriptional coactivators, and stimulates its binding to the circadian regulator period homolog 2 (PER2), which reduces the binding of PPARγ to target gene promoters (Grimaldi et al., 2010). The phosphorylation of Ser273 via CDK5 decreases PPARγ target gene expression in adipocytes, but did not affect the regulation of adipocyte differentiation by PPARγ (Choi et al., 2010). Polypeptide modifiers such as ubiquitin and sumo also affect adipogenesis by regulating the function of adipogenic factors. PPARγ2 is also SUMOylated by PIAS or PIASx at Lys107, which negatively regulates PPARγ2's transcriptional activity (Ohshima et al., 2004). Interestingly, the relationship between polypeptide modifiers and obesity is supported by DNA microarray data. White adipose tissue from obese mice expressed ubiquitin less than that from lean control; conversely, NEDD8 expression is increased in fat tissues of obese mice (Nadler, et al., 2000). However, the reversal of the expression of these genes with adipocyte functions such as adipocyte differentiation and adipocyte fat storage was not clearly verified.

NEDD8 is ubiquitously expressed in mammalian tissues, and structurally similar to ubiquitin, NEDD8 is conjugated to substrates covalently though E1-E2-E3 enzyme cascades, which are called NEDDylation. Previously, our research group reported that hypoxia-inducible factor-1α (HIF-1α) stabilizes NEDD8 conjugation (Ryu et

al., 2011). NEDDylation regulates activity, stability, and localization of its substrates. For example, (1) NEDDylation of p53 inhibits its translation activity (Xirodimas et al., 2004). (2) NEDDylation of BCA3 promotes their interactions with SIRT1 and suppresses NF-κB-dependent transcription (Gao et al., 2006). (3) The NEDDylation of pVHL reduces its interaction with Cul2-containing complexes (Russell and Ohh, 2008). (4) The NEDDylation of pVHL leads to a proper fibronectin matrix assembly (Stickle et al., 2004). Yet, the physiological significance of NEDD8 as a posttranslational modifier remains to be elucidated in obesity.

In this study, I pursued the possibility that NEDDylation might play a role in regulating adipogenesis. To identify NEDDylated target proteins, proteomic approaches using over-expressed NEDD8 in 3T3-L1 cells were carried out to identify the substrates associated with adipogenesis. Intriguingly, PPARγ, a major transcriptional factor in adipogenesis, turned out to be a novel substrate of NEDDylation. Here, this study demonstrates that NEDDylation is essential for adipogenic differentiation, and PPARγ, one of the main transcriptional factors in adipogenesis, is stabilized by NEDDylation. Consistent with these observations, I propose that NEDDylation controls adipocyte differentiation and fat accumulation, and that NEDD8 is a new physiological regulator of PPARγ stability during adipogenesis. Furthermore, the results of this study implicate MLN4924 as a potential therapeutic target for obesity.

MATERIALS AND METHODS

Antibodies and Reagents

Antibodies against PPARγ (sc-7196, sc-1984), C/EBPα (sc-61), C/EBPβ (sc-150), C/EBPδ (sc-636), Tubulin (sc-9104), MDM2 (sc-965), SUMO (sc-9060) and Ub (sc-9133) were obtained from Santa Cruz Biotechnology (Santa Cruz, CA, USA). Antibodies against NEDD8 (2745) and perilipin (9349) were obtained from Cell signaling Technology (Beverly, MA, USA). Anti-HA was obtained from Roche (Basel, Switzerland). The antibody against APPBP1 (NBP1-92162) was obtained from NOVUS (St.Charles, MO, USA). Chemicals of 3-Isobutyl-1-methylxanthine: IBMX (I5879), dexamethasone (D4902), insulin (I1507), 1-(4-Chlorobenzoyl)-5-methoxy-2-methyl-3-indoleacetic acid: indomethacin (I7378), cycloheximide (C1988), HA-affinity bead (E6779), (D)-glucose (G7021), human insulin (I9278), Oil-red O (O0624) and EZview™RedAnti-HA AffinityGel (E6779) were obtained from Sigma-Aldrich (St. Louis, MO, USA). Nutlin-3 (10004372) was obtained from Cayman Chemical Company (Ann Arbor, MI, USA). MG132 (BML-PI102) was obtained from ENZO Life Sciences (Farmingdale, NY, USA). Ni-NTA Agarose beads were obtained from Qiagen (Hilden, Germany). MLN4924 was kindly gift from Lak Shin Jeong (Lee et al., 2011). Bovine serum, fetal bovine serum (FBS) and Dulbecco's modified eagle's medium (DMEM) were obtained from Thermo Fisher Scientific (Waltham, MA, USA).

Cell culture and adipocyte differentiation

HEK293 (human embryonic kidney, ATCC CRL-1573) was obtained from American Type Culture Collections (Manassas, VA, USA). 3T3-L1 and 3T3-F442A pre-adipocytes were kindly gift from Dr. Jae-Woo Kim (Yonsei University, Seoul, South Korea). Pre-adipocyte was maintained in DMEM supplemented with 10% bovine serum. Differentiation of 3T3-L1 cells were induced by the treatment of 1 μM dexamethasone, 500 μM IBMX, and 5 μg/ml insulin, which is designated DMI in DMEM supplemented with 10% FBS. Two days after starting differentiation cells were maintained in DMEM with 10% FBS and 1 μg/ml insulin up to 8 days with medium change every two day. Human adipose derived stem cells (H-ADSCs) were kindly gift from Dr. Seoung-Who Kim (Ulsan University, Seoul, South Korea). H-ADSCs were obtained from patients who provided informed consent, and the institutional review board of Asan Hospital (Seoul, Korea) approved the use of the clinical samples for this research (approve, #2012-0283). Human adipose tissue-derived stem cells (H-ADSCs) were isolated from 35–55 years old women undergoing liposuction and passage 3–5 cells were used in this study. The cells were isolated using ADSC markers under flow cytometry (BD Biosciences, Franklin Lakes, NJ). More than 95% of H-ADSCs were identified to express CD105, CD90, CD73, and HLA-abc. Adipocyte differentiation of H-ADSCs were induced with DMI and 200 μM indomethacin in α-MEM supplemented with 10% FBS. Cells were incubated in 5% CO_2 and 20% O_2 at 37°C.

Plasmid DNA, siRNA and transient transfection

The expression vectors for HA-tagged mouse PPARγ was kindly gift from Kyong-

Soo Park (Seoul National University, Seoul, South Korea). NEDD8 cDNA was obtained by reverse transcription-PCR was cloned into His_6-tagged pcDNA3. NEDD8-ΔGG mutant which is unable to conjugate target proteins was made by site-directed mutagenesis (Ryu et al., 2011). Ubiquitin, PPARγ-NT (1-140), PPAR γ-M (141-281) and PPAR γ-CT (282-505) amplified by PCR were constructed into HA-tagged pcDNA3 (Clontech Laboratories, Inc. Mountain View, CA, USA). pcMDM2 amplified by PCR was cloned into pcDNA (Clontech Laboratories). Myc-SENP8 amplified by PCR was constructed into Myc-tagged pcDNA (Clontech Laboratories). All siRNAs for each gene were synthesized from IDT Integrated DNA Technologies (Coralville, IA, USA) and were listed in Table1. Two different siRNAs were designed to target mouse NEDD8 and APPBP1. Plasmid and siRNA were transiently transfected into cells using Lipofectimine (Invitrogen, Carlsbad, CA, USA) according to the manufacturer's instructions.

Stable pre-adipocyte cell line

For stably knockdown to 3T3-L1 and 3T3-F442A cells, the shRNAs containing a hairpin loop were synthesized and inserted into pLKO.1-puro vector (Sigma-Aldrich). sh-NEDD8-I and -II, sh-APPBP1-I and -II, sh-Control were inserted into pLKO.1-puro vector and were listed in Table 2. Two different shRNAs were designed to target mouse NEDD8 and APPBP1. The viral vectors were co-transfected into HEK293 cells with pMD2-VSVG, pRSV-Rev and pMDLg/pRRE plasmids to make viral particles. To establish stable cell lines, lentiviruses were collected from the supernatant of HEK293 cells. 3T3-L1 or 3T3-F442A cells were

infected with viruses and then selected using puromycin (5 μg/ml). For generation of stable expression in 3T3-L1 cells, cDNA for His-NEDD8 and HA-PPARγ plasmids were subcloned into the lentiviral shuttle vector pLVX-IRES-puro (Clontech Laboratories). The viral vectors were co-transfected into HEK293 cells with pMD2-VSVG, pRSV-Rev and pMDLg/pRRE plasnids to make viral particles. To establish stable cell lines, lentiviruses were collected from the supernatant of HEK293 cells. 3T3-L1 cells were infected with viruses and then selected using puromycin (5 μg/ml).

RNA preparation and real-time PCR

Total RNAs were isolated from cultured cells or tissue using TRIzol (Invitrogen). For cDNA synthesis, we used Easy Script™ cDNA Synthesis Kit (Applied Biological Materials Inc, Richmond, BC, Canada). The cDNAs of pparg, c/ebpa, c/ebpb, c/ebpd, adiponectin, resistin, cd36, fabp4, scd1, perilipin, lpl, acs, fasn, nedd8, tnfa, il6, mcp1, f40/80, c11b, c11c, and 18S rRNA were amplified with EvaGreen qPCR master mix reagent (Applied Biological Materials) in StepOne™ Real-time PCR System (Applied Biosystems, BC, Foster City, CA, USA). The level of each cDNA was relatively quantified by being divided by the 18S rRNA level in the corresponding sample. The sequences of qPCR primers are listed in Table 3.

Adipogenesis induction and Oil-red O staining

3T3-L1 cells were grown to confluent and induced with adipogenesis media that include DMEM with 10% FBS, 1μM dexamethasone, 500 μM IBMX and 5 μg/ml

insulin (DMI). 3T3-F442A cells were grown to confluent and induced with adipogenesis media that include DMEM with 10% FBS and 5 μg/ml insulin. H-ADSCs were grown to confluent and induced with adipogenesis media that include αMEM with 10% FBS, 1 μM dexamethasone, 500 μM IBMX, 5 μg/ml insulin (DMI) and 0.2 μM indomethacin. Media were changed with DMEM or αMEM with 10% FBS and 5 μg/ml insulin after 2 days. After differentiation, cells were fixed in 0.5% formalin for 20 min at RT. Fixed cells were incubated 1h with 0.3% Oil-red O solution (Sigma-Aldrich) in 60% isopropanol.

Western blotting and immunoprecipitation analysis

Cell lysates in a 2 x SDS sample buffer were separated on SDS-polyacrylamide gels and transferred to Immobilon-P membranes (Millipore, Billerica, MA, USA). Membranes were blocked from nonspecific proteins with 5% skim milk in TTBS (Tris-buffered saline containing 0.1% Tween 20) for 30 min and incubated overnight with primary antibody diluted at 1:500 to 1:3000 in the blocking solution. The membranes were incubated with a horseradish peroxidase-conjugated secondary antibody for 1h with blocking solution and blots visualized using Pierce ECL Plus western blotting substrate kit. For immunoprecipitation assay, cells were lysed in 5 mM EDTA, 50 mM Tris-Cl, 100 mM NaCl, and 0.1% NP-40 buffer and freshly added protease inhibitor. Cell lysates (1 mg) were incubated with EZview™RedAnti-HA AffinityGel for 4 h at 4°C. Precipitates were eluted by 2 x SDS buffer and subjected to SDS-polyacrylamide gel electrophoresis, followed by western blotting analysis. 10 μg anti-PPARγ and anti-MDM2 antibody were

incubated with 1 mg protein for overnight at 4°C. After incubation, precipitates were bound with protein A/G-sepharose beads (GE Health care) for 4 h at 4°C. After beads washing, precipitates were eluted by 2 x SDS buffer and subjected to SDS-polyacrylamide gel electrophoresis, followed by western blotting analysis.

Identification of His_6-tagged NEDD8 conjugation

For NEDD8 conjugation, we modified protocol in Jaffray and Hay (2006, Methods). After transfection with His_6-tagged NEDD8 or NEDD8ΔGG plasmid, cells were divided into two dishes. One was lysed with 2 x SDS sample buffer and analyzed by western blotting to confirm the expression level of input proteins. The other was lysed by denaturing buffer (6 M guanidine hydrochloride, 0.1 M Na_2HPO_4/NaH_2PO_4, 0.01 M Tris-Cl (pH 8), 10 mM imidazole and 10 mM β-mercaptoethanol). The lysates were bound with Ni^{2+}-NTA-agarose bead (Qiagen) for 4 h at RT. The beads were washed for 5 min in each step with the washing solution: washing buffer 1 (pH 8: 8 M urea, 0.1 M Na_2HPO_4/NaH_2PO_4, 0.01 M Tris-Cl (pH 8), 20 mM imidazole and 10 mM β-mercaptoethanol), washing buffer 2 (pH 6.3: 8 M urea, 0.1 M Na_2HPO_4/NaH_2PO_4, 0.01 M Tris-Cl (pH 8), 20 mM imidazole and 10 mM β-mercaptoethanol) with 0.2% Triton-X100 and washing buffer 2 with 0.1% Triton-X100. Then, beads were eluted with 2 x SDS sample buffer and analyzed western blotting.

Enzymatic in-gel digestion

pLVX-IRES-His-NEDD8 expressed in 3T3-L1 stable cells were differentiated to

adipocytes. After 4 day adipocyte differentiation, cells were lysed. His-NEDD8-conjugated proteins were bound to Ni^{2+}-NTA-agarose beads under denaturing conditions and eluted with a SDS sample buffer and then the eluents were subjected to SDS-polyacrylamide gel electrophoresis. The SDS-polyacrylamide gel stained with PlusOne ™ Silver staining kit (GE Healthcare, Uppsala, Sweden) according to the manufacturer instructions. For in-gel digestion, the proteins separated by SDS-PAGE were excised from the gel and the gel pieces containing protein were destained with 50% acetonitrile (ACN) containing 50 mM NH_4HCO_3 and vortexed until CBB was completely removed. These gel pieces were then dehydrated in 100% acetonitrile and vacuum-dried for 20 min with speedVac. For the digestion, gel pieces were reduced using 10 mM DTT in 50 mM NH_4HCO_3 for 45 min at 56°C, followed by alkylation of cysteines with 55 mM iodoacetamide in 50 mM NH_4HCO_3 for 30 min in dark. Finally, each gel pieces were treated with 12.5 ng/μl sequencing grade modified trypsin (Promega, Madison, WI) in 50 mM NH_4HCO_3 buffer (pH 7.8) at 37°C for overnight. Following digestion, tryptic peptides were extracted with 5% formic acid in 50% ACN solution at RT for 20 min. The supernatants were collected and dried with SpeedVac. Re-suspended samples in 0.1% formic acid were purified and concentrated using C18 ZipTips (Millipore, MA) before MS analysis.

LC-MS/MS analysis

The tryptic peptides were loaded onto a fused silica microcapillary column (12 cm

x 75 μm) packed with C18 reversed phase resin (5 μm, 200 Å). LC separation was conducted under a linear gradient as follows: a 3-40% solvent B (ACN containing 0.1% formic acid) gradient (solvent A; DW containing 0.1% formic acid), with a flow rate of 250 nL/min, for 60 min. The column was directly connected to LTQ linear ion-trap mass spectrometer (Finnigan, CA) equipped with a nano-electrospray ion source. The electrospray voltage was set at 1.95 kV, and the threshold for switching from MS to MS/MS was 500. The normalized collision energy for MS/MS was 35% of main radio frequency amplitude (RF) and the duration of activation was 30 ms. All spectra were acquired in data-dependent scan mode. Each full MS scan was followed by five MS/MS scan corresponding from the most intense to the fifth intense peaks of full MS scan.

Database searching and validation

The acquired LC-ESI-MS/MS fragment spectrum was searched in the BioWorksBrowser™ (version Rev. 3.3.1 SP1, Thermo Fisher Scientific Inc., CA) with the SEQUEST search engines against National Center for Biotechnology Information (http://www.ncbi.nlm.nih.gov/) Mus musculus database. The searching conditions were trypsin enzyme specificity, a permissible level for two missed cleavages, peptide tolerance; ±2 amu, a mass error of ±1 amu on fragment ions and variable modifications of carbamidomethylation of cysteine (+57 Da) and oxidation of methionine (+16 Da) residues.

Chomatin Immunoprecipitation

Lysates from 1×10^7 cells were cross-linked with 1% formaldehyde for 10 min at RT, and glycine (final 125 mM) was added to quench the cross-linking reaction. Lysed cell extracts were subjected to sonication until the DNA fragments become less than 500 base pair. Chromatin complexes were precipitated with indicated antibodies overnight at 4°C. Protein G sepharose (Life technologies) beads were added and incubated 2 more hs. After washing with saline, DNA-protein complexes were eluted with 1% SDS and incubated overnight at 65°C to reverse crosslinking. The eluted DNAs were purified with Mega-quick spin DNA purification kit (Intron, Seoul, Korea). The precipitated DNAs were amplified and quantified on ABI StepOne^{TM} Real-Time PCR System using the Evagreen qPCR mastermix. PCR primer sequences used for ChIP are listed in Table 4.

Implantation of 3T3-L1 and 3T3-F442A preadipocytes and analysis of fat pads

All animals were maintained in compliance with the Guide for Experimental Animal Research from the Laboratory for Experimental Animal Research, Seoul National University Institutional Animal Care and Use Committee (SNUIACUC) (SNU-110718-1). 3T3-L1, 3T3-F442A cells were grown completely and infected with pLKO.1-puro-shControl and pLKO.1-puro-sh-NEDD8. Cells were trypsinized and suspended in DMEM with 10% bovine serum. 3×10^7 cells were injected into the subcutis of the abdomens of 9-wk-old BALB/c male nude mice (Orient Bio, Inc., Gyeonggi-Do, South Korea). After 5 wks, fat pads produced from the implanted

cells were fixed in formalin buffer and stained with hematoxylin and eosin (H&E) (Mandrup et al., 1997).

Immunofluorescence

Implanted fat fad was fixed in formalin solution and was cut into 4 μm slices. The fat slices were deparaffinized and hydrated, and then antigens were retrieved by in 10 mM sodium citrate buffer in a microwave for 20 min. After blocking, sections were incubated overnight with anti-perilipin (1:500). For visualizing specific protein, Alexa Fluor® 488 Goat Anti-Rabbit IgG (H+L) (Invitrogen) was used incubating sections and nucleus stained with DAPI (1:5000 in PBS, Sigma Aldrich).

Animals and animal care

Animal study was approved by the Seoul National University Animal Experiments Ethics Committee (SNU-130318-1-4). Mice were housed in pathogen free facility during 12 h light and 12 h dark cycle. We fed C57BL/6J mice (Central Lab. Animal Inc. Seoul Korea) HFD consisting of 60% of calories from fat (D12492 Research diets Inc. New Brunswick, NJ, USA) starting from 4 wks of age to 16 wks of age. MLN4924 30 mg/kg was injected intraperitoneally into mice once per 3 days. Daily food consumption and body weight provided food was measured every three day for singly housed mice. At the ends of MLN4924 treatments, blood was collected by eye and cardiac puncture. Fats and livers were rapidly excised and weighed and then frozen in liquid nitrogen. Samples were kept -80°C and portion of fats were fixed in 4% formalin for histology experiments.

Body composition

Computed tomography

128-slice multi-detector computed tomography multi-detector computed tomography (MDCT) was used (Ingenuity CT, Philips Healthcare, Cleveland, OH). The tube voltage was set at 120 kV with a constant 175 mA current. The slice-thickness was 0.7mm and the field of view (FOV) was set at 50×50 mm^2. Reconstruction in the axial, sagittal, and coronal planes was acquired for all CT scans.

Before CT scan, mice were anesthetized with a mixture of Zoletil (Virbac, Carros, France) (50 mg/kg) and xylazine (10 mg/kg) administered by intraperitoneal injection. They were placed prone in the appropriate holders. First, a scannogram of whole body was made to ensure proper placement in the holder and to set the scan area. Second, Whole-body scans of the entire mice were done. To avoid artificially including S leg fat in the abdominal area, mice' hind limbs were extended.

Measurement of intra-abdominal adipose tissue

Intra-abdominal adipose tissue *(IAAT)*

I selected the optimal single slice in which both renal hila were well observed around L3-L5. Cross-sectional abdominal contour was estimated by delineating the skin manually with a graph pen though the muscular structures and vertebral corpora. Hounsfield unit (HU) cut-off values of -250 to -50 were assigned for adipose tissue in the slice. The area between -250 HU and -50 HU pixels was

calculated automatically by the post-processing CT software (Rapidia 2.8, INFINITT, Seoul, Korea). IAAT inside the abdominal wall was measured. Abdominal fat was assessed by computed tomography (Dixon, 1983).

Blood chemistry analysis

Serum was isolated from the whole blood out of mice fasted for 12 h. The content of glucose in blood was measured by one touch glucometer Accu-Chek Active® system (Roche, Basel, Switzerland). The level of insulin and leptin was measured with ELISA kit (ALPCO Diagnostics, Salem, NH, USA) according to the manufacturer's instructions. The level of free fatty acid was quantified with the kit (Sigma-Aldrich, St. Louis, Missouri, USA) according to the manufacturer's instructions.

Glucose and insulin tolerance test

For glucose tolerance test (GTT), mouse was fasted for overnight and then intraperitoneally injected with D-glucose at a dose of 2 g per kg body weight. For insulin tolerance test (ITT), mouse was fasted 4 h and then intraperitoneally injected with insulin at a dose of 1 U per kg body weight. The level of glucose was measured at 0, 15, 30, 60, 90 and 120 min.

Statistical analysis

Mean and standard deviation (SD) were analyzed using Microsoft Excel software. Comparing two groups were determined statistical significance using Student's t

test P values < 0.05 were considered to be statistically significant.

Tables

Table 1. Targets and Nucleotide Sequences of siRNAs

Target Genes	GeneBank accession number	siRNA Sequences
hNEDD8	NM_006156.2	5’-CAGACAAGGUGGAGCGAAUCAAGGA-3’
mNEDD8-I	NM_008683.3	5’-UCCUUGAUUCGCUCCACCUUGUCUGUG-3’,
mNEDD8-II	NM_008683.3	5’-UUCACUUUAAUUAGCAUCUUCUUCCCA-3’
mAPPBP1-I	NM_144931.3	5’-GAGCAGAUUCCAAAGCUUCUUGUCCAU-3’
mAPPBP1-II	NM_144931.3	5’-AGGUAAAUUUCCUUGACCCUCCUUGGC-3’
hMDM2	NM_002392.5	5’-UUCCUGAAGCUCUUGUACAAGGUCCUU-3’
mMDM2	NM_010786.3	5’-GCAAUGAUCUACAGAAAUUUAGUGG-3’
Non-target		5’-UUGAGCAAUUCACGUUCAUTT-3’

Table 2. Targets and DNA Sequences for shRNAs

Target Genes	Sequences (5’ to 3’): Sense and Antisense strands
mNEDD8-I	Sense: CGGTTGATTCGCTCCACCTTGTCTCTCGAGAGACAAGGTGGAGCGAATCAATTTTT Antisence: ATTAAAAATTGATTCGCTCCACCTTGTCTCTCGAGAGACAAGGTGGAGCGAATCAA
mNEDD8-II	Sense: CCGGACTTTAATTAGCATCTTCTTCCTCGAGGAAGAAGATGCTAATTAAAGTTTTTT

	Antisence: ATTAAAAAACTTTAATTAGCATCTTCTTCCTCGAGGAAGAAGATGCTA ATTAAAGT
mAPPBP1-I	Sense: CGGCAGAATTCAAAGCTTCTTGTCCTCGAGGACAAGAAGCTTTGGAA TCTGTTTTT Antisence: ATTAAAAACAGATTCCAAAGCTTCTTGTCCTCGAGGACAAGAAGCTT TGGAATCTG
mAPPBP1- II	Sense: CGGTAAATTTCCTTGACCCTCCTTCTCGAGAAGGAGGGTCAAGGAAA TTTATTTTT Antisence: AATTAAAAATAAATTTCCTTGACCCTCCTTCTCGAGAAGGAGGGTCAA GGAAATTTA
Non-target (GFP)	Sense: CCGGCGTGATCTTCACCGACAAGATCTCGAGATCTTGTCGGTGAAGA TCACGTTTTT Antisence: AATTAAAAACGTGATCTTCACCGACAAGATCTCGAGATCTTGTCGGT GAAGATCACG

Table 3. Nucleotide Sequences of Primers used for RT-PCR

Mouse Genes	Primer sequence: forward (For) and reverse (Rev)
Pparg	For 5'- AGTGGAGACCGCCCAGGCTT -3' Rev 5'- CAGTTCCAGGGCCTGCAGCA-3'
Cebpa	For 5'-CTCGCCATGCCGGGAGAACTCTA-3' Rev 5'-GAGGTGACTGCTCATCGGGGGC-3'
Cebpb	For 5'- ACCACGACTTCCTCTCCGACCTCT -3' Rev 5'- CGTAGTCGGCCGGCTTCTTGC -3'
Cebpd	For 5'-ATCGACTTCAGCGCCTACA-3' Rev 5'-GCTTTGTGGTTGCTGTTGAA-3'
Adiponectin	For 5'-ATGACGGCAGCACTGGCA-3' Rev 5'-CGGCCTTGTCCTTCTTGA-3'

Resistin	For 5’-CGCTTCCTGATGTCGGTC-3’ Rev 5’-ATGCCCACTTCGCCATCC-3’
Cd36	For 5’- GCTTGCAACTGTCAGCACAT - 3’ Rev 5’- GCCTTGCTGTAGCCAAGAAC- 3’
Fabp4	For 5’- CATGGCCAAGCCCAACAT -3’ Rev 5’- CGCCCAGTTTGAAGGAAATC -3’
Scd1	For 5’-GCGATACACTCTGGTGCTCA-3’ Rev 5’-CCCAGGGAAACCAGGATATT-3’
Perilipin	For 5’-TGCTGGATGGAGACCTC-3’ Rev 5’-ACCGGCTCCATGCTCCA-3’
Lpl	For 5’-GCACTTTCCAGCCAGGATGC-3’ Rev 5’-GGCCTGGTTGTGTTGCTTGC-3’
Acs	For 5’-GCTGATCCAGAAGGGGTTCA-3’ Rev 5’-CCACCCCACACTTCTTGCCT-3’
Fasn	For 5’-CTGGCCCCGGAGTCGCTTGAGTATA-3’ Rev 5’-GGAGCCTCCGAAGCCAAATGA-3’
Nedd8	For 5’-AACCCACAGACAAGGTGGAG -3’ Rev 5’-CAAGGAGGTAAACGGAACCA -3’
Tnfa	For 5’- ACGGCATGGATCTCAAAGAC-3’ Rev 5’-AGATAGCAAATCGGCTGACG-3’
Il6	For 5’-TAGTCCTTCCTACCCCAATTTCC-3’ Rev 5’- TTGGTCCTTAGCCACTCCTTC-3’
Mcp1	For 5’-CCACTCACCTGCTGCTACTCAT-3’ Rev 5’-GGTGATCCTCTTGTAGCTCTCC-3’
F40/80	For 5’-CCCCAGTGTCCT TACAGAGTG-3' Rev 5’-GTGCCCAGAGTGGATGTCT-3'
C11b	For 5’- 5'-CCTTGT TCTCTT TGATGCAG-3' Rev 5’- 5'-GTGATGACAACTAGGATCTT-3'
C11c	For 5’-CCTGAGGGTGGGCTGGAT-3' Rev 5’-GCCAATTTCCTCCGGACAT-3'
18S RNA	For 5’- TTCGTATTGAGCCGCTAGA-3’ Rev 5’- CTTTCGCTCTGGTCCGTCTT-3’

Table 4.Chip-PCR primer sequences.

Purposes	Targets	Forward primers (5’ to 3’)	Reverse primers (5’ to 3’)
ChIP PCR	Mouse Fabp4	TTTGCTTCCACTTAATTCCT	GCTCAGGGTGTGCAAGCAGG
	Mouse C/ebpa	CTGAGCTACACCCTCGGCTC	TCCCCACCGGAGGGCATGAG
	Mouse Fabp4 (NS)	TTTCTCAGAGCATCCCGTGG	TTACAAGACAGCCAGAGAAA

RESULTS

NEDD8 was induced during adipocyte differentiation.

Adipocyte differentiation is temporally controlled through the hormonal stimulation of glucocorticoids, cAMP, and insulin, which are known to consistently induce C/EBPβ and δ, followed by PPARγ and C/EBPα expression (Rosen and Spiegelman, 2000). To examine whether NEDD8 was related to adipocyte differentiation, the differentiation of mouse 3T3-L1 pre-adipocyte cells were induced by dexamethasone, IBMX, and insulin (DMI): adipogenesis stimuling cocktail. NEDD8 expression gradually increased during adipogenesis and reached a peak at day 6, and other adipogenic transcription factors of PPARγ and C/EBPs were also induced (Fig 1A, B). To identify the NEDD8-conjugated substrates during adipogenesis, His-NEDD8 stable cell lines were established using lentivirus overexpression system in 3T3-L1 preadipocytes. After selection with puromycin, adiopogenesis was induced. His-NEDD8-conjugated proteins were isolated using Ni^{2+} affinity beads, electrophoresed, and identified by LC-MS analysis (Fig 2). Interestingly, PPARγ, the major adipogenic transcription factor, was identified as one of the NEDDylated proteins (Fig 2B). 3T3-L1 cell lines, which stably express His-NEDD8, were far more differentiated than that harboring control vector (Fig 3). Particularly, Oil-red O staining revealed that dexamethasone-treated His-NEDD8 cell lines were more differentiated than control cell lines. In addition, PPARγ protein levels were obviously increased by differentiation induction in His–NEDD8 stable cells compared with the control cell line. Thus NEDD8 enhances the actions

of glucocorticoid in adipogenesis. Collectively, these results suggest that NEDD8 is a positive regulator of adipogenesis.

The knockdown of NEDD8 reduced the expression of PPARγ and adipogenesis capacity of 3T3-L1 pre-adipocytes.

To understand the role of NEDD8 in the adipogenesis, I established stable knockdown cell lines using a lentiviral shRNA expression vector in 3T3-L1 pre-adipocytes. After selection with antibiotics, a control, NEDD8, and NEDD8-activating enzyme APPBP1 shRNA stable expressing cell lines were induced to differentiate into adipocytes. Two different shRNAs were designed to target mouse NEDD8 and APPBP1, and the efficiency of NEDD8 and APPBP1 knockdown were analyzed by western blotting (Fig 4A). Western blotting and Oil-red O staining revealed that the knockdown of both NEDD8 and APPBP1 significantly decreased adipogenesis; in particular, the knockdown of NEDD8 more dramatically inhibited adipogenesis and PPARγ protein expression. The differentiation of mouse 3T3-F442A pre-adipocyte cells was induced by insulin. Corresponding with this result, another preadipocyte, 3T3-F442A producing shRNAs against mouse NEDD8 and mouse APPBP1 was less differentiated compared with the control cells. In addition, the expression level of PPARγ was decreased, compared with the control cells (Fig 4B). In order to examine dose-dependent effect of the knockdown, I tried transient transfections of different doses of siRNA into 3T3-L1 cells. The efficient knockdown effects were confirmed by western blot analysis 8 days after transfection (Fig 5A). The knockdown of mouse NEDD8 and APPBP1 by siRNA

suppressed adipocyte differentiation dose-dependently in 3T3-L1 cells. Furthermore, kinetic expression analysis during adipogensis showed that NEDD8 expression paralleled with PPARγ, because both proteins were induced during the middle stage of adipogenesis. This induction of PPARγ was decreased by the knockdown of NEDD8 (Fig 5B). These results suggest that adipocyte differentiation might be associated with the NEDDylation process through the regulation of PPARγ protein levels.

The depletion of NEDD8 decreased adipogenic genes in 3T3-L1 pre-adipocytes.

To address the functional role of NEDD8 in adipogenesis, and which adipogenic factors are regulated by NEDD8, 3T3-L1 pre-adipocytes were transfected with control siRNA or anti-NEDD8 siRNA two days before adipogenesis. 3T3-L1 cells were induced for adipogenesis for eight days, and then were harvested on the indicated day. RT-qPCR analyses revealed that the NEDD8 knockdown significantly attenuated pparg and c/ebpa mRNA expression, and lipid deposition–related factors such as fatty acid binding protein 4 (fabp4), cluster of differentiation 36 (cd36), and fatty acid synthase (fasn). In addition, adipokines such as resistin and adiponectin were suppressed when PPARγ was inhibited by knockdown of NEDD8 (Fig 6), whereas c/ebpb and c/ebpd mRNA expression were not dependent on NEDD8 because the expression of c/ebpb and c/ebpd were induced prior to PPARγ expression. These results further demonstrate that NEDD8 is essential for adipogenesis.

NEDD8 was recruited to the peroxisome proliferator hormone response

elements (PPRE) of C/EBPα and FABP4 promoters during adipogenesis.

As PPARγ and NEDD8 were co-induced during adipogenesis, I examined whether NEDD8 regulates PPARγ. Western blot analysis showed a significant reduction of PPARγ protein in NEDD8 knockdown cell lines, compared to that in control cell lines. On the contrary, the PPARγ protein levels were dramatically increased in NEDD8-overexpressed cell lines (Fig 7). These results suggest that NEDD8 was required to induce PPARγ in 3T3-L1 cells was dependent on NEDD8 expression. As PPARγ is known to be transcriptional activator for the expression of C/EBPα and FABP4, the chromatin immunoprecipitation (ChIP) analysis with PPARγ antibodies was performed on the well-known PPRE sites for these proteins. The binding of PPARγ on the FABP4 and C/EBPα promoter was more enriched in 3T3-L1 cells after the adipogenesis stimuli, while was diminished in NEDD8 shRNA stable cell lines. (Fig 8A left and B left). On the contrary, the binding of PPARγ on the fabp4 and c/ebpa promoter was increased in NEDD8-overexpressed stable cell lines (Fig 8 A right and B right). These results suggest that enhanced expression of PPARγ by NEDD8 correlated with increased binding of PPARγ to downstream target promoters.

NEDD8 had an essential role in *in vivo* adipogenesis.

NEDD8 plays important role in *in vitro* adipocyte differentiation. To investigate the *in vivo* role of NEDD8, I established NEDD8-deficient 3T3-L1 (Fig 9) and 3T3-F442A cell lines (Fig 10), and implanted them into the subcutaneous tissue of mouse abdomen. Five wks after implantation, the grafted fat pads were examined

with the histology and the expression of anti-perilipin (a lipid droplet scaffold protein) via immunostaining. Upon comparison with the control fat pad, both NEDD8-deficient cell lines showed dramatic inhibition in adipose tissue formation. These results indicate that NEDD8 is necessary for *in vivo* adipocyte differentiation.

NEDDylation of PPARγ was required for its stability.

As shown above, proteomics analysis revealed that PPARγ was conjugated with NEDD8 during adipogenesis. Among the major adipogenic transcription factors, PPARγ turned out solely to be endogenously NEDDylated via Ni^{2+} pull-down assay (Fig 11). Ectopically expressed PPARγ in HEK293 cells was identified to be conjugated with NEDD8, but not with NEDD8ΔGG (conjugation-defective due to Gly-75/76 deletion) or SENP8 (deNEDDylase) overexpression (Fig 12 A). Moreover, since HIF-1α reported to be stabilized by NEDDylation (Ryu et al., 2011), I tested whether PPARγ is able to be stabilized with NEDD8. Ectopically expressed PPARγ was stabilized with NEDD8 dose dependently, but not with NEDD8ΔGG (Fig 12 B left). To solidify that NEDD8 increased the PPARγ stability, HEK293 cells were transfected either with PPARγ only or PPARγ and NEDD8 (Fig 12 B right). After 48 h incubation, the cells were treated with cycloheximide to inhibit de novo protein synthesis and PPARγ degradation was attenuated by NEDD8. To determine whether NEDDylation affects PPARγ ubiquitination, HEK293 cells were co-transfected with PPARγ and NEDD8 or Ub, which were incubated with or without MG132, an inhibitor of the proteasome (Fig 13 upper). In the presence of MG132, the combination of PPARγ and Ub, together with NEDD8 blocked the

PPARγ ubiquitination more strongly. NEDD8 siRNA was co-transfected with either PPARγ or PPARγ and Ub, and then the cells were incubated with or without MG132 (Fig 13 lower). In the presence of MG132, the co-express with PPARγ and Ub in NEDD8 siRNA knockdown cells up-regulated PPARγ ubiquitination. On the base of these results, NEDDylation is required for PPARγ stabilization by blocking its ubiquitination.

Identification of the PPARγ domain conjugated with NEDD8.

Next, to analyze which domain of PPARγ might be associated with NEDD8, HEK293 cells expressed with each domain of PPARγ were treated with MG132 or co-transfected with NEDD8 (Fig 14). Interestingly, western blot revealed that the expression levels of middle and C-term peptides increased with NEDD8 co-expression. To speculate the NEDDylated region of PPARγ, each of PPARγ fragments co-expressed with His-NEDD8 was subjected to Ni^{2+} pull-down assay. The middle and C-terminal regions turned out to be NEDDylated (Fig 15 upper), but abolished in His-NEDD8ΔGG co- expressed cells(Fig 15 lower). NEDD8 physically interacts with the PPARγ middle and C-terms.

MDM2 as an E3 ligase promoted PPARγ NEDDylation.

It was recently reported that murine double minute 2 (MDM2), the E3 ubiquitin ligase, has an important role in regulating the stability of p53 tumor suppressors and the expression level of MDM2 is amplified in 3T3-L1 preadipocytes (Berberich et al., 1999). A recent study showed that MDM2 is required for the cAMP-mediated

induction of C/EBPδ by the recruitment of cAMP regulatory element-binding protein (CREB), and promotes adipogenesis (Hallenborg et al., 2012). Yet, the reason for MDM2 amplification in adipogenesis was not clarified. On the base of previous reports, I expected that MDM2 has the role of E3 ligase for PPARγ NEDDylation. 3T3-L1 pre-adipocytes transfected with control siRNA or anti-MDM2 siRNA two days before adipogenesis were induced for adipogenesis for eight days, then harvested (Fig 16 A). Oil-red O staining revealed that MDM2 knockdown significantly decreased adipogenesis dose dependently. As expected, western blotting showed that the PPARγ protein level was significantly reduced, when MDM2 depleted. Furthermore, nutlin-3, an MDM2 inhibitor, also blocked adipocyte differentiation and reduced PPARγ protein levels dose dependently, suggesting that MDM2 has a crucial role in adipogenesis (Fig 16 B). As expected, MDM2 physically interacted with PPARγ in HEK293 cells (Fig 17). Ni^{2+} pull-down assay showed that ectopically expressed MDM2 mediated PPARγ NEDDylation. Conversely, PPARγ NEDDylation was down regulated by knockdown of MDM2 in HEK293 cells (Fig 18 left). Nutlin-3 also inhibited PPARγ NEDDylation (Fig 18 right). These results suggest that MDM2 physically interacts with PPARγ and specifically mediates PPARγ NEDDylation.

MLN4924 inhibited adipogenesis in 3T3-L1 and H-ADSC.

Searching for inhibitors that ubiquitin-proteasome system (UPS) and ubiquitin-like proteins (UBLs) may allow control over dynamic genes and be the key to find novel therapeutics for diseases; NEDDylation is activated by a NEDD8 activation enzyme

complex, which is a combination of APPBP1 and UBA3 during the first process (Rabut and Peter 2008). MLN4924, the adenosine sulfamate analog that targets NEDD8 E1 activating enzyme has a crucial therapeutic effect in the treatment of cancer (Soucy et al., 2009). Pharmaceutically, MLN4924 has possibility as a NEDDylation-targeting therapy that has a potential effect on other diseases. To address the effect on adipogenesis of NEDDylation, MLN4924 was treated in mouse and human pre-adipocytes, and then adipocyte differentiation was induced using adipogenic stimuli cocktails. Oil-red O staining showed that MLN4924 suppressed adipocyte differentiation. As assumed, western blotting showed that the PPARγ protein level was reduced in 3T3-L1 cells and human adipose tissue-derived mesenchymal stem cells (H-ADSCs) isolated from obese patients (Fig 19). I further checked the expression of adipogenic markers and lipid deposition-related genes in MLN4924 treatment (Fig 20). MLN4924 significantly reduced the expression of pparg, c/ebpa, and other adipogenic target genes such as fabp4, cd36, adiponectin, and resistin during adipogenesis. Furthermore, the expression of lipid metabolic genes such as fasn and scd1 were also suppressed, whereas c/ebpb and c/ebpd mRNA expression was not implicated in MNL4924. These data suggest that MLN4924 dramatically reduced adipogenesis in both mouse and human cell lines.

MLN4924 reduced fat accumulation.

To address whether MLN4924 reduces fat storage in 3T3-L1 and H-ADSCs, 3T3-L1 was treated with either 0.1 or 0.5 μM of MLN4924 daily from third or sixth day during 20 days-differentiation. After the daily treatment of MLN4924, the fat

accumulation was reduced by MLN4924 (Fig 21). The same results have shown in human cells (Fig 22). Furthermore, quantitative PCR showed that the expression of lipid metabolic genes such as perilipin, lpl, acs, scd1, cd36, and fabp4 was significantly reduced by MLN4924 in 3T3-L1 cells (Fig 23). The same results have been shown in human cells (Fig 24). These results indicate that MLN4924 can block fat accumulation.

MLN4924 effected on weight loss and improves glucose tolerance and insulin sensitivity in high fat diet–induced obesity mice.

MLN4924 diminished the number and size of lipid droplets in both 3T3-L1 cells and H-ADSCs dramatically. The above experiments lead to the question of whether MLN4924 can be an anti-obesity drug. As the early stages of adipogenesis are attenuated by the inhibition of NEDDylation, MLN4924 was expected to prevent childhood obesity. To systemically access weight gain, we fed young C57BL/6 mice with a 60% fat diet, injecting the mice intraperitoneally once every three days with vehicle or MLN4924 (30 mg/kg). Anti-obesity drugs should be less toxic than anticancer drugs, thus the drug treatment interval was increased for this study. Interestingly, MLN4924 prevented the high fat diet (HFD)-induced weight gain (Fig 25 A). Body weight was reduced by MLN4924 during 12 wks in HFD. As expected, MLN4924 did not reduce the body weight in normal chow diet (NCD) mice, suggesting that MLN4924 is not substantially toxic at the dose used in the experiment. Withdrawal of the drug after six wks of treatment restored weight gain, indicating that the action of MLN4924 is reversible (Fig 25 B). Food intake was not

influenced by the MLN4924 treatment, and the preventative effect of MLN4924 against weight gain was not dependent on the loss of appetite (Fig 25 C). Moreover, obesity is associated with type 2 diabetes (Kahn et al., 2006); to determine whether MLN4924 treatment could attenuate diabetic symptoms in HFD-fed mice, obesity was established 10 wks after, and then their metabolic parameters were examined. Consequently, the fasting serum glucose level was increased in HFD-fed mice, and HFD-induced hyperglycemia was reduced by MLN4924 treatment. Similarly, the fasting insulin level was significantly increased by HFD, and HFD–insulin overproduction was restored by MLN4924 (Fig 26 A). This result indicates that the insulin sensitivity in diet induced obesity (DIO) mice can be significantly improved by MLN4924. Following the confirmation that characterized HFD-induced hyperglycemia, I next employed a glucose tolerance test and insulin tolerance test, which revealed that MLN4924 relived HFD-induced glucose and insulin intolerance, while not affecting glucose tolerance and insulin sensitivity in NCD-fed mice (Fig 26 B). Moreover, MLN4924 reduced plasma leptin concentrations in the DIO mice model (Fig 26 C). These results indicate that MLN4924 significantly enhanced glucose homeostasis and insulin sensitivity in DIO mice.

MLN4924 reduced adipose tissue size in DIO mice.

As described above, this study observed that the body weight of HFD-fed mice was reduced via treatment with MLN4924. To analyze how obese HFD-fed mice were, the abdominal fat of mice was analyzed using Computed Tomography (CT). The analysis of the body fat composition revealed a remarkable reduction of adipose

deposition in HFD-fed MLN4924-treated mice compared with HFD-fed control mice (Fig 27 A). This CT-based analysis of the fat area and volume that were enormously reduced in HFD-fed mice treated with MLN4924 (Fig 27 B). As expected, the size of white adipose tissues (WAT), epididymal fat, subcutaneous fat, and visceral fat restored to normal in MLN4924-treated HFD-fed mice treated with MLN4924 (Fig 27 C). Next, I determined which genes were down regulated by MLN4924 in DIO mice. As shown in fig 11, PPARγ was NEDDylated at adipocyte differentiation and the expected target of MLN4924. These results indicate that the down regulation of PPARγ expression is a potential therapeutic effect of anti-obesity drugs. From western blotting, the MLN4924-treated HFD-fed mice showed reduced PPARγ expression in WAT (Fig 28). Furthermore, the patients with obesity had adipose tissue dysfunction, which leads to adipocyte hypertrophy and inflammatory processes in the adipose tissue (Ouchi et al., 2011). Interestingly, the expression of adipogenic genes, lipid metabolic genes, and inflammatory cytokines increased in the epididymal fat of HFD-fed mice, MLN4924 also prevents this response (Fig 29, 30). From the *in vivo* results, MLN4924 prevents obesity in HFD-fed mice by reducing the adipogenesis and fat accumulation; yet this mode of action did not disturb the development of normal fat tissue. Taken together, this study suggests that MLN4924 might have an advantageous effect for anti-obesity drugs.

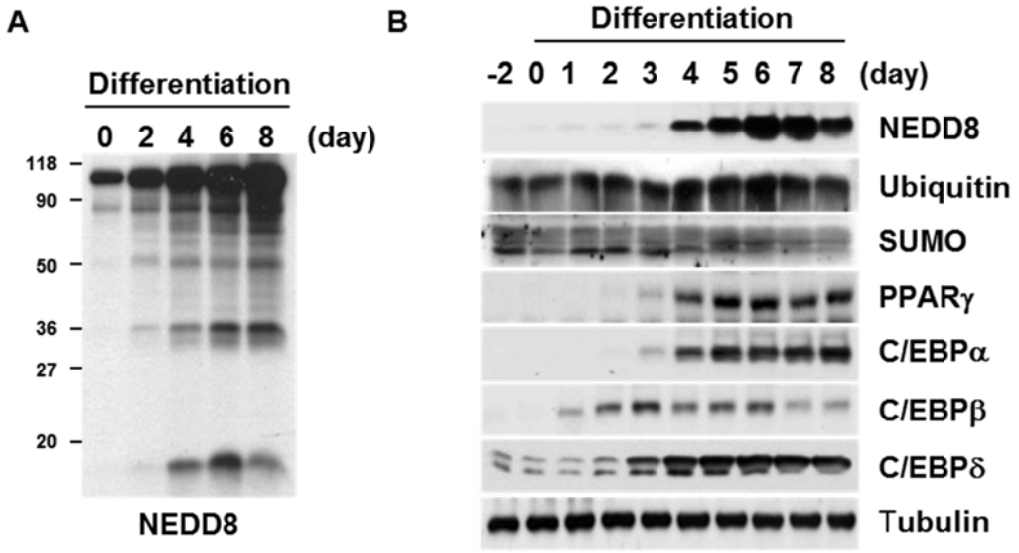

Figure 1. NEDD8 is induced during adipocyte differentiation.

(A) 3T3-L1 cells were incubated with adipogenesis stimuli cocktail (DMI) for the indicated lengths of time. The protein level of NEDD8 was determined by western blotting analysis during adipogenesis. (B) Before or after treatment of DMI for the indicated lengths of time, NEDD8, Sumo, Ubiquitin, PPARγ and C/EBPs protein levels were determined by western blotting analysis using indicated antibodies. Tubulin was used as a loading control with particular total protein samples.

A

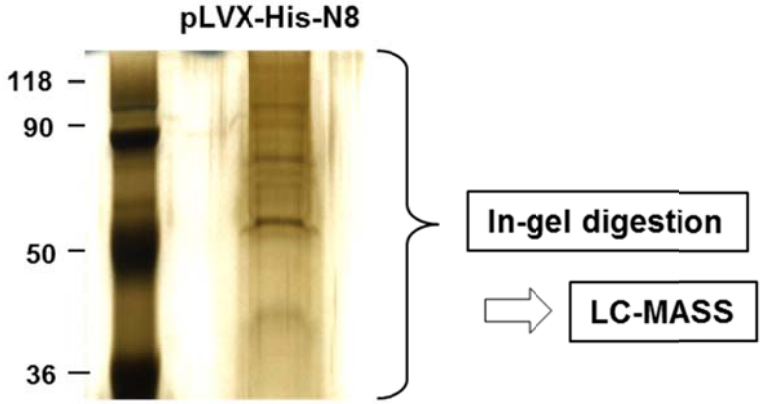

B

NEDDyated proteins by proteomics in the adipocytes

Non-POU domain-containing octamer-binding protein

Putative pre-mRNA-splicing factor ATP-dependent RNA helicase

Ataxin-2

Insulin-like growth factor 2 mRNA-binding protein 2

Mannosyl-oligosaccharide glucosidase

DNA topoisomerase 1

E3 ubiquitin-protein ligase CBL

GDH/6PGL endoplasmic bifunctional protein

1,4-alpha-glucan-branching enzyme

NADH-cytochrome b5 reductase 3

Serine/threonine-protein phosphatase 1 regulatory subunit 10

60S ribosomal protein L15

ATP-binding cassette sub-family D member 3

Constitutive coactivator of PPAR-gamma-like protein 2

60S ribosomal protein L27a

Trimethyllysine dioxygenase, mitochondrial

Peroxisome proliferator-activated receptor gamma

Figure 2. Proteomic analysis of NEDDylated protein that might play important roles in adipogenesis in 3T3-L1 cells.

(A) 3T3-L1 cells were infected with viral pLVX-His-NEDD8 vector. After selections with puromycin, stable cells were treated with DMI. After 4 days, cells were lysed. His-NEDD8-conjugated proteins were bound to Ni^{2+}-NTA-agarose beads under denaturing conditions and subjected to silver staining and then LC/MS analysis was performed after in-gel digestion. (B) LC/MS data for His-NEDD8-conjugated proteins.

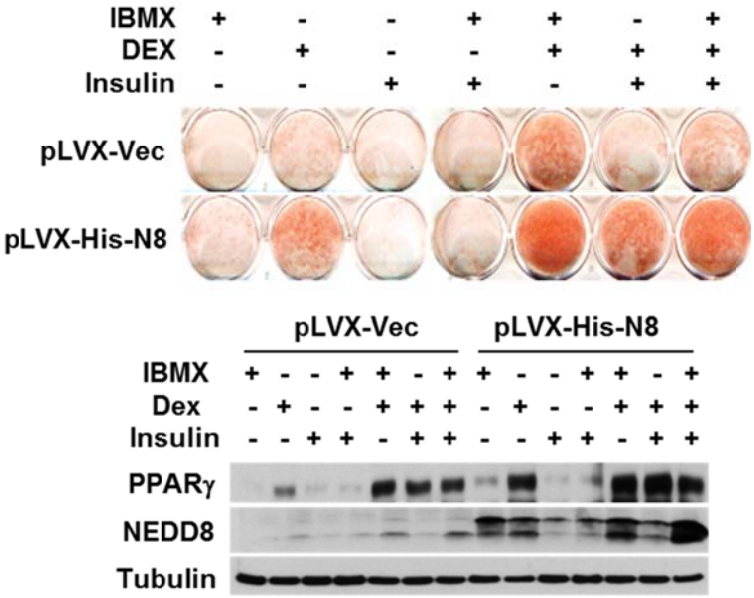

Figure 3. NEDD8 mediates actions of glucocorticoid in the adipogenesis.

Stably expressed pLVX-IRES-Control (pLVX-Vec) or pLVX-IRES-His-NEDD8 (pLVX-His-N8) 3T3-L1 cells were differentiated with indicating conditions (1 μM dexamethasone, 500 μM IBMX, 5 μg/ml insulin) and then at day 8, cells were stained with Oil-red-O staining (upper). Cell lysates were analyzed for PPARγ and NEDD8 protein levels by western blotting using anti-PPARγ and anti-NEDD8 antibodies. Tubulin was used as a loading control (lower).

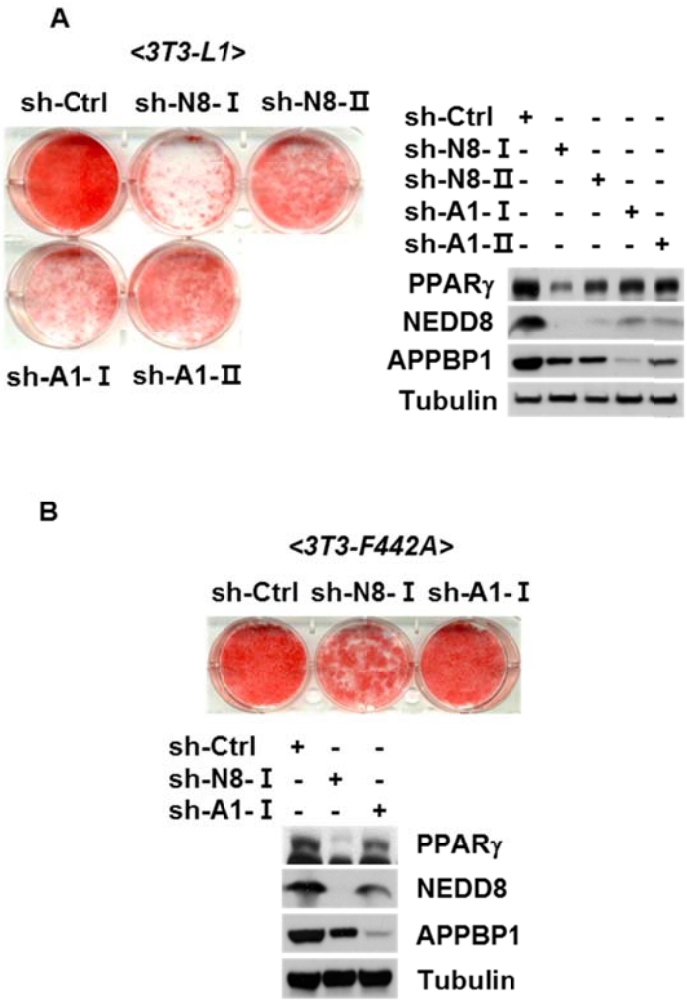
A
<3T3-L1>
sh-Ctrl
sh-N8-Ⅰ
sh-N8-Ⅱ
sh-A1-Ⅰ
sh-A1-Ⅱ
sh-Ctrl + - - - -
sh-N8-Ⅰ - + - - -
sh-N8-Ⅱ - - + - -
sh-A1-Ⅰ - - - + -
sh-A1-Ⅱ - - - - +
PPARγ
NEDD8
APPBP1
Tubulin
B
<3T3-F442A>
sh-Ctrl
sh-N8-Ⅰ
sh-A1-Ⅰ
sh-Ctrl + - -
sh-N8-Ⅰ - + -
sh-A1-Ⅰ - - +
PPARγ
NEDD8
APPBP1
Tubulin

Figure 4. NEDD8 knockdown reduced the adipogenesis capability of preadipocytes.

(A) 3T3-L1 cells were stably knock downed with each targeting shRNA viruses, pLKO.1-sh-Control (sh-Ctrl), two different NEDD8-targeting pLKO.1-sh-NEDD8 (sh-N8-I and -II）or pLKO.1-sh-APPBP1 (sh-A1-I and -II）and then stimulated with DMI. After adipogenesis cells were stained with Oil-red O at day 8. PPARγ, NEDD8 and APPBP1 protein levels were determined by western blotting analysis at 8 day. Tubulin was used as a loading control with particular total protein samples. (B) 3T3-F442A cells were stably knockdowned with pLKO.1-sh-Control (sh-Ctrl), pLKO.1-sh-NEDD8-I (sh-N8-I) and pLKO.1-sh-APPBP1-I (sh-A1-I) and then stimulated with DMI. Cells were stained with Oil-red O at day 8 (upper). PPARγ, NEDD8 and APPBP1 protein levels were determined by western blotting analysis. Tubulin was used as a loading control with particular total protein samples (lower).

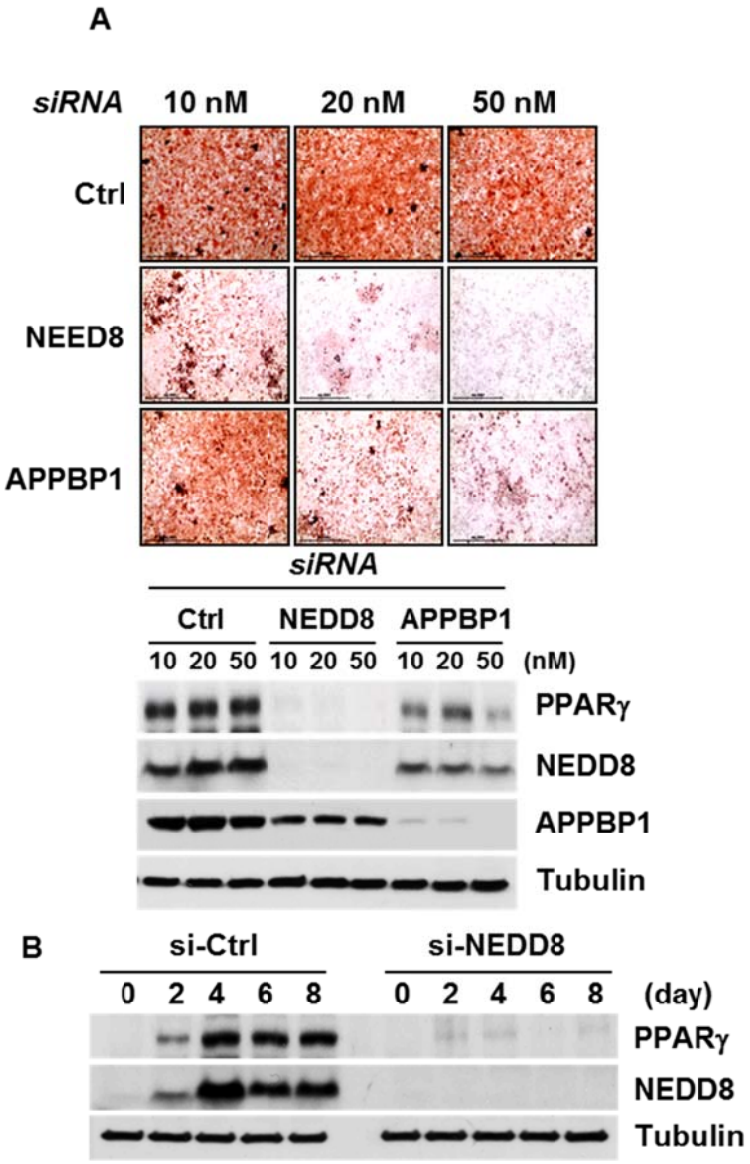
A
siRNA
10 nM
20 nM
50 nM
Ctrl
NEED8
APPBP1
siRNA
Ctrl
NEDD8
APPBP1
10 20 50 10 20 50 10 20 50 (nM)
PPARγ
NEDD8
APPBP1
Tubulin
B
si-Ctrl
si-NEDD8
0 2 4 6 8 0 2 4 6 8 (day)
PPARγ
NEDD8
Tubulin

Figure 5. Analysis of dose-dependency and kinetics of NEDD8 knockdown in 3T3-L1 cells.

(A) 3T3-L1 cells were transiently transfected with si-Control (si-Ctrl), si-NEDD8 or si-APPBP1 to 10, 20, 50 nM at 2 day before differentiation and then stimulated with DMI. After differentiation, cells were stained with Oil-red-O at day 8 (upper). Cell lysates were analyzed by western blotting using anti-PPARγ, anti-NEDD8 or anti-APPBP1 antibodies. Tubulin was used as a loading control with particular total protein samples (lower). (B) 3T3-L1 cells were transiently transfected with si-Control or si-NEDD8 (50 nM) at 2 days before differentiation. 3T3-L1 cells treated with DMI and then harvested at 0, 2, 4, 6 and 8 day. Cell lysates were analyzed by western blotting using anti-PPARγ, anti-NEDD8 or anti-APPBP1 antibodies. Tubulin was used as a loading control with particular total protein samples.

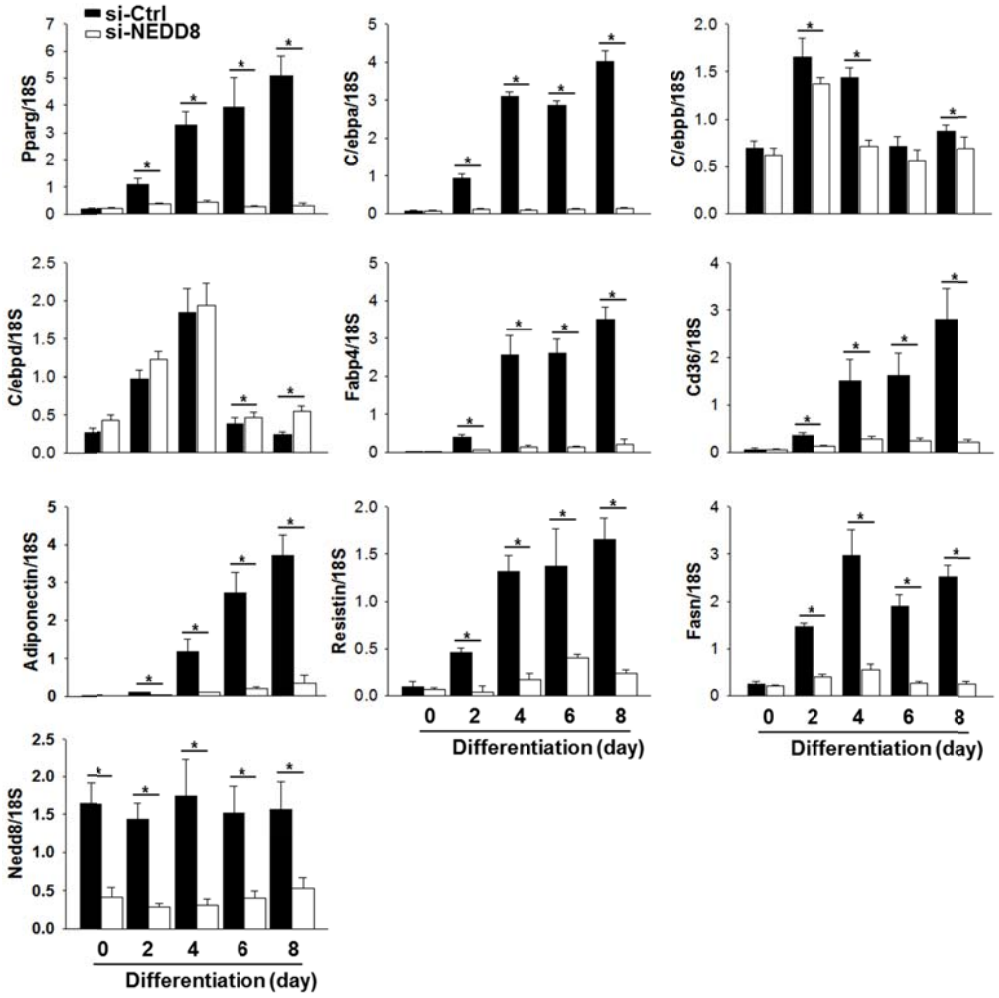
si-Ctrl
si-NEDD8
Pparg/18S
C/ebpa/18S
C/ebpb/18S
C/ebpd/18S
Fabp4/18S
Cd36/18S
Adiponectin/18S
Resistin/18S
Fasn/18S
Nedd8/18S
0 2 4 6 8
Differentiation (day)

Figure 6. NEDD8 knock down by si-NEDD8 down regulated the expression of adipogenic genes during adipogenesis.

3T3-L1 cells were transfected with si-Ctrl or si-NEDD8 (50 nM) at 2 days before differentiation and then stimulated with DMI for the indicated lengths of time. Total RNA was extracted from cells, and RT-qPCR was applied to measure the expression levels of pparg, c/ebpa, c/ebpb, c/ebpd, fabp4, cd36 resistin, adiponectin, fasn, and nedd8. Results were quantified as the relative levels versus 18S RNA level. Data shown represent the mean±SD (n=3) and * denotes $p < 0.05$.

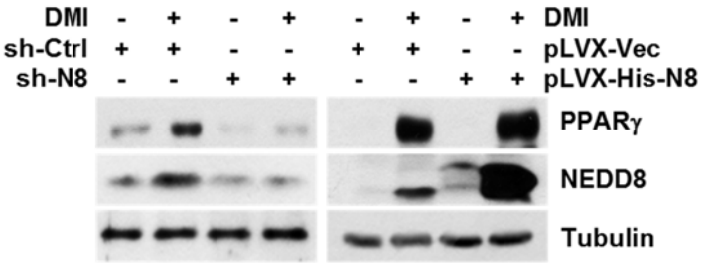

Figure 7. PPARγ induction in 3T3-L1 cells required NEDD8 during adipogenesis.

3T3-L1 stable cell lines expressing non-targeting sh-RNA (pLKO.1-sh-Ctrl) and NEDD8-targeting shRNA (pLKO.1-sh-N8) (left) and cells stably over-expressing each targeting vector viruses, pLVX-IRES-Control (pLVX-Vec) or pLVX-IRES-His-NEDD8 (pLVX-His-N8) (right) were treated with DMI. After 4 days cell lysates were analyzed by western blotting using anti-PPARγ and anti-NEDD8 antibodies. Tubulin was used as a loading control with particular total protein samples

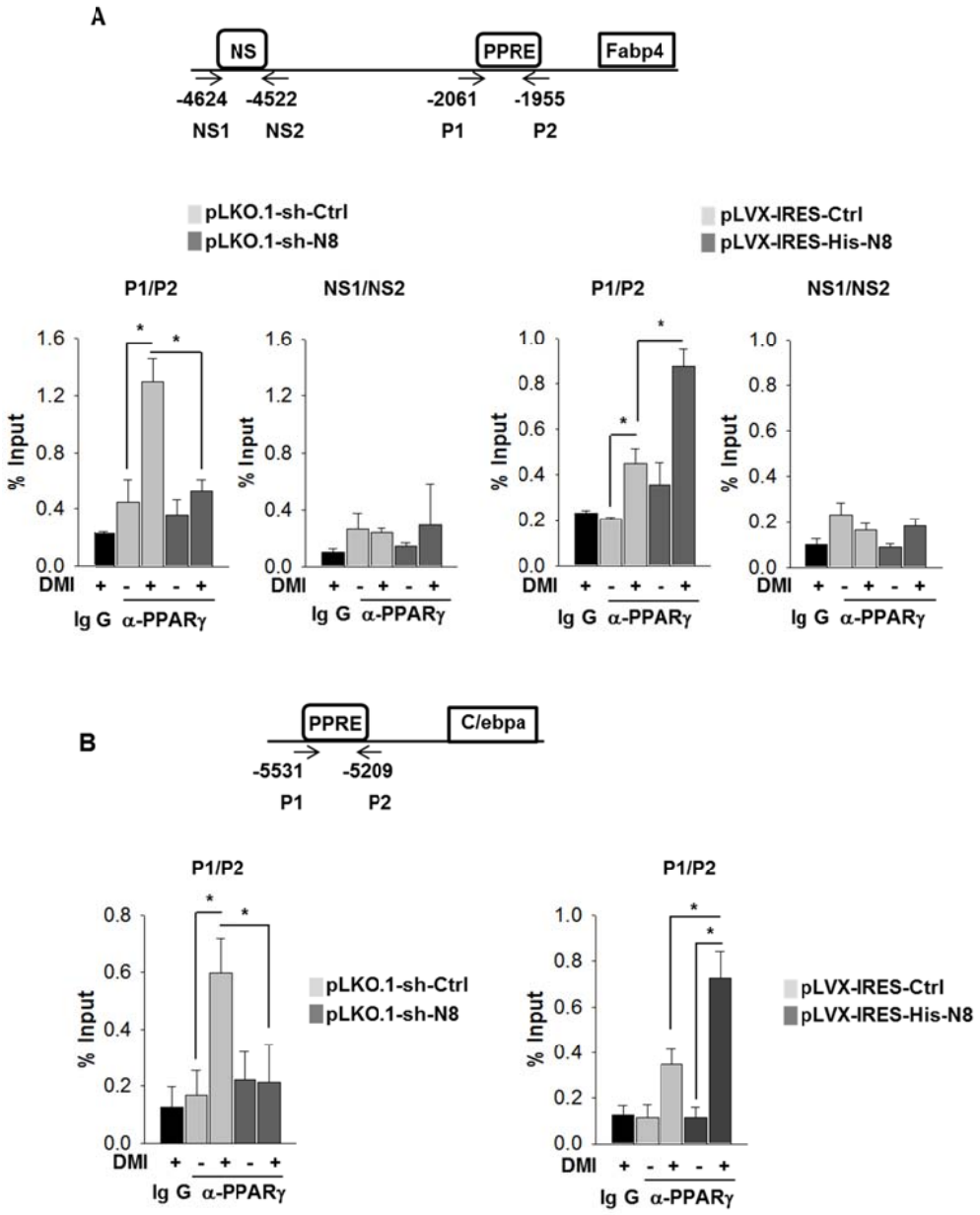
A
NS
PPRE
Fabp4
-4624
-4522
-2061
-1955
NS1
NS2
P1
P2
pLKO.1-sh-Ctrl
pLKO.1-sh-N8
pLVX-IRES-Ctrl
pLVX-IRES-His-N8
P1/P2
NS1/NS2
% Input
DMI
Ig G
α-PPARγ
B
PPRE
C/ebpa
-5531
-5209
P1
P2

Figure 8. Enhanced NEDD8 expression correlates with enhanced binding of PPARγ on PPRE.

(A) Chromatin immunoprecipitation (ChIP) was performed to reveal the binding of PPARγ to the promoter of its target genes. A schematic representation of fabp4 PPRE and segments amplified by PCR (upper). P1/P2 was fabp4 promoter sequence and NS1/NS2 was non-specific promotor sequence. 3T3-L1 stable cell lines expressing non-targeting sh-RNA (pLKO.1-sh-Ctrl) and NEDD8-targeting shRNA (pLKPO.1-sh-N8) or pLVX-IRES-Control and pLVX-IRES-His-NEDD8 vectors were treated with DMI and then after 4 days chromatin complexes were precipitated with anti-PPARγ antibody. The precipitated DNAs were amplified and quantified on RT-qPCR system using fabp4 primers. The results (mean±SD, n=3) are expressed as percentages of the input level (lower). (B) A schematic representation of c/ebpa PPRE and segments amplified by PCR (upper). P1/P2 was c/ebpa promoter sequence. 3T3-L1 stable cell lines expressing non-targeting sh-RNA (pLKO.1-sh-Ctrl) and NEDD8-targeting shRNA (pLKPO.1-sh-N8) or pLVX-IRES-Control and pLVX-IRES-His-NEDD8 vectors were treated with DMI and then after 4 days chomatin complexes were precipitated with indicated anti-PPARγ antibody. The precipitated DNAs were amplified and quantified on RT-qPCR system using c/ebpa primers. The results are expressed as percentages of the input level. Data shown represent the mean±SD (n=3) and * denotes $p < 0.05$.

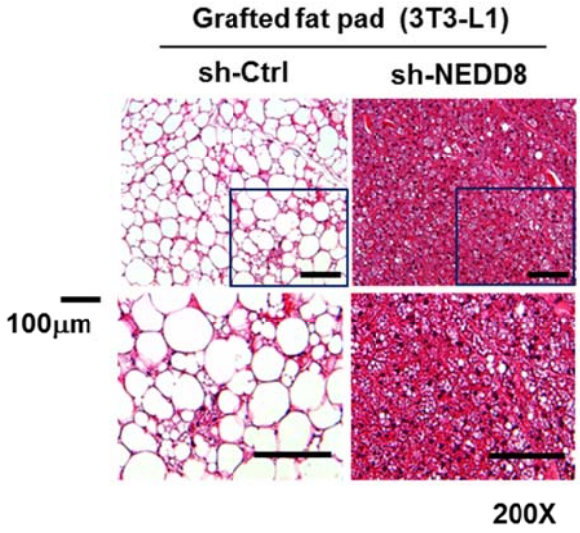
Grafted fat pad (3T3-L1)
sh-Ctrl
sh-NEDD8
100μm
200X

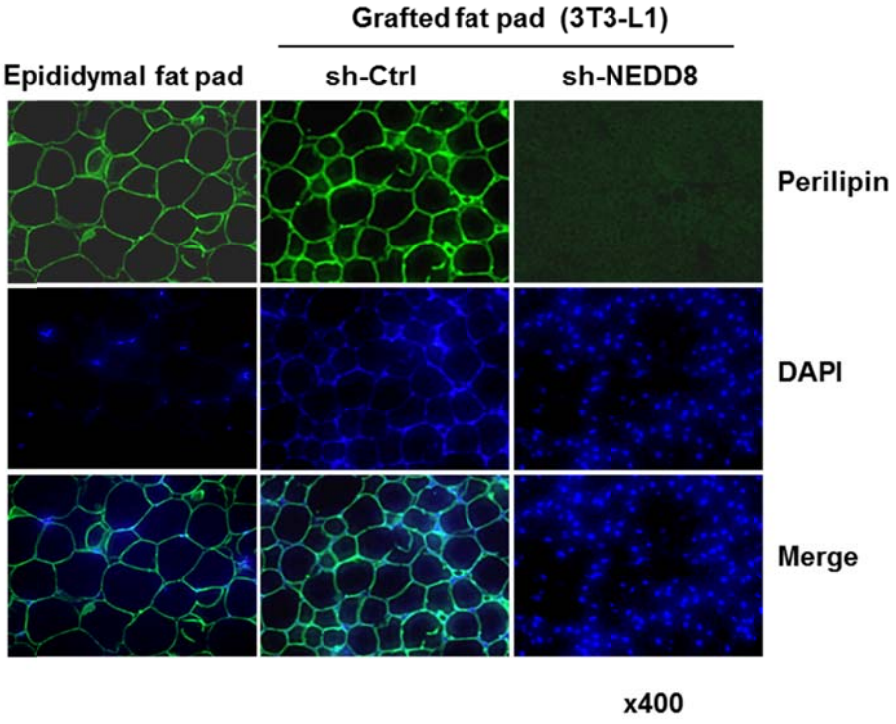
Grafted fat pad (3T3-L1)
Epididymal fat pad
sh-Ctrl
sh-NEDD8
Perilipin
DAPI
Merge
x400

Figure 9. NEDD8 is essential for the adipogenesis in implanted mouse fat pad. 3T3-L1 cells stably expressing by pLKO.1-sh-Control (sh-Ctrl) or pLKO.1-sh-NEDD8 (sh-NEDD8) were implanted into the subcutis of the abdomens of 9-wk-old male BALB/c nude mice. 5 wks after implantation, implanted fat pads were stained with hematoxylin and eosin (H&E, upper panel) or subjected to immunofluorescence analysis with anti-perilipin antibody (lower panel). Nuclei were stained with DAPI.

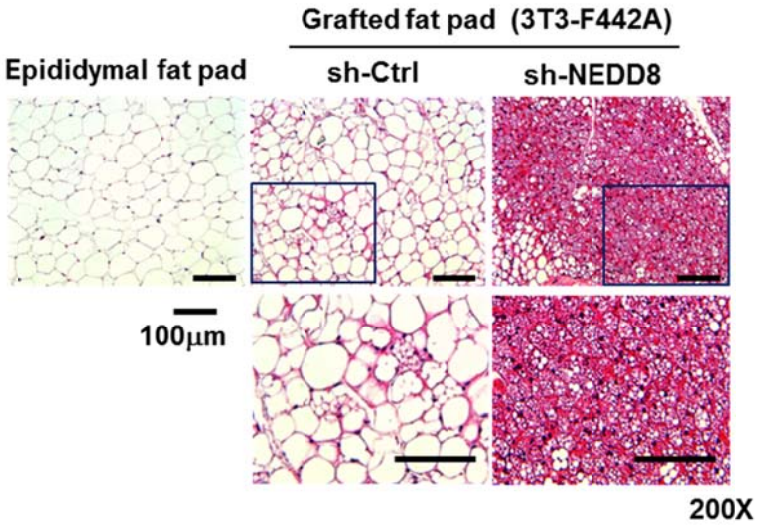
Grafted fat pad (3T3-F442A)
Epididymal fat pad
sh-Ctrl
sh-NEDD8
100μm
200X

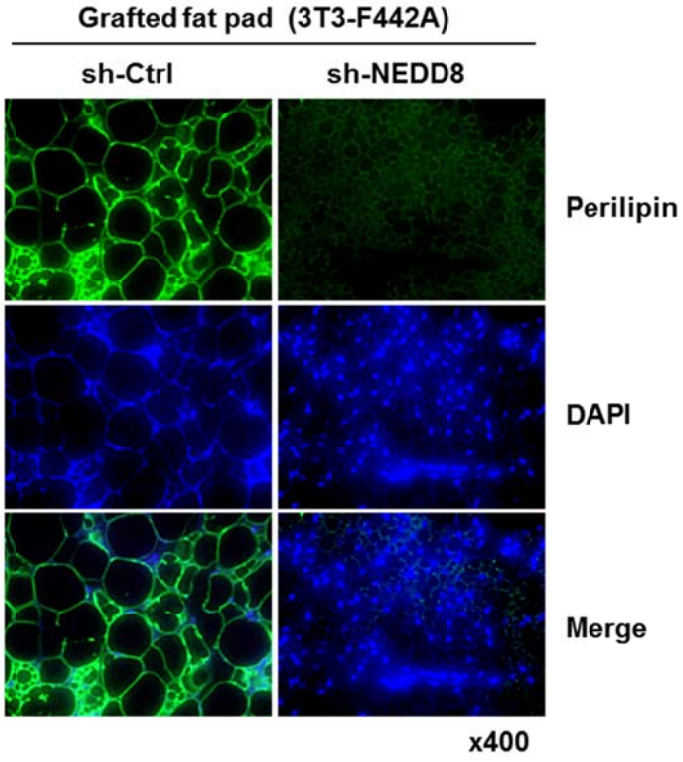
Grafted fat pad (3T3-F442A)
sh-Ctrl
sh-NEDD8
Perilipin
DAPI
Merge
x400

Figure 10. NEDD8 is essential for the adipogenesis in implanted mouse fat pad.

3T3-F442A cells stably expressing by pLKO.1-sh-Control (sh-Ctrl) or pLKO.1-sh-NEDD8 (sh-NEDD8) were implanted into the subcutis of the abdomens of 9-wk-old male BALB/c nude mice. 5 wks after implantation, implanted fat pads were stained with hematoxylin and eosin (H&E, upper panel)) or subjected to immunofluorescence analysis with anti-perilipin antibody (lower panel). Nuclei were stained with DAPI.

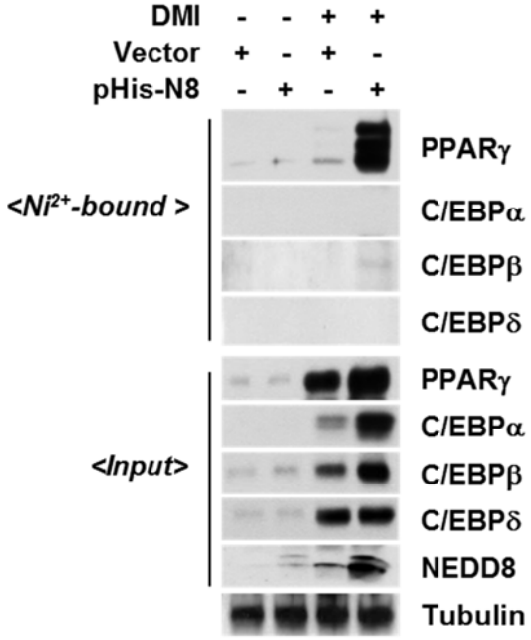

Figure 11. Endogenous PPARγ conjugates with NEDD8 during adipogenesis.

3T3-L1 cells stably expressing pLVX-IRES-vector or pLVX-IRES-His-NEDD8 cell lines were induced to adipogenesis using DMI. After 4 days, cells were lysed. His-NEDD8-conjugated proteins were bound to Ni^{2+}-NTA-agarose beads under denaturing conditions. His-NEDD8-conjugations were analyzed by western blotting analysis using the indicated antibodies. Tubulin was used as a loading control.

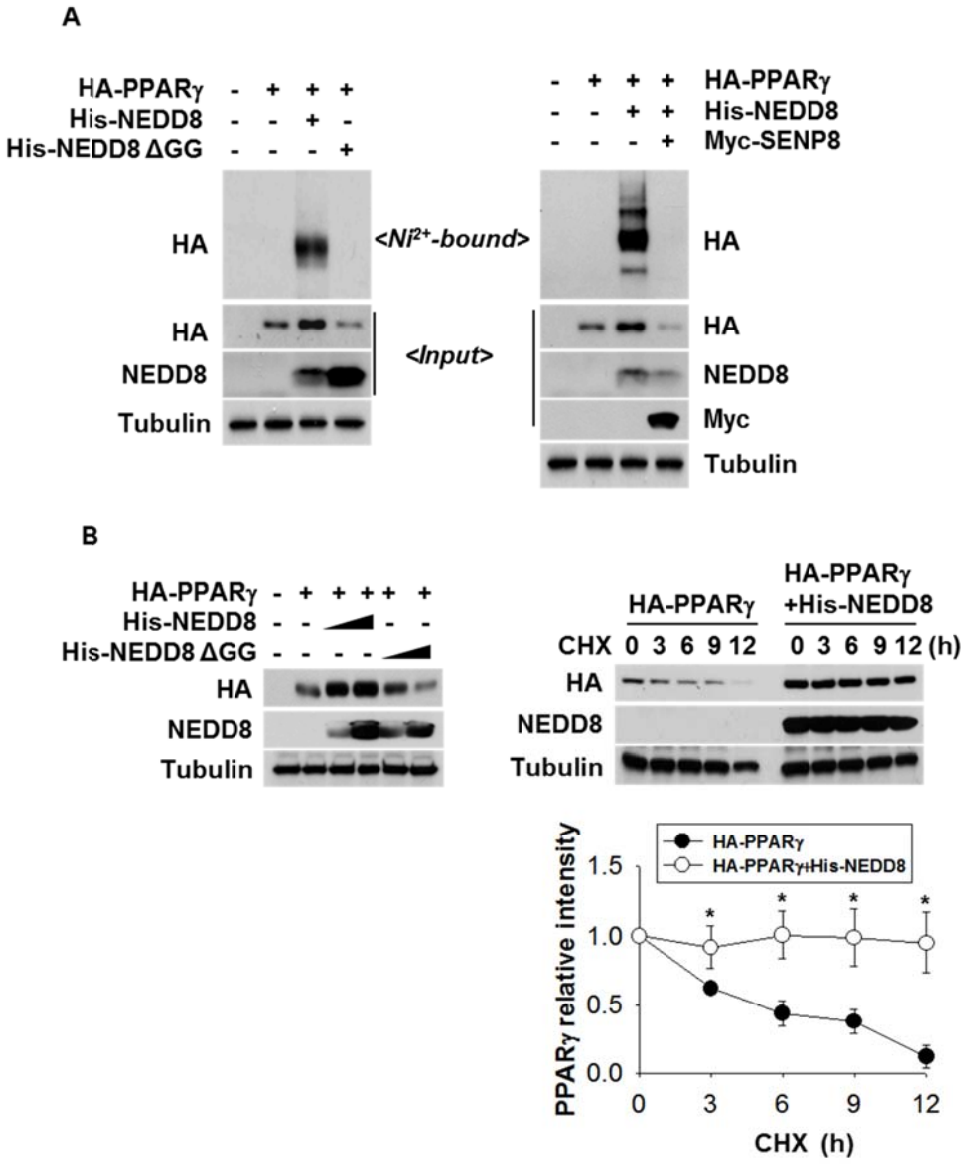
A
HA-PPARγ - + + +
His-NEDD8 - - + -
His-NEDD8 ΔGG - - - +
HA
<Ni2+-bound>
HA
NEDD8
Tubulin
<Input>
- + + + HA-PPARγ
- - + + His-NEDD8
- - - + Myc-SENP8
HA
HA
NEDD8
Myc
Tubulin
B
HA-PPARγ - + + + + +
His-NEDD8 - - - -
His-NEDD8 ΔGG - - - -
HA
NEDD8
Tubulin
HA-PPARγ
HA-PPARγ +His-NEDD8
CHX 0 3 6 9 12 0 3 6 9 12 (h)
HA
NEDD8
Tubulin
HA-PPARγ
HA-PPARγ+His-NEDD8
PPARγ relative intensity
1.5
1.0
0.5
0.0
0 3 6 9 12
CHX (h)

Figure 12. NEDDylation of PPARγ increased its stability.

(A) NEDDylation of PPARγ is blocked by mutant NEDD8 (NEDD8ΔGG) and deNEDDylating enzyme SENP8. HEK293 cells were transfected with HA-PPARγ, or co-transfected HA-PPARγ and His-NEDD8 or His-NEDD8ΔGG. After 48 h, cells were lysed. His-NEDD8-conjugated proteins were bound to Ni^{2+}-NTA-agarose beads under denaturing conditions. The His-NEDD8-conjugated PPARγ was purified and analyzed by western blotting using anti-HA or anti-NEDD8 antibodies. Tubulin was used as a loading control (left). HEK293 cells were transfected with HA-PPARγ, or co-transfected HA-PPARγ and His-NEDD8 or His-NEDD8 and Myc-SENP8. After 48 h, cells were lysed. His-NEDD8-conjugated proteins were bound to Ni^{2+}-NTA-agarose beads under denaturing conditions. The His-NEDD8-conjugated PPARγ was purified and analyzed western blotting using anti-HA anti-NEDD8 or anti-Myc antibodies. Tubulin was used as a loading control (right). (B) HA-PPARγ was co-transfected with His-NEDE8 or His-NEDD8ΔGG into HEK293 cells. After 48 h, cell lysates were analyzed by western blotting by using anti-HA or anti-NEDD8 antibodies. Tubulin was used as a loading control (left). HEK293 cells were transfected with HA-PPARγ only or HA-PPARγ and His-NEDD8 and then incubated 0, 3, 6, 9, 12 h with 50 μM cycloheximide. Proteins were analyzed by western blotting using anti-HA or anti-NEDD8 antibodies. Protein intensities form the western blottings were analyzed using ImageJ 1.36b software (NIH, Bethesda, MD, USA) and plotted. Tubulin was used as a loading control (right). Data shown

represent the mean±SD (n=3) and * denotes $p < 0.05$.

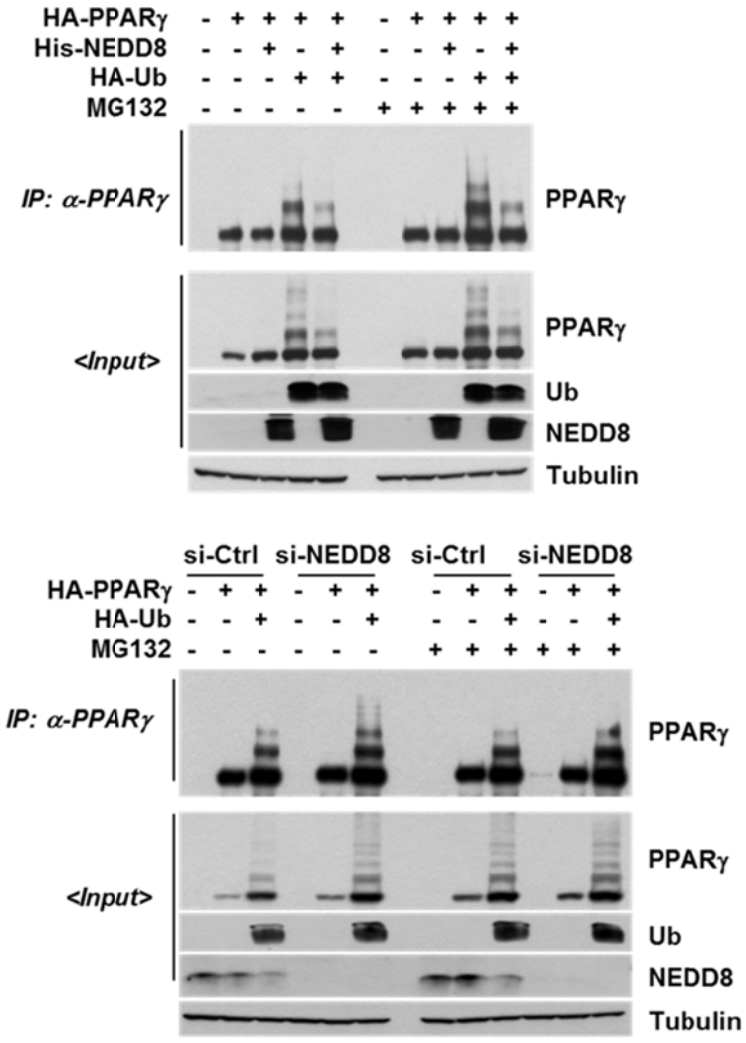
HA-PPARγ - + + + + - + + + +
His-NEDD8 - - + - + - - + - +
HA-Ub - - - + + - - - + +
MG132 - - - - - + + + + +
IP: α-PPARγ
PPARγ
<Input>
PPARγ
Ub
NEDD8
Tubulin
si-Ctrl si-NEDD8 si-Ctrl si-NEDD8
HA-PPARγ - + + - + + - + + - + +
HA-Ub - - + - - + - - + - - +
MG132 - - - - - - + + + + + +
IP: α-PPARγ
PPARγ
<Input>
PPARγ
Ub
NEDD8
Tubulin

Figure 13. NEDDylation of PPARγ attenuates its ubiquitination.

HEK293 cells were co-transfected with HA-PPARγ, His-NEDD8 or HA-Ub as indicated and then stabilized 48 h. After incubation with MG132 (10 μM) for 8 h, cell lysates were immunoprecipitated using anti-PPARγ antibody and analyzed by western blotting analysis using indicated antibodies. Tubulin was used as a loading control (upper). HEK293 cells were co-transfected with 50 nM Control si-RNA or anti-NEDD8 siRNA and indicated plasmids and then stabilized 48 h. After incubation with MG132 (10 μM) for 8 h, cell lysates were immunoprecipitated using anti-PPARγ antibody and analyzed by western blotting analysis using indicated antibodies. Tubulin was used as a loading control (lower).

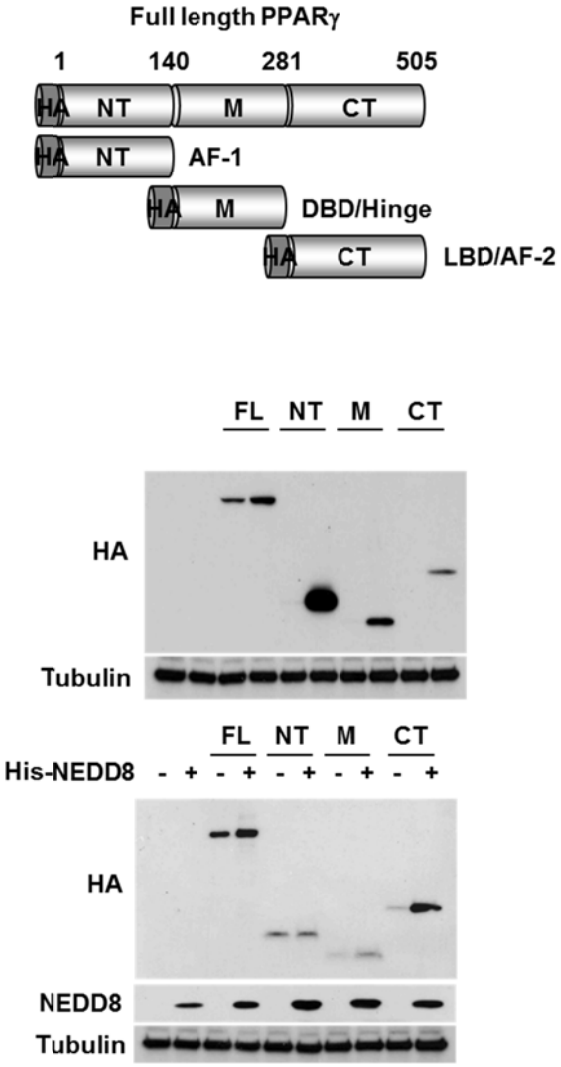
Full length PPARγ
1
140
281
505
HA
NT
M
CT
AF-1
DBD/Hinge
LBD/AF-2
FL
NT
M
CT
HA
Tubulin
His-NEDD8
NEDD8

Figure 14. PPARγ domains stabilize with NEDD8.

HEK293 cells were transfected with HA-PPARγ domains. After incubation with MG132 (10 μM) for 8 h, cell lysates were analyzed by western blotting analysis using anti-HA antibody. Tubulin was used as a loading control (upper). Ectopic PPARγ domains were stabilized by NEDD8. HA-PPARγ or PPARγ domains were co-transfected with His-NEDE8 into HEK293. After 48 h, cell lysates were analyzed by western blotting analysis using anti-HA and anti-NEDD8 antibodies. Tubulin was used as a loading control (lower).

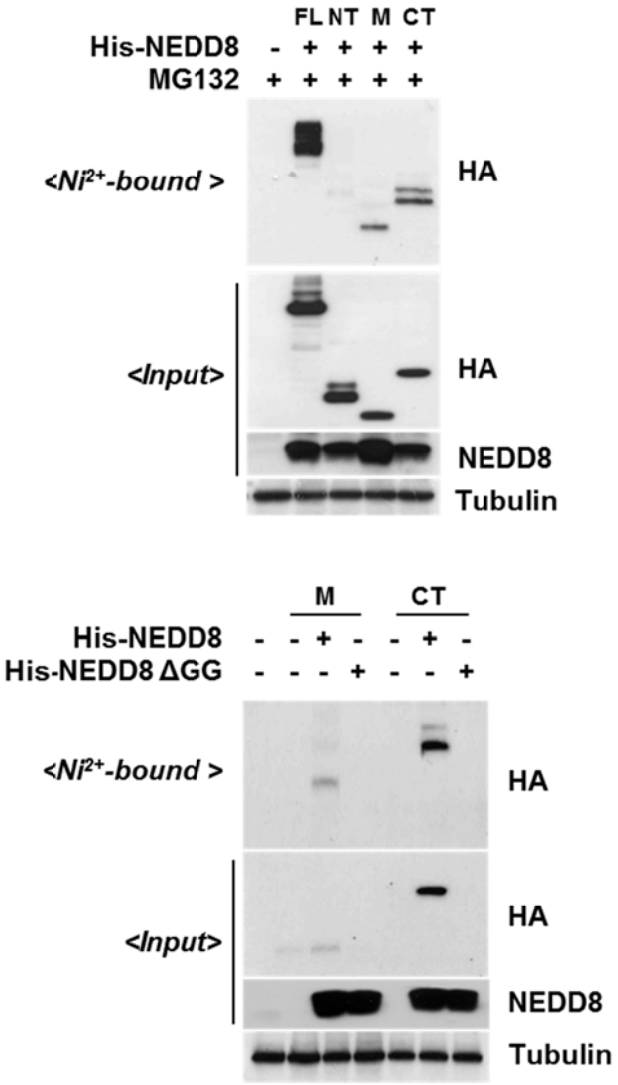
FL NT M CT
His-NEDD8 - + + + +
MG132 + + + + +
<Ni2+-bound >
HA
<Input>
HA
NEDD8
Tubulin
M CT
His-NEDD8 - - + - - + -
His-NEDD8 ΔGG - - - + - - +
<Ni2+-bound >
HA
<Input>
HA
NEDD8
Tubulin

Figure 15. Identification of the NEDDylated domains of PPARγ.

HEK293 cells were co-transfected with HA-PPARγ domains and His-NEDD8. PPARγ FL: full length (aa 1-505), NT: N-terminus (aa 1-140), M: middle (aa 141-281) and CT: C terminus (aa 281-505). After 48 h, 10 μM MG132 was treated with 8 h. HEK293 cells were lysed. His-NEDD8-conjugated proteins were bound to Ni^{2+}-NTA-agarose beads under denaturing conditions. His-NEDD8 conjugated PPAR-γ domains were isolated with Ni^{2+} affinity resin. Proteins were analyzed by western blotting using anti-HA and anti-NEDD8 antibodies. Tubulin was used as a loading control (upper). HA-PPARγ M and CT were co-transfected with His-NEDE8 or His-NEDD8ΔGG plasmids into HEK293 cells. After 48 h cells were lysed. His-NEDD8-conjugated proteins were bound to Ni^{2+}-NTA-agarose beads under denaturing conditions. His-NEDD8 conjugated PPARγ domains were isolated with Ni^{2+} affinity resin and eliminated by His-NEDD8ΔGG. Proteins were analyzed by western blotting using anti-HA and anti-NEDD8 antibodies. Tubulin was used as a loading control (lower).

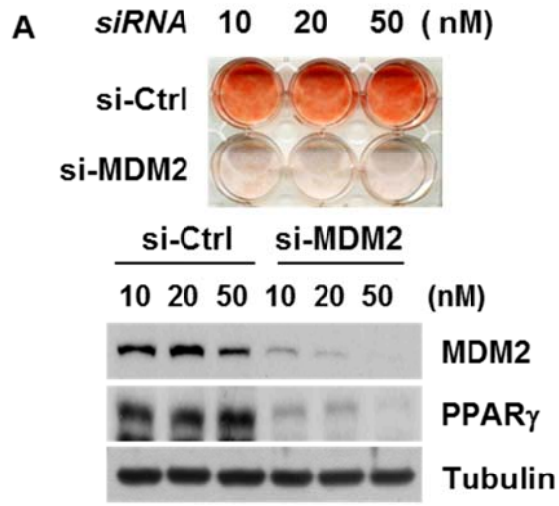
A
siRNA 10 20 50 (nM)
si-Ctrl
si-MDM2
si-Ctrl si-MDM2
10 20 50 10 20 50 (nM)
MDM2
PPARγ
Tubulin
B
Nutlin-3 - 10 20 (μM)
Nutlin-3 - 10 20 (μM)
MDM2
PPARγ
Tubulin

Figure 16. MDM2 is essential for the adipogenesis.

(A) Knockdown of MDM2 by si-Mdm2 blocked the adipogenesis and PPARγ expression. 3T3-L1 cells were transfected with control si-RNA or anti-MDM2 siRNA to 10, 20, 50 nM and then stimulated with DMI. After differentiation, cells were stained with Oil-red-O and cell lysates were analyzed by western blotting at 8 day using anti-MDM2 and anti-PPARγ antibodies. (B) 3T3-L1 cells were treated with nutlin-3 to 10, 20 μM for 48 h and then stimulated with DMI. After differentiation, Cells were stained with Oil-red O (upper) and cell lysates were analyzed by western blotting at 8 day using anti-MDM2 and anti-PPARγ antibodies. Tubulin was used as a loading control (lower).

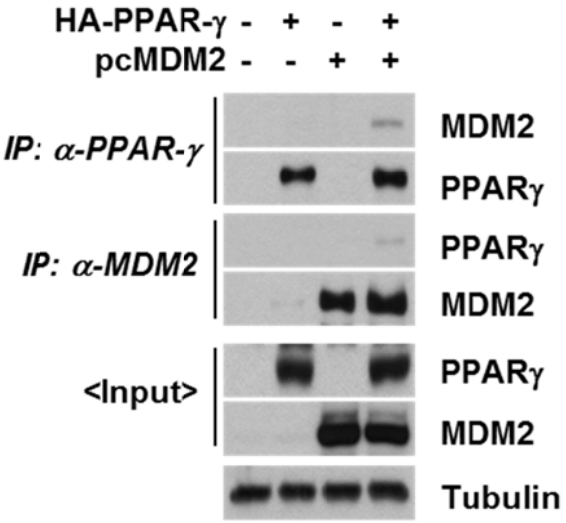

Figure 17. PPARγ physically interacts with MDM2.

HEK293 cells were co transfected with HA-PPARγ and pcMDM2. After stabilized 48 h, cell lysates were immunoprecipitated using anti-PPARγ antibody and analyzed by western blotting using indicated antibodies. Tubulin was used as a loading control.

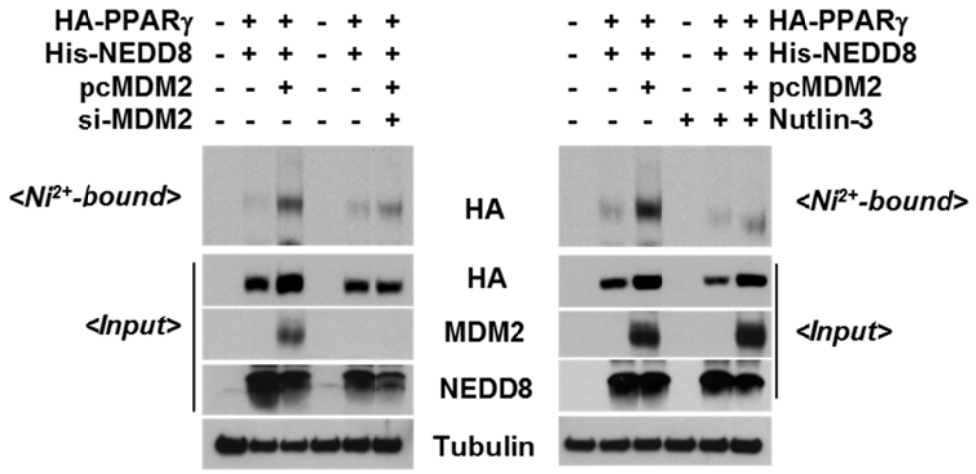

Figure 18. MDM2 is a specific E3 ligase for PPARγ NEDDylation.

Knockdown of MDM2 by si-MDM2 blocked PPARγ NEDDylation. HEK293 cells were co-transfected with indicated plasmids together with si-MDM2. After 48 h, cells were lysed in denaturing conditions. His-NEDD8 conjugated PPARγ was isolated with Ni^{2+} affinity resin. Proteins were analyzed by western blotting using anti-HA, anti-MDM2 and anti-NEDD8 antibodies. Tubulin was used as a loading control (left). Blocking of MDM2 by nutlin-3 diminished PPARγ NEDDylation. HEK293 cells were co-transfected with indicated plasmids. After 48 h, nutlin-3 treated to 20 μM for 8 h and then cells were lysed in denaturing conditions. His-NEDD8 conjugated PPARγ was isolated with Ni^{2+} affinity resin. Proteins were analyzed by western blotting using anti-HA, anti-MDM2 and anti-NEDD8 antibodies (right). Tubulin was used as a loading control.

<3T3-L1>

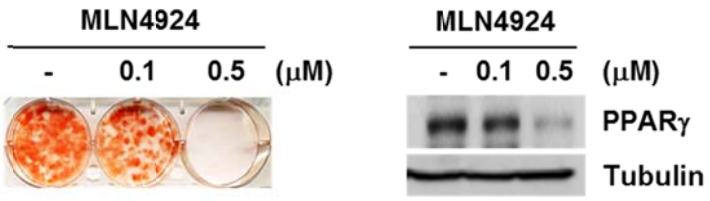

<H-ADSCs>

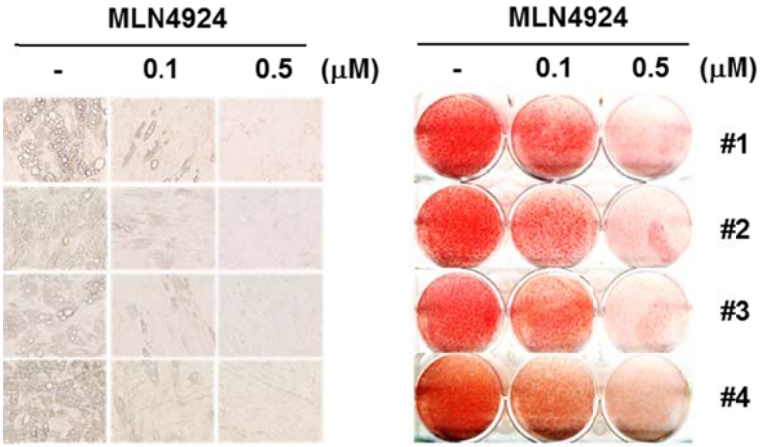

x400

<H-ADSCs#1>

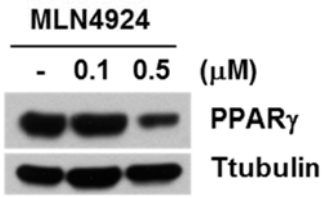

Figure 19. MLN4924, an E1 inhibitor of NEDDylation, inhibits adipogenesis in 3T3-L1 cells and H-ADSCs.

3T3-L1 cells were pre-incubated with MLN4924 (0.1 and 0.5 μM) for 2 days and then stimulated with DMI. After adipogenesis cells were stained with Oil-red-O at day 8 (upper). Cell lysates were analyzed by western blotting using anti-PPARγ antibody (lower). Tubulin was used as a loading control. H-ADSCs from four donors were pre-incubated with MLN4924 (0.1 and 0.5 μM) for 2 days and then stimulated with DMI+indomethacin (200 μM). After adipogenesis cells were stained with Oil-red-O at day 21 (upper). Cell lysates were analyzed by western blotting using anti-PPARγ antibody (lower). Tubulin was used as a loading control.

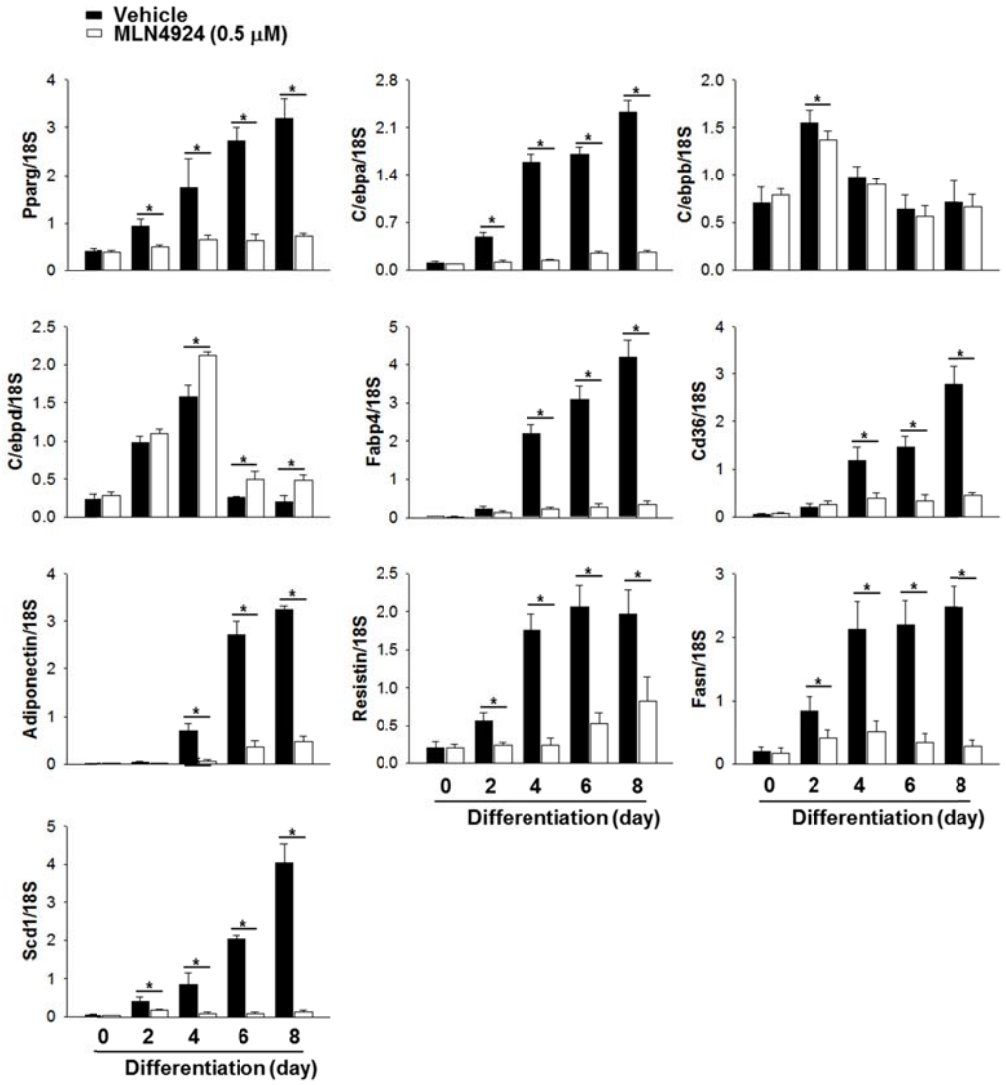
Vehicle
MLN4924 (0.5 μM)
Pparg/18S
C/ebpa/18S
C/ebpb/18S
C/ebpd/18S
Fabp4/18S
Cd36/18S
Adiponectin/18S
Resistin/18S
Fasn/18S
Scd1/18S
0 2 4 6 8
Differentiation (day)

Figure 20. MLN4924 down-regulates the expression level of adipogenic genes during adipogenesis.

3T3-L1 cells were pre incubated with MLN4924 to 0.5 μM at 2 days before differentiation and then stimulated with DMI for the indicated lengths of time. After differentiation total RNAs were prepared from cells and RT-qPCR was applied to measure the expression levels of pparg, c/ebpa, c/ebpb, c/ebpd, fabp4, resistin, adiponectin, fasn, cd36 and scd1. Results were quantified as the relative levels versus 18S RNA level. Data shown represent the mean±SD (n=3) and * denotes $p < 0.05$.

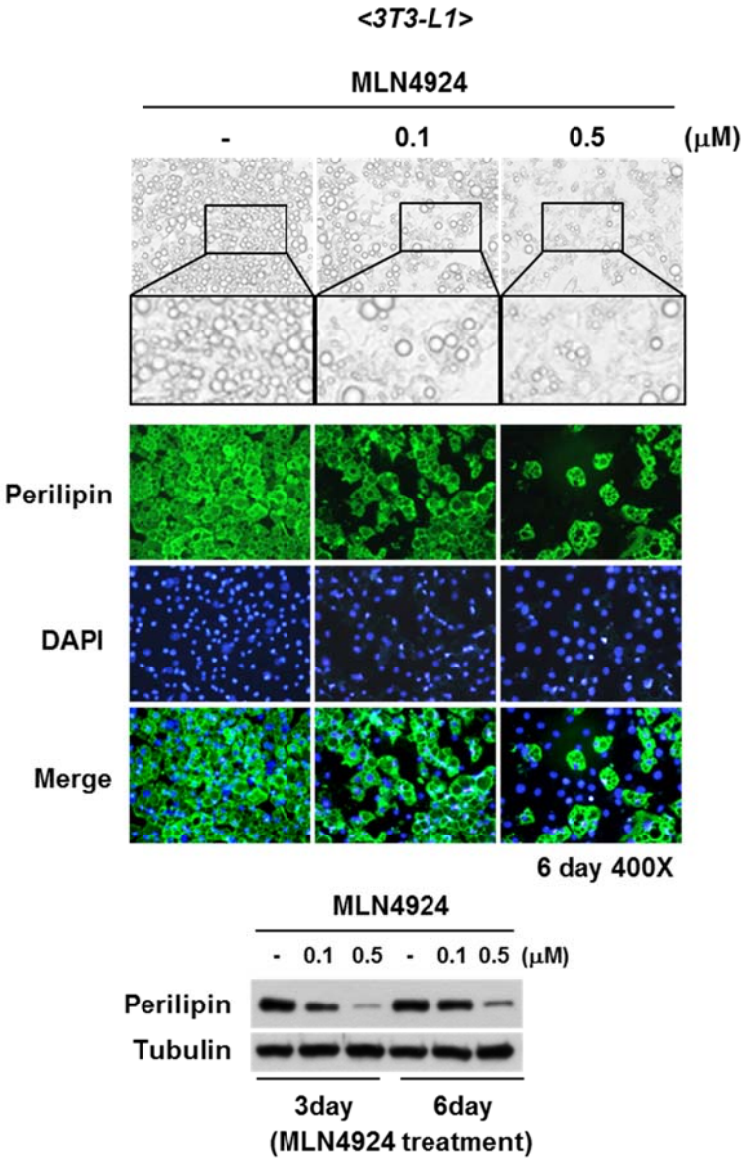
<3T3-L1>
MLN4924
-
0.1
0.5
(μM)
Perilipin
DAPI
Merge
6 day 400X
MLN4924
- 0.1 0.5 - 0.1 0.5 (μM)
Perilipin
Tubulin
3day
6day
(MLN4924 treatment)

Figure 21. MLN4924 reduces lipid accumulation in 3T3-L1.

3T3-L1 cells were differentiated with DMI and then treated with MLN4924 (0.1 and 0.5 μM) at 3 day and 6 day. After 20 day, cells were subjected to immunofluorescence analysis with anti-perilipin antibody and cell lysates were determined by western blotting analysis. Nuclei were stained with DAPI. Tubulin was used as a loading control.

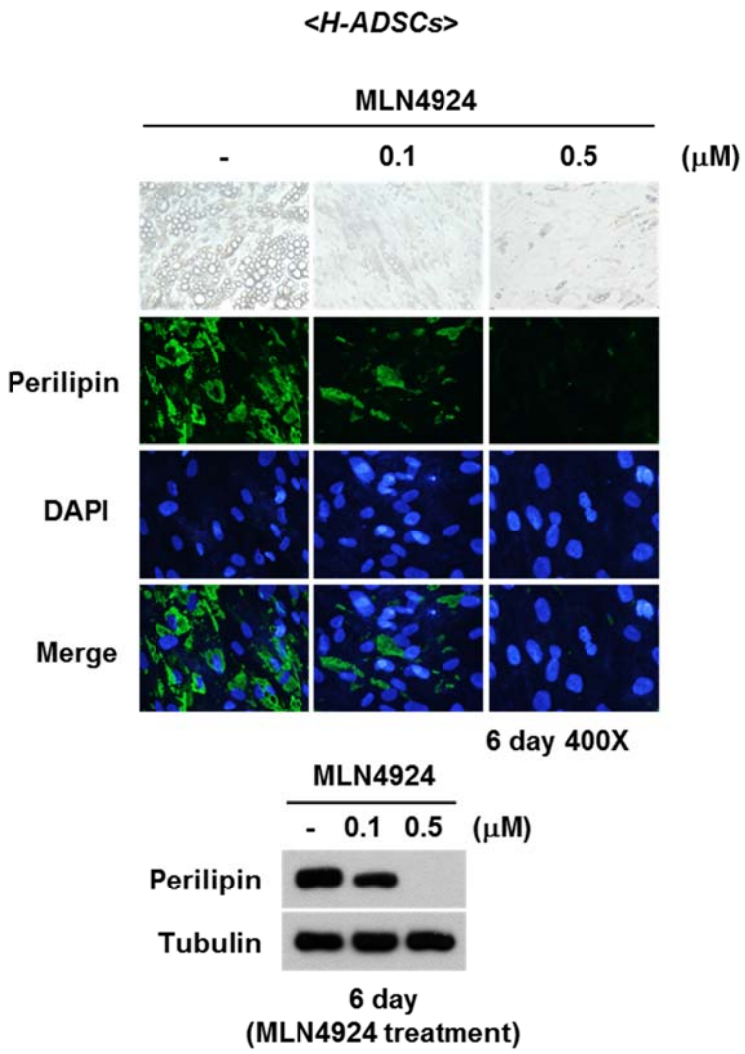
<H-ADSCs>
MLN4924
-
0.1
0.5
(μM)
Perilipin
DAPI
Merge
6 day 400X
MLN4924
- 0.1 0.5 (μM)
Perilipin
Tubulin
6 day
(MLN4924 treatment)

Figure 22. MLN4924 inhibits fat accumulation in H-ADSCs.

H-ADSCs were differentiated with DMI+ indomethacin (200 μM) and then treated with 0.1 and 0.5 μM MLN4924 at 6 day. After 30 day, cells were subjected to immunofluorescence analysis with anti-perilipin antibody and cell lysates were determined by western blotting analysis. Nuclei were stained with DAPI. Tubulin was used as a loading control.

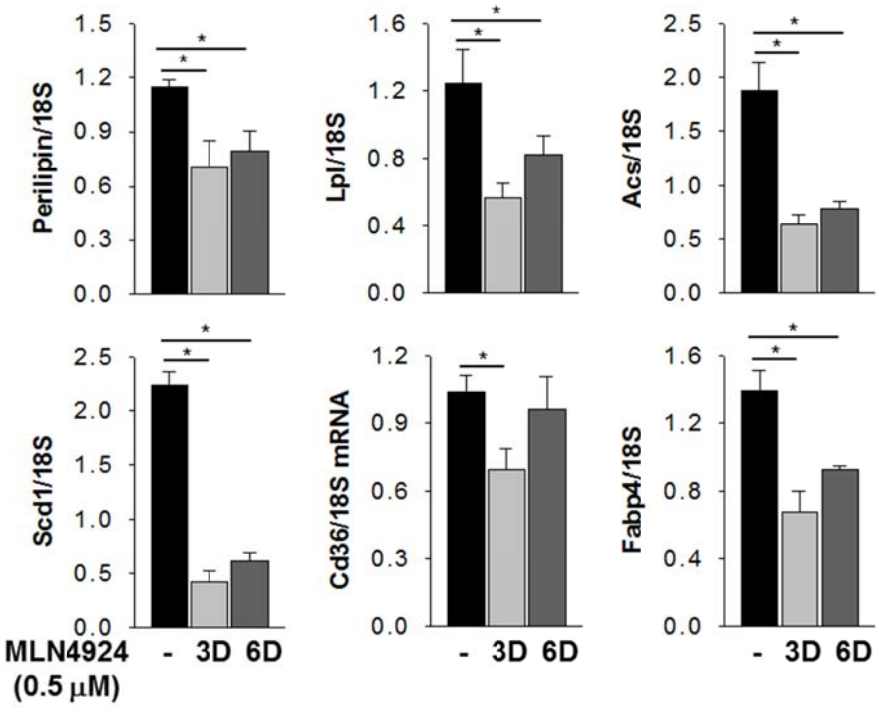
<3T3-L1>
Perilipin/18S
Lpl/18S
Acs/18S
Scd1/18S
Cd36/18S mRNA
Fabp4/18S
MLN4924 (0.5 μM)
- 3D 6D
- 3D 6D
- 3D 6D

Figure 23. Lipid metabolic genes are decreased by MLN4924 in 3T3-L1 cells.

3T3-L1 cells were differentiated with DMI and then treated with 0.5 μM MLN4924 at day 3 and 6. After 20 days, total RNAs were analyzed for genes involved in lipid metabolism. perilipin, lpl, acs, scd1, cd36 and fabp4 mRNA levels were quantified by RT-qPCR. Results were quantified as the relative levels versus 18S RNA level. Data shown represent the mean±SD (n=3) and * denotes $p < 0.05$.

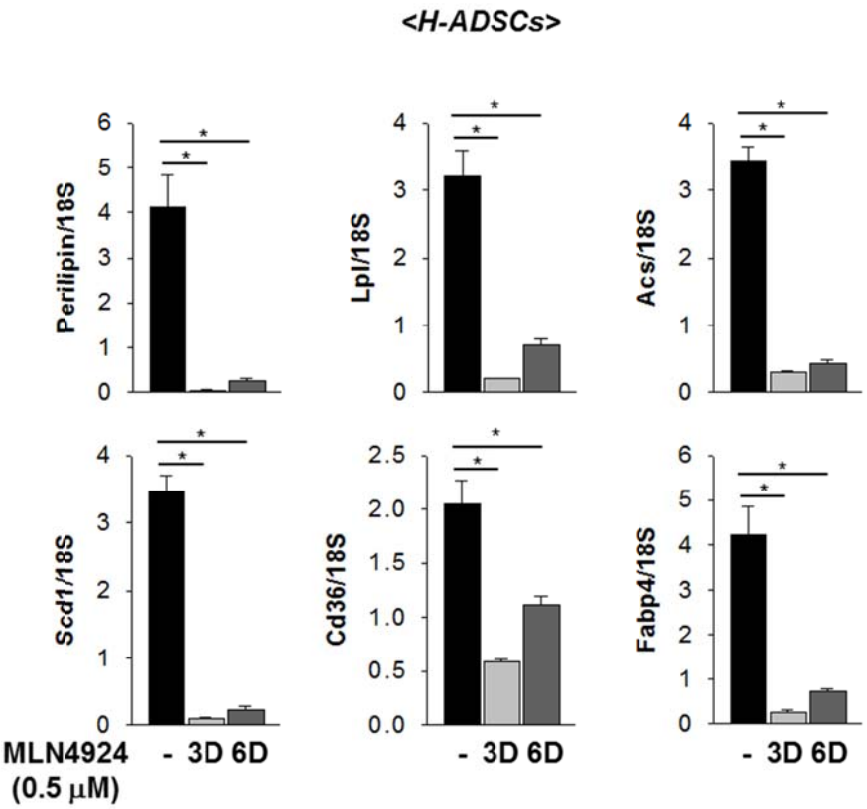
<H-ADSCs>
Perilipin/18S
Lpl/18S
Acs/18S
Scd1/18S
Cd36/18S
Fabp4/18S
MLN4924 - 3D 6D
(0.5 μM)
- 3D 6D
- 3D 6D

Figure 24. Lipid metabolic genes are decreased by MLN4924 in H-ADSCs.

H-ADSCs were differentiated with DMI+ indomethacin (200 μM) and then treated with MLN4924 (0.5 μM) at day 3 and 6. After 20 days, total RNAs were analyzed of lipid metabolic genes. perilipin, lpl, acs, scd1, cd36 and fabp4 mRNA levels were quantified by RT-qPCR. Results were quantified as the relative levels versus 18S RNA level. Data shown represent the mean±SD (n=3) and * denotes $p < 0.05$.

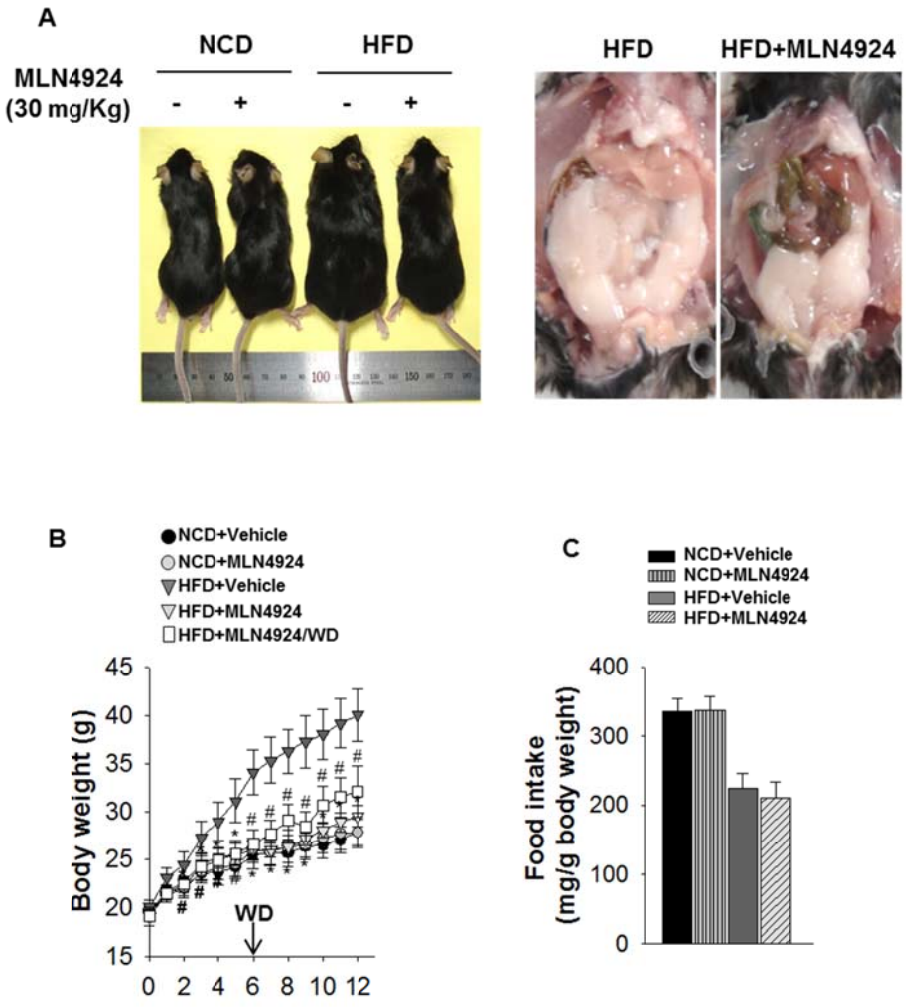
A
NCD
HFD
MLN4924
(30 mg/Kg)
- + - +
HFD
HFD+MLN4924
B
NCD+Vehicle
NCD+MLN4924
HFD+Vehicle
HFD+MLN4924
HFD+MLN4924/WD
Body weight (g)
WD
C
NCD+Vehicle
NCD+MLN4924
HFD+Vehicle
HFD+MLN4924
Food intake
(mg/g body weight)

Figure 25. MLN4924 prevents HFD-induced obesity in mice.

(A) Representative photographs of mice (left). Representative photographs of mice abdomen (right). (B) Weekly increases in the body weights of mice. Mice were divided into five groups: vehicle treatment in NCD-fed and HFD-fed mice, MLN4924 treatment (30 mg/Kg) in NCD-fed and HFD-fed mice and HFD with withdrawal of MLN4924 (30 mg/kg) after 6 wks treatment. (C) Weekly food intakes of mice. All data were presented as the mean±SD (n=8 per group) and * denotes $p < 0.05$ (HFD+vehicle vs HFD+MLN4924) and # denotes $p < 0.05$ (HFD+vehicle vs HFD+MLN4924 withdrawal)

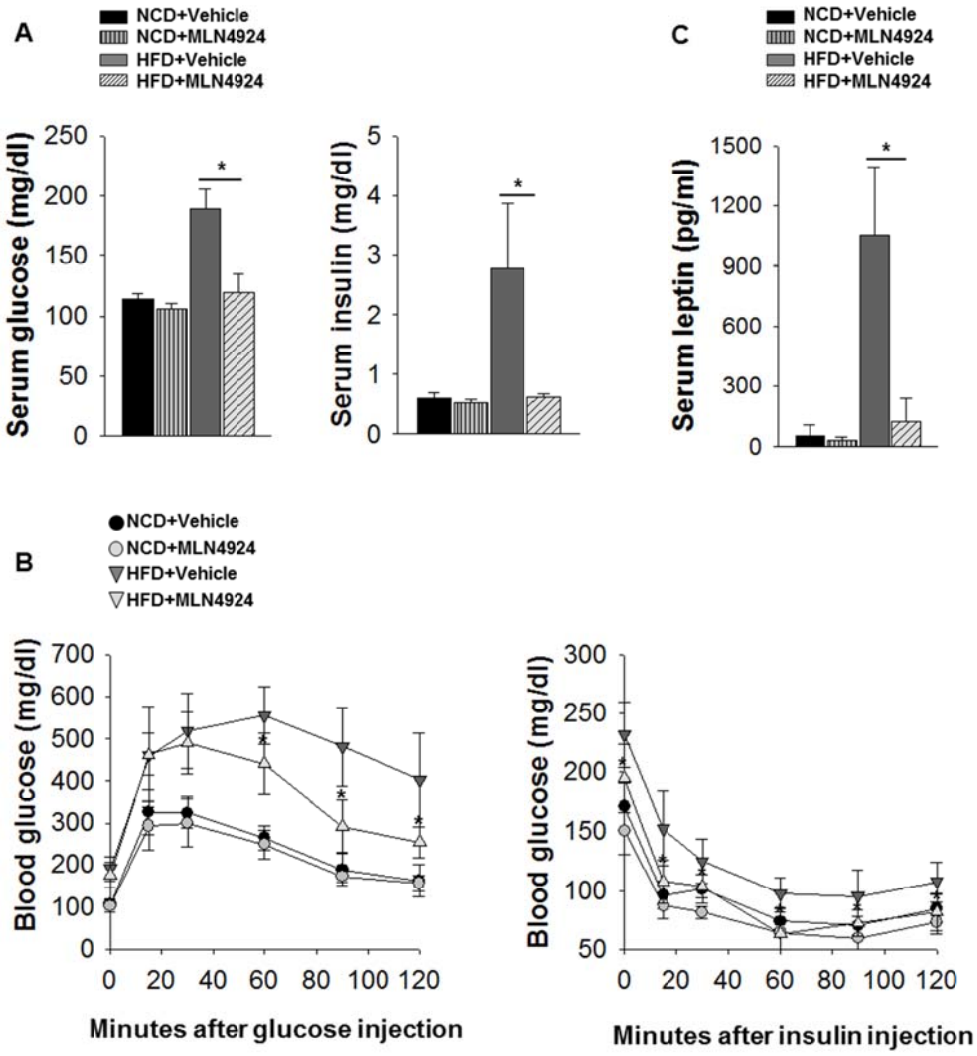
A
NCD+Vehicle
NCD+MLN4924
HFD+Vehicle
HFD+MLN4924
Serum glucose (mg/dl)
250
200
150
100
50
0
*
Serum insulin (mg/dl)
5
4
3
2
1
0
*
C
NCD+Vehicle
NCD+MLN4924
HFD+Vehicle
HFD+MLN4924
Serum leptin (pg/ml)
1500
1200
900
600
300
0
*
B
NCD+Vehicle
NCD+MLN4924
HFD+Vehicle
HFD+MLN4924
Blood glucose (mg/dl)
700
600
500
400
300
200
100
0
0 20 40 60 80 100 120
Minutes after glucose injection
Blood glucose (mg/dl)
300
250
200
150
100
50
0 20 40 60 80 100 120
Minutes after insulin injection

Figure 26. The effects of MLN4924 recover glucose, insulin homeostasis and physiological parameters.

(A) After 12 h fasting, insulin level was measured in serum. After 12 h fasting, glucose level was measured in serum (*n*=8 per group). (B) Glucose tolerance test (GTT) and insulin tolerance test (ITT) in mice (*n*=8 per group). Glucose was injected into intraperitoneal. Insulin tolerance test in mice (*n*=8 per group). Insulin was injected into intraperitoneal. (C) After 12 h fasting, leptin level was measured in serum (n=8 per group). All data were presented as the mean±SD (n=8 per group) and * denotes $p < 0.05$ (HFD+vehicle vs HFD+MLN4924).

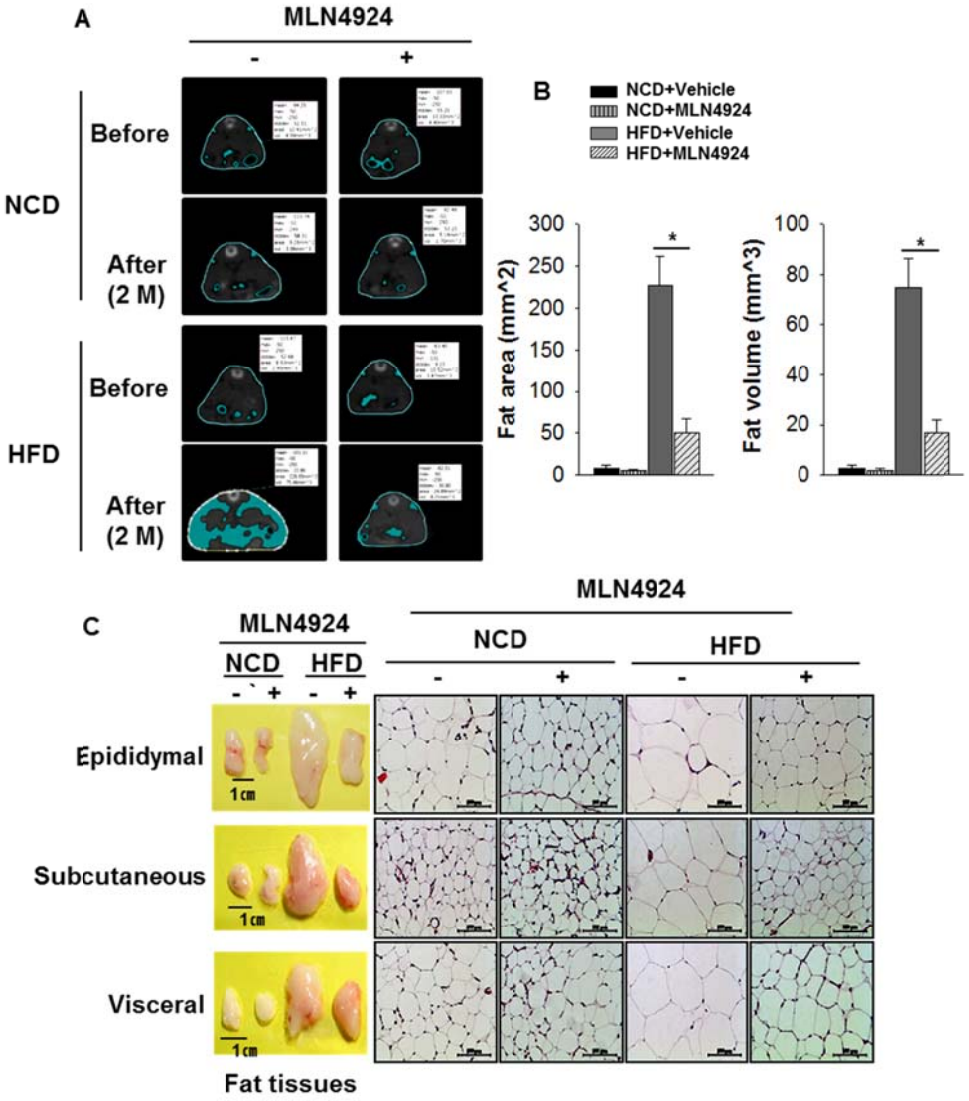
A
MLN4924
-
+
NCD
Before
After (2 M)
HFD
Before
After (2 M)
B
NCD+Vehicle
NCD+MLN4924
HFD+Vehicle
HFD+MLN4924
Fat area (mm^2)
300
250
200
150
100
50
0
*
Fat volume (mm^3)
100
80
60
40
20
0
*
C
MLN4924
NCD
HFD
- + - +
MLN4924
NCD
HFD
- + - +
Epididymal
Subcutaneous
Visceral
1 cm
Fat tissues

Figure 27. MLN4924 reduces fat size in HFD model.

(A) Representative CT image of mice abdomen. (B) Fat area and volume of mice. All data were presented as the mean±SD (n=8 per group) and * denotes $p < 0.05$ (HFD+vehicle vs HFD+MLN4924). (C) Representative photographs of mouse epididymal, subcutaneous, visceral fat (left). Representative H/E staining of mouse epididymal, subcutaneous, visceral fat (right).

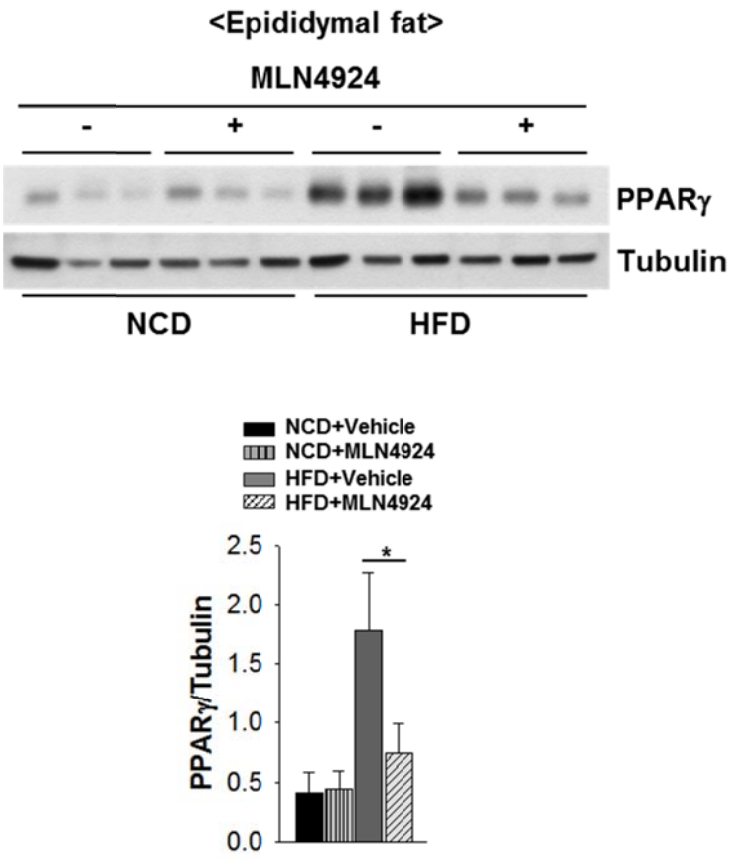

Figure 28. MLN4924 decreases PPARγ protein levels in HFD model.

In epididymal fat, protein expression of PPARγ was measured using 15 μg lysates from NCD-fed, NCD-fed+MLN4924, HFD and HFD-fed+MLN4924 and analyzed by western blotting. Tubulin was used as a loading control. Data shown represent the mean±SD (n=3 per group) and * denotes $p < 0.05$ (HFD+vehicle vs HFD+MLN4924).

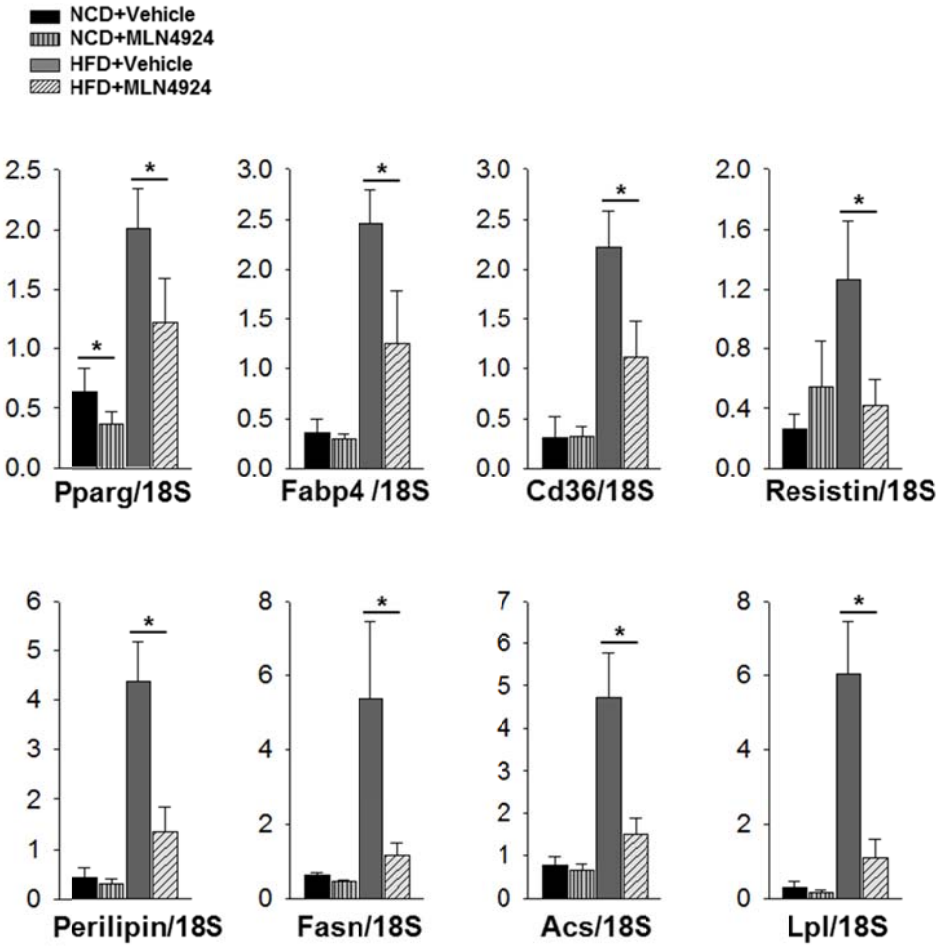

Figure 29. Lipid metabolism in HFD is recovered by MLN4924 treatment.

Total RNAs were prepared from WAT. pparg, fabp4, cd36, resistin, perilipin, fasn, acs and lpl, mRNA levels were quantified by RT-qPCR. Results were quantified as the relative levels versus 18S RNA level. All data were presented as the mean±SD (n=8 per group) and * denotes $p < 0.05$ (HFD+vehicle vs HFD+MLN4924).

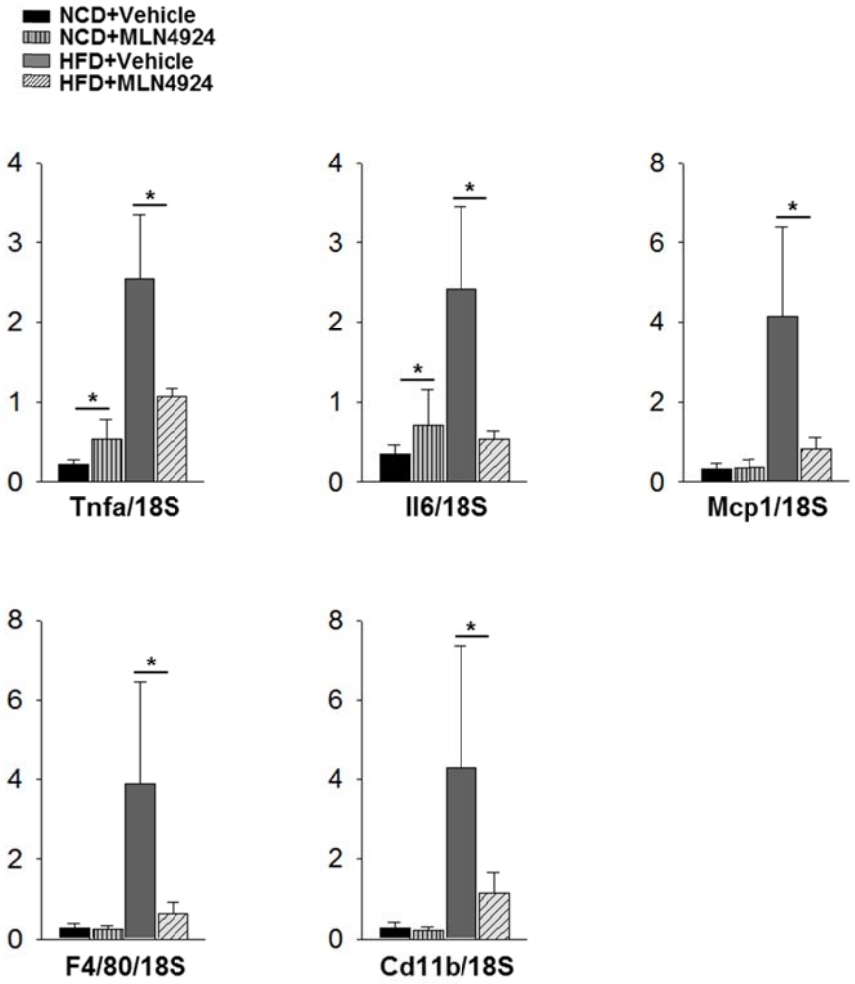

Figure 30. The expression of inflammatory cytokines in HFD is recovered by MLN4924 treatment.

Total RNAs were prepared from WAT. Tnfa, il6, mcp1, f4/80 and cd11b mRNA levels were quantified by RT-qPCR. Results were quantified as the relative levels versus 18S RNA level. All data were presented as the mean±SD (n=8 per group) and * denotes $p < 0.05$ (HFD+vehicle vs HFD+MLN4924).

DISCUSSION

Adipogenesis is controlled by a network of transcription factors that lead to the induction of the expression of the necessary adipogenic gene products for gaining the specialized function and morphology of adipocytes. The major question that motivates this study is: what is the role of NEDD8 in adipogenesis? In this study, I have demonstrated that NEDD8 plays an important role in adipogenesis and fat accumulation. PPARγ acts as a transcription factor in adipogenesis, and lipid sensor in metabolism. Endogenous NEDD8 turns out to be covalently conjugated to PPARγ during adipogenesis in 3T3-L1 cells (Fig 11). Prior studies have addressed that PPARγ is regulated by ubiquitination or SUMOylation, which is the down-regulating PPARγ activity or stability. NEDDylation has a crucial role in PPARγ stability, by interfering in its ubiquitination. Moreover, MDM2 is a specific E3 ligase that promotes PPARγ NEDDylation, and MLN4924, a NEDDylation E1 enzyme inhibitor was found to have a potential therapeutic effect on obesity by functioning as a negative regulator of adipogenesis and fat accumulation in both 3T3-L1 cells and H-ADSCs. Based on these results, I suggest that the NEDDylation of PPARγ plays an important role in adipogenesis and fat accumulation.

The molecular mechanism that governs increasing the number of fat cells (hyperplasia) in obesity is unclear, and the function of NEDD8 during adipogenesis has not yet been elucidated, but that of SUMO and Ub have been uncovered for other adipogenic transcription factors such as C/EBPα, β, δ, and PPARγ. In this

study, we first reported that NEDD8 expression was up regulated during adipocyte differentiation (Fig 1). Similar to PPARγ, NEDD8 expression is also increased in the middle stage of adipogenesis. Further studies of the upstream signaling for NEDD8 regulation in adipogenesis remain to be done.

PPARγ was activated by various fatty acids, eicosanoids, and linoleic acid. In lipid metabolism, PPARγ regulates the expression of targets that participate in fatty acid release, transport, and storage such as lipoprotein lipase (LPL), fatty acid binding proteins (FABP4), and fatty acid transporters or cluster of differentiation 36 (CD36). PPARγ was shown to stimulate adipogenesis alone in mouse fibroblasts (Tontonoz et al., 1994). Previous studies have shown that C/EBPβ is capable of inducing PPARγ in Ppar-γ+/- MEFs, which leads to the activation of adipogenesis, involving C/EBPα expression, which follows exposure to a PPARγ ligand. Constantly, C/EBPβ was unable to induce C/EBPα expression or adipogenesis in Pparγ-/- MEFs. (Zuo et al., 2006). C/EBPβ and C/EBPδ stimulate PPARγ expression, and PPARγ activates C/EBPα expression. Helix-loop-helix (HLH) transcription factor SREBP-1c, another up regulatory factor of PPARγ, has been found to play an important role in stimulating adipogenesis using insulin-induced 3T3-L1 cells (Kim et al., 1998). In NEDD8-overexpressed 3T3-L1 cells, dexamethasone, a synthetic member of the glucocorticoids, accelerates adipocyte differentiation (Fig 3). NEDD8 probably participates in the regulation of hormone signaling, yet this remains to be clarified. Currently, the NEDD8 regulatory mechanism remains unknown in adipogenesis. The knockdown of NEDD8 in 3T3-L1 cells down

regulates PPARγ expression, and blocks several PPARγ downstream genes and adipogenic target genes in 3T3-L1 cells (Fig 6). Furthermore, mice that are implanted with NEDD8-stably-knockeddown 3T3-L1 and 3T3-F442A cells failed to form a fat pad (Fig 9, 10). Our ChIP data clearly shows that NEDD8 is a key modulator of PPARγ promoter binding capability. The NEDDylation of PPARγ dynamically changed the assembly of transcriptional regulatory chromatin structure, and enhanced expression of PPARγ by NEDD8 correlated with increased binding of PPARγ to downstream target promoters (Fig 8).

PPARγ proteins have a short half-life (t½=2 h), and were degraded by a poly-ubiquitination proteasome system (Kilroy et al., 2009). Paradoxically, PPARγ protein levels were sustained during adipogenesis, while the molecular mechanism by which PPARγ stability was maintained is still unclear. From previous studies, in adipocytes, ubiquitination or SUMOylation do not increase PPARγ protein levels. In addition, PPARγ targets the proteasome via ubiquitin-independent or dependent manners. The ligand-binding domain (LBD) occurred in the ubiquitin-dependent degradation of PPARγ (Gail et al., 2009). Interestingly, our data suggests that PPARγ NEDDylation dominantly occurred in LBD (Fig 15) and blocked ubiquitination (Fig 13). In this study, that the claim is made that PPARγ NEDDylation inhibits ubiquitination and stabilizes the protein. Another important finding of this study is that MDM2 mediates the NEDDylation of PPARγ (Figure 18). A RING finger-type E3 ligase MDM2 has been reported for which p53, the tumor suppressor protein, was NEDDylated by MDM2, leading to an increase in its

transactivation activity (Xirodamas et al., 2004). MDM2 has reported self-NEDDylation, which regulates its stability (Watson et al., 2010). TAp73 is also NEDDylated though MDM2, and suppresses its transactivity and reduces its cytoplasmic localization (Watson et al., 2006). In addition, the MDM2 gene was up regulated in 3T3-L1 cells (Berberich et al., 1999).

The current therapies for obesity are based on exercise, diet, surgery, and pharmacological drugs. The available anti-obesity drugs can be divided into two modes of action: Central actors (central nervous system: CNS) and peripheral actors (muscle, fat, kidneys, and gastrointestinal tract) (Schwartz et al., 2000). To reduce the appetite and induce a sensation of satiation, anti-obesity drugs may act on serotoninergic, noradrenergic, dopaminergic, cannabinoid, and hormone receptor mechanisms in the brain (Dietrich and Horvath, 2012). Anti-obesity drugs should also increase energy expenditure and fat oxidation via activating the catecholaminergic system in the CNS and peripheral tissues. Lipase inhibition in the gastrointestinal tract reduces fat absorption (Hainer and Hainerová, 2012). In the past, available pharmacological therapies have been thyroid hormones, dinitrophenol, and amphetamines. Thyroid hormones activate the basal metabolic rate (BMR) and induce energy expenditure, which may lead to side effects such as sleep problems and heart failure. Dinitrophenol, a well-known anti-obesity agent, is reported to cause rapid weight loss by increasing the energy expenditure. The biological process of dinitrophenol results in heat instead of APT, by uncoupling the oxidative phosphorylation in mitochondria. Overheating, sweating, and fatal

hyperthermia are attributable side effects (Harper 2001). Amphetamines decrease food intake and increase locomotors activity by releasing noradrenaline (NA) from the presynaptic vesicles in the lateral hypothalamus. Increasing NA leads to the stimulation of β2-adreneric receptors and inhibition of appetite (Valentino et al., 2010). Since the 1930s, amphetamines have been discarded as a treatment, due to the occurrence of cardiovascular diseases and their addictive properties. The next generation of obesity drugs includes Sibutramine, a noradrenalin and serotonin reuptake inhibitor utilized by the hepatic cytochome P450 system that affects both food intake and energy expenditure. Rimonabant, a cannabinoid 1(CB1) receptor antagonist that acts by blocking the CB1 receptor in the nervous system and inhibiting food intake (Colombo 1998). Orlistat, a gastric and pancreatic lipase inhibitor that blocks enzyme activity. Unfortunately, these drugs come with side effects. Sibutramine has cardiovascular side effects, and was withdrawn in 2010. Rimonabant lost tis approval in 2008, when an association with anxiety and depression was discovered. Orlistat may cause hypoglycemia, headaches, and respiratory infections. Recently, Qsymia and locaserin have been approved by the FDA, but they also have side effects. Lorcaserin, a serotonin 2C agonist, acts in the CNS and reduces food intake. It may cause headaches, dizziness, insomnia, and carcinogenesis. Qsymia, a noradrenalin releaser and phentermine/topiramate combination has side effects including increased dizziness, headaches, insomnia, and heart rate. The market for obesity drugs is potentially huge, but the drugs' safety levels do not allow the realization of the market. From the limitations of drug

responses, anti-obesity drug research requires a more effective approach and developing the new therapy target. Fundamentally, obesity drugs should be developed to reduce the fat size or fat cell numbers, and controlling these factors is crucial for obesity drugs. New therapeutic insights have been made into the molecular regulation of adipogenesis and the reduction of fat storage. PPARγ adipose knockout mice had reduced fat formation and were protected from HFD-induced obesity and insulin resistance in mice (Jones et al., 2005). Thiazolidinediones (TZDs) activated PPARγ, and led to altered adipocytes, skeletal muscle, and liver metabolism, by regulating insulin sensitivity (Way et al., 2001). However, few reports have described the PPARγ antagonist. Bisphenol A diglycidyl ether (BADGE) was reported as a PPARγ antagonist that negatively regulated PPARγ activity and adipogenesis in 3T3-L1 and 3T3-FF2A cells (Wright et al, 2000). Dimethyl a-(dimethoxyphophinyl)-p-chlorobenzyl phosphate (SR-202) blocks PPARγ transcriptional activity and improves insulin sensitivity in ob/ob mice (Rieusset et al., 2002). In the present study, MLN4924, a PPARγ NEDDylation inhibitor, is therapeutically beneficial for obesity and insulin sensitivity, MLN4924 has an effect on highly proliferating cancers in *in vivo* xenograft models (Soucy et al., 2009). Another study has verified that MLN4924 also affected acute myeloid leukemia (AML) by inducing apoptosis (Swords et al., 2010). MLN4924 also reduced the outgrowth of liver cancer cells both *in vivo* and *in vitro* via induced autophagy (Luo Z et al., 2012). Preclinical models of solid tumors and acute lymphoblastic leukemia xenografts were tested from the pediatric preclinical testing

program (Smith et al., 2012). Furthermore, searching for inhibitors of the ubiquitin-proteasome system (UPS) and ubiquitin-like proteins (UBLs) may control dynamic genes and be the key to novel disease therapies.

Visceral fat surrounds the internal organs and is associated with peripheral and hepatic insulin resistance (Cases and Barzilai, 2000). From the *in vivo* experiments, MLN4924 reduced subcutaneous, visceral, and epididymal fats in DIO mice (Figure 13). The abnormal accumulation of fatty acyl-CoA and triglycerides in muscles and the liver lead to insulin resistance by inhibiting insulin receptor signaling (liver: IRS-1 and muscle: IRS-2) (Kim et al., 2001; Yu et al., 2002). My findings support that MLN4924 can inhibit adipocyte differentiation and fat accumulation by decreasing the genes involved in adipogenesis and lipid metabolism *in vitro*. In the treatment of MLN4924 in DIO mice, abnormal fat accumulation is reduced and lipid metabolism is normalized by decreasing the expression of lipid metabolic genes. PPARγ can modulate both adipocyte function and endothelial cells by regulating inflammation and atherosclerosis (Marx et al., 1999). MLN4924 treatment in DIO mice can also recover glucose tolerance, insulin sensitivity, body weight, leptin level, and the expression of inflammatory cytokine genes.

In conclusion, taken together with these data, I suggest that NEDD8 is a novel posttranslational modification that can regulate the stability of PPARγ in adipogenic differentiation. MLN4924 recovered lipid metabolism via normalizing the glucose tolerance, insulin sensitivity, lipid metabolic target genes, and

inflammatory cytokine target genes in DIO mice. Based on these results, MLN4924 can be suggested as a therapeutic target for obesity.

REFERENCES

Berberich SJ, Litteral V, Mayo LD, Tabesh D, Morris D. Mdm-2 gene amplification in 3T3-L1 preadipocytes. Differentiation. 1999;64:205-212.

Bourlier V, Zakaroff-Girard A, Miranville A, De Barros S, Maumus M, Sengenes C, Galitzky J, Lafontan M, Karpe F, Frayn KN, Bouloumié A. Remodeling phenotype of human subcutaneous adipose tissue macrophages. Circulation. 2008;117:806-815.

Cao Z, Umek RM, McKnight SL. Regulated expression of thee C/EBP isoforms during adipose conversion of 3T3-L1 cells. Genes Dev. 1991;5:1538-1552.

Cases JA, Barzilai N. The regulation of body fat distribution and the modulation of insulin action. Int T Obes Relat Metrab Disord. 2000;24:S63-S66.

Chandra V, Huang P, Hamuro Y, Raghuram S, Wang Y, Burris TP, Rastinejad F. Structure of the intact PPAR-gamma-RXR- nuclear receptor complex on DNA. Nature. 2008;456:350–356.

Choi JH, Banks AS, Estall JL, Kajimura S, Boström P, Laznik D, Ruas JL, Chalmers MJ, Kamenecka TM., Blüher M. Griffin PR, Spiegelman BM. Anti-diabetic drugs inhibit obesity-linked phosphorylation of PPARγ by Cdk5. Nature. 2010;466: 451-456.

Colombo G, Agabio R, Diaz G, Lobina C, Reali R, Gessa GL. Appetite suppression and weight loss after the cannabinoid antagonist SR 141716. Life Sci. 1998;63:PL113-PL117.

Dietrich MO, Horvath TL. Limitations in anti-obesity drug development: the critical role of hunger-promoting neurons. Nat Rev Drug Discov. 2012 ;11:675-691

Dixon, A.K. Abdominal fat assessed by computed tomography: sex difference in distribution. Clin. Radiol. 1983;34:189-191.

Drolet R, Richard C, Sniderman AD, Mailloux J, Fortier M, Huot C, Rhéaume C, Tchernof A. Hypertrophy and hyperplasia of abdominal adipose tissues in women. Int J Obes (Lond). 2008;32:283–291.

Fabbrini E, Sullivan S, Klein S. Obesity and nonalcoholic fatty liver disease: biochemical, metabolic, and clinical implications. Hepatology. 2010;51:679-689

Gail E. Kilroy, Xiaoying Zhan, Elizabeth Floyd. PPAR-g AF-2 domain functions as a cmponent of a Ubuiquitin-dependent degradation signal. Obesity. 2009;17:665-673.

Gao F, Cheng J, Shi T, Yeh ET. NEDDylation of a breast cancer-associated protein recruits a class III histone deacetylase that represses NFkappaB-dependent transcription. Nat Cell Biol. 2006;8:1171-1177.

Grimaldi B, Bellet MM., Katada S, Astarita G, Hirayama J, Amin RH, Grannema JG, Piomelli D, Leff T, Sassone-Corsi P. PER2 controls lipid metabolism by direct regulation of PPARg. Cell Metab. 2010;12:509-520.

Hainer V, Hainerová IA. Do we need anti-obesity drugs? Diabetes Metab Res Rev. 2012;28:Suppl 2:8-20.

Hallenborg P, Feddersen S, Francoz S, Murano I, Sundekilde U, Petersen RK, Akimov V, Olson MV, Lozano G, Cinti S, Gjertsen BT, Madsen L, Marine JC, Blagoev B, Kristiansen K. Mdm2 controls CREB-dependent transactivation and initiation of adipocyte differentiation. Cell death and diffrentiation. 2012;19:1381–1389.

Harper JA, Dickinson K, Brand MD. Mitochondrial uncoupling as a target for drug development for the treatment of obesity. Obes Rev. 2001; 2:255-265.

Henegar C, Tordjman J, Achard V, Lacasa D, Cremer I, Guerre-Millo M, Poitou C, Basdevant A, Stich V, Viguerie N, Langin D, Bedossa P, Zucker JD, Clement K. Adipose tissue transcriptomic signature highlights the pathological relevance of extracellular matrix in human obesity. Genome Biol. 2008;9:R14.

Hirsch J, Batchelor B. Adipose tissue cellularity in human obesity. Clin Endocrinol Metab. 1976;5:299-311.

Hofbauer KG, Nicholson JR. Pharmacotherapy of obesity. Exp Clin Endocrinol Diabetes 2006;114:475–484

Jaffray, E.G., and Hay, R.T. Detection of modification by ubiquitin-like proteins. Methods. 2006;38:35-38.

Jones JR, Barrick C, Kim KA, Lindner J, Blondeau B, Fujimoto Y, Shiota M, Kesterson RA, Kahn BB, Magnuson MA. Deletion of PPARgamma in adipose

tissues of mice protects against high fat diet-induced obesity and insulin resistance. Proc Natl Acad Sci U S A. 2005;102:6207-6212.

Kahn SE, Hull RL, Utzschneider KM. Mechanisms linking obesity to insulin resistance and type 2 diabetes. Nature. 2006;444:840-846.

Kilroy GE, Zhang X, Floyd ZE. PPAR-gamma AF-2 domain functions as a component of a ubiquitin-dependent degradation signal. Obesity. 2009;17:665-673.

Kim JB, Sarraf P, Wright M, Yao KM, Mueller E, Solanes G, Lowell BB, Spiegelman BM. Nutritional and insulin regulation of fatty acid synthetase and leptin gene expression though ADD1/SREBP1. J. Clin.Invest. 1998;101:1–9.

Kim JK, Fillmore JJ, Chen Y, Yu C, Moore IK, Pypaert M, Lutz EP, Kako Y, Velez-Carrasco W, Goldberg IJ, Breslow JL, Shulman GI. Tissue-specific overexpression of lipoprotein lipase causes tissue-specific insulin resistance. Proc. Natl. Acad. Sci. USA. 2001;98:7522-7527.

Lee HW, Nam SK, Choi WJ, Kim HO, Jeong LS. Stereoselective synthesis of MLN4924, an inhibitor of NEDD8-activating enzyme. J Org Chem. 2011;76:3557-3361.

LeRoith D, Novosyadlyy R, Gallagher EJ, Lann D, Vijayakumar A, Yakar S. Obesity and type 2 diabetes are associated with an increased risk of developing cancer and a worse prognosis; epidemiological and mechanistic evidence. Exp Clin Endocrinol Diabetes. 2008;116:S4-6.

Lowell BB. PPARgamma: an essential regulator of adipogenesis and modulator of fat cell function. Cell. 1999;99:239-242.

Luo Z, Yu G, Lee HW, Li L, Wang L, Yang D, Pan Y, Ding C, Qian J, Wu L, Chu Y, Yi J, Wang X, Sun Y, Jeong LS, Liu J, Jia L. The NEDD8-activationg enzyme inhibitor MLN4924 induces autophagy and apoptosis to suppress liver cancer cell growth. Cancer res. 2012;72:3360-3371.

Mandrup S, Loftus TM, MacDougald OA, Kuhajda FP, Lane MD. Obese gene expression at in vivo levels by fat pads derived from s.c. implanted 3T3-F442A preadipocytes. Proc Natl Acad Sci U S A. 1997;94:4300-4305.

Marx N, Brourcier T, Sukhova GK, Libby P, Plutzky J. PPARgamma activation in human endothelial cells increases plasminogen activator inhibitor type 1 expression: PPAR gamma as a potential mediator in vascular disease. Arterioscler Thomb Vasc Biol. 1999;19:546-551.

Nadler ST, Stoeh JP, Schueler KL, Tanimoto G, Yandell BS, Attie AD. The expression of adipogenic genes is decreased in obesity and diabetes mellitus. Proc Natl Acad Sci U S A. 2000;97:11371-11376.

Ohshima T, Koga H, Shimotohno K. Transcriptional activity of peroxisome proliferator-activated receptor gamma is modulated by SUMO-1 modification. J Biol Chem. 2004;279:29551-29557.

Ouchi N, Parker JL, Lugus JJ, Walsh K. Adipokines in inflammation and metabolic disease. Nat Rev Immunol. 2011;11:85-97

Rabut G, Peter M. Function and regulation of protein neddylation. 'Protein modifications: beyond the usual suspects' review series. EMBO Rep. 2008;9:969-976.

Rieusset J, Touri F, Michalik L, Escher P, Desvergne B, Niesor E, Wahli W. A new selective peroxisome proliferator-activated receptor-g antagonist with antiobesity and antidiabetic acitivity. Mol Endocrinol. 2002;11:2628-2644 .

Rosen ED, MacDougald OA. Adipocyte differentiation from the inside out. Nat. Rev. Mol. Cell Biol. 2006;7:885-896.

Rosen ED, Spiegelman BM. Molecular regulation of adipogenesis. Annu Rev Cell Dev Biol. 2000;16:145-171.

Russell RC, Ohh M. NEDD8 acts as a 'molecular switch' defining the functional selectivity of VHL. EMBO Rep. 2008;9:486-491.

Ryu JH, Li SH, Park HS, Park JW, Lee B, Chun YS. Hypoxia-inducible factor α subunit stabilization by NEDD8 conjugation is reactive oxygen species-dependent. J Biol Chem. 2011;28:6963-6970.

Salans LB, Horton ES, Sims EA. Experimental obesity in man: cellular character of the adipose tissue. J Clin Invest. 1971;50:1005-1011.

Schwartz MW, Woods SC, Porte D Jr, Seeley RJ, Baskin DG. Central nervous system control of food intake. Nature. 2000;404:661-671.

Smith MA, Maris JM, Gorlick R, Kolb EA, Lock R, Carol H, Keir ST, Reynolds CP, Kang MH, Morton CL, Wu J, Smith PG, Yu J, Houghton PJ. Initial testing of the investigational NEDD8-activating enzyme inhibitor MLN4924MLN4924 by the pediatric preclinical testing program. Pediatr Blood Cancer. 2012;59:246-253.

Soucy TA, Smith PG, Milhollen MA, Berger AJ, Gavin JM, Adhikari S, Brownell JE, Burke KE, Cardin DP, Critchley S, Cullis CA, Doucette A, Garnsey JJ, Gaulin JL, Gershman RE, Lublinsky AR, McDonald A, Mizutani H, Narayanan U, Olhava EJ, Peluso S, Rezaei M, Sintchak MD, Talreja T, Thomas MP, Traore T, Vyskocil S, Weatherhead GS, Yu J, Zhang J, Dick LR, Claiborne CF, Rolfe M, Bolen JB, Langston SP. An inhibitor of NEDD8-activating enzyme as a new approach to treat cancer. Nature. 2009;458:732-736.

Spalding KL, Arner E, Westermark PO, Bernard S, Buchholz BA, Bergmann O, Blomqvist L, Hoffstedt J, Näslund E, Britton T, Concha H, Hassan M, Rydén M, Frisén J, Arner P. Dynamics of fat cell turnover in humans. Nature. 2008;453:783-787.

Steger DJ, Grant GR., Schupp M., Tomaru T, Lefterova MI, Schug J, Manduchi E, Stoeckert CJ, Lazar MA. Propagation of adipogenic signals though an epigenomic transition state. Genes Dev. 2010;24:1035-1044.

Stickle NH, Chung J, Klco JM, Hill RP, Kaelin WG Jr, Ohh M. pVHL modification by NEDD8 is required for fibronectin matrix assembly and suppression of tumor development. Mol Cell Biol. 2004 ;24:3251-3261.

Swords RT, Kelly KR, Smith PG, Garnsey JJ, Mahalingam D, Medina E, Oberheu K, Padmanabhan S, O'Dwyer M, Nawrocki ST, Giles FJ, Carew JS. Inhibition of NEDD8-activating enzyme: a novel approach for the treatment of acute myeloid leukemia. Blood. 2010;115:3796-3800.

Tontonoz P, Hu E, Spiegelman BM. Stimulation of adipogenesis in fibroblasts by PPARγ, a lipid-activated transcription factor. Cell. 1994;79:1147–1156.

Valentino MA, Lin JE, Waldman SA. Central and peripheral molecular targets for antiobesity pharmacotherapy. Clin Pharmacol Ther. 2010;87:652-662.

Van Gaal LF, Mertens IL, De Block CE.Mechanisms linking obesity with cardiovascular disease. Nature. 2006;7121:875-880.

Watson IR, Blanch A, Lin DC, Ohh M, Irwin MS. Mdm2-mediated NEDDylation of RAp73 regulates its transacivation function. J Biol Chem. 2006;281:34096-34103.

Watson IR, Li BK, Roche O, Blanch A, Ohh M, Irwin MS. Chemotherapy induces NEDP1-mediated destabilization of MDM2. Oncogene. 2010;29:297-304.

Way JM, Harrington WW, Brown KK, Gottschalk WK, Sundseth SS, Mansfield TA, Ramachandran RK, Willson TM, Kliewer SA. Comprehensive messenger

ribonucleic acid profiling reveals that peroxisome proliferator-activated receptor-g activation has coordinate effects on gene expression in multiple insulin sensitive tissue. Endocinology. 2001;6:763-774.

Wright HM, Clish CB, Mikami T, Hauser S, Yanagi K, Hiramatsu R, Serhan CN, Spiegelman BM. A synthetic antagonist for the peroxisome proliferator-activated receptor-g inhibits adipocyte differentiation. J Biol Chem. 2000;3:1873-1877.

Xirodimas DP, Saville MK, Bourdon JC, Hay RT, Lane DP. Mdm2-mediated NEDD8 conjugation of p53 inhibits its transcriptional activity. Cell. 2004;118:83-97.

Yamauchi T, Kamon J, Waki H, Murakami K, Motojima K, Komeda K, Ide T, Kubota N, Terauchi Y, Tobe K, Miki H, Tsuchida A, Akanuma Y, Nagai R, Kimura S, Kadowaki T. The mechanisms by which both heterozygous peroxisome proliferator-activated receptor gamma (PPARgamma) deficiency and PPARgamma agonist improve insulin resistance. J Biol Chem. 2001;276:41245-41254.

Yu C, Chen Y, Cline GW, Zhang D, Zong H, Wang Y, Bergeron R, Kim JK, Cushman SW, Cooney GJ, Atcheson B, White MF, Kraegen EW, Shulman GI. Mechanism by which fatty acids inhibit insulin acitivation of insulin receptor substrate-1 (IRS-1)- associated phosphatidylinositol 3-Kinase activity in muscle. J Biol. Chem. 2002;277:50230-50236.

Zuo Y, Qiang L, Farmer SR. Activation of C/EBPalpha expression by C/EBPbeta during adipogenesis requires a PPARgamma-associated repression of HDAC1 at the C/EBPalpha gene promoter. J. Biol. Chem. 2006;281:7960–7967.

국 문 초 록

비만은 과잉 섭취된 음식과 에너지 소비의 불균형에 의해 생기는 대사성 질환으로써 지방세포 수와 크기를 증가시켜 에너지 대사에 이상을 유발시킬 뿐만 아니라 다른 대사성 질환에 원인이 된다. 비만연구에 있어 지방세포의 분화 연구와 기능 연구는 필수적이다. 특히 분자 수준에서 가장 중요한 인자라고 알려진 PPARγ는 핵 수용체일 뿐만 아니라 전사인자로써 retinoid X receptor (RXR)와 heterodimer를 이루며 타깃 유전자의 promoter의 peroxisome proliferator hormone response elements (PPREs) 위치에 결합하여 타깃 유전자 발현을 유도한다고 알려져 있다. PPARγ의 주된 기능은 지방세포 분화를 유도하고 당과 지질 대사에 관여하며, 염증유발 인자를 조절한다고 알려져 있다. 본 연구에서는 PPARγ 안정화를 증가시키는 새로운 post-translation modification인 NEDDylation을 소개하고, 이는 PPARγ의 분해를 매개하는 ubiquitination을 억제 함으로써 PPARγ 안정화 시킨다. 또한 PPARγ의 NEDDylation을 매개하는 E3 ligase가 MDM2임을 밝히고 이 또한 지방세포 분화에 중요한 역할을 하고 있음을 연구하였다. 나아가 NEDDylation의 E1 효소의 inhibitor라고 알려진 MLN4924가 지방분화 억제 효과가 있을 뿐만 아니라, 지방축적을 감소시키며, 비만 쥐에서 몸무게와 지방 대사가 정상적으로 회복됨으로써 비만 치료제로의 효과가

있음을 확인하였다. 이러한 결과는 새로운 PPARγ의 NEDDylation을 통해 지방세포 기능이 조절 될 수 있으며, 지방세포 분화 자체를 조절함으로써 새로운 비만 치료 메커니즘을 제시하고자 한다.

주요어: 지방세포 분화, PPARγ, NEDDylation, MDM2, MLN4924, 비만

학번: 2010-30610

의학박사 학위논문

PPARγ와 NEDD8의 결합에 의한 지방세포 분화 조절기전의 연구 및 이를 표적으로 하는 새로운 비만 치료제의 발굴

Regulation of adipogenesis via NEDDylation of PPARγ and discovery of a novel anti-obesity agent to target this mechanism

2015년 2월

서울대학교 대학원

의과학과 의과학 전공

박 형 숙

PPARγ와 NEDD8의 결합에 의한 지방세포 분화 조절기전의 연구 및 이를 표적으로 하는 새로운 비만 치료제의 발굴

지도 교수 전 양 숙

이 논문을 의학박사 학위논문으로 제출함

2014 년 12 월

서울대학교 대학원

의과학과 의과학 전공

박 형 숙

박형숙의 의학박사 학위논문을 인준함

2014 년 12 월

위 원 장_____

부위원장_____

위 원_____

위 원_____

위 원_____

Regulation of adipogenesis via NEDDylation of PPARγ and discovery of a novel anti-obesity agent to target this mechanism

by

Hyoung Sook Park

A thesis submitted to the Department of Biomedical science in partial fulfillment of the requirements for the degree of Doctor of Philosophy in Biomedical science at Seoul National University College of Medicine

December, 2014

Approved by Thesis Committee:

Professor _____ Chairman

Professor _____ Vice Chairman

Professor _____

Professor _____

Professor _____

Abstract

Neural precursor cell expressed developmentally down-regulated 8 (NEDD8), an ubiquitin-like protein, regulates the activity, stability, and subcellular localization of target proteins. NEDD8 is covalently conjugated to lysine residues of substrates though E1-E2-E3 enzyme cascades, which is called NEDDylation. Here, I characterized the prominent role of NEDDylation for adipogenesis. The depletion of NEDD8 decreased the expression of adipogenic genes, thereby inhibiting adipogenic differentiation. In particular, the expression of peroxisome proliferator-activated receptor gamma (PPARγ), a master regulator of adipogenesis, was reduced by knocking down NEDD8, and was enhanced by over-expressing NEDD8 in 3T3-L1 cells. Moreover, PPARγ covalently conjugated with NEDD8 during adipogenesis, as shown by Ni^{2+} pull-down assay with His-NEDD8-overexpressed 3T3-L1 cells. In addition, the stability of PPARγ protein was sustained due to decreased ubiquitination during adipogenesis. Notably, mouse double minute 2 (MDM2) was found to be a specific E3 ligase of PPARγ NEDDylation. Based on these results, I tested whether a NEDD8-activating enzyme inhibitor, MLN4924, had an anti-obesity effect. The results showed that MLN4924 can inhibit both adipocyte differentiation and fat accumulation in both 3T3-L1 cells and human adipocyte-derived stem cells (H-ADSCs). Consistently, MLN4924 treatment in diet-induced-obesity (DIO) mice model diminished weight gain, accompanied with recovered lipid metabolism to a normal range. Furthermore, MLN4924 treatment in DIO mice recovered glucose tolerance, insulin sensitivity, body weight, leptin level, and the expression of inflammatory cytokine genes. Taken together, these results suggest

that NEDD8 leads to crucial post-translational modification to regulate the stability of PPARγ proteins in adipogenesis. Accordingly, I report that MLN4924 could be developed as a therapeutic agent for obesity.

Key words: adipocyte differentiation, PPARγ, NEDDylation, MDM2, MLN4924, obesity.

Student Number: 2010-30610

CONTENTS

Page

LIST OF FIGURES

LIST OF ABBREVIATIONS

NEDD8: Neural precursor cell-expressed developmentally down-regulated 8

PPARγ: Peroxisome proliferator-activated receptor gamma

C/EBPs: CCAAT/enhancer binding proteins

MDM2: Mouse double minute 2

LPL: Lipoprotein lipase

FABP4: Fatty acid binding protein 4

CD36: Cluster of differentiation 36

Fasn: Fatty acid synthase

PTM: Post-translational modifications

TZDs: Thiazolidinediones

NCD: Normal chow diet

HFD: High fat diet

DIO: Diet induced obesity

INTRODUCTION

Globally, obesity remains a serious unsolved medical problem, and is a critical contributor to type 2 diabetes mellitus, hypertension, hyperlipidemia (high triglycerides and low high-density lipoproteins), atherosclerosis, cardiovascular disease, cancer, and nonalcoholic fatty liver (Kahn et al., 2006; Hofbauer and Nicholson, 2006; Van Gaal et al., 2006; LeRoith et al., 2008; Fabbrini et Al., 2010). Obesity is also related with abnormal adipokine secretion, macrophage infiltration, and inflammatory cytokine secretion (Bourlier et al., 2008, Henegar et al., 2008). Previously, it was suggested that overfeeding increases adipocyte size, but creates no changes in cell number (Sanlans et al., 1971). However, hyperplasia is correlated strongly with obesity severity, and is most marked in severely obese individuals (Hirsch and Batchelor, 1976). Especially, increasing adipocyte number is an important cause of juvenile obesity, and an increased adipocyte number in the juvenile period persists throughout the lifetime. An increase in adipocyte number may contribute to obesity severity by prolonging periods of weight gain in adulthood. Recent studies have proposed that adipocyte turnover is very dynamic, and approximately 10% of fat cells are renewed annually at all adult ages (Spalding et al., 2008). Lipoaspirates of fat tissues contain a high proportion of mesenchymal stem cells (MSC), which can differentiate into adipocytes, which strongly supports that new fat cells constantly arise from undifferentiated progenitor cells or

preadipocytes, even in adults (Drolet et al., 2008). Therefore, adipogenesis is critical for maintaining adipocyte number in obesity, and high adipogenic potential could be an important therapeutic target for pharmacological intervention in obesity.

Adipocytes are derived from multipotent mesenchymal stem cells that have the ability to develop into adipocytes, chondrocytes, myocytes, and osteocytes. Adipogenesis and adipocyte differentiation are determined by the activation of transcriptional factors, including the nuclear hormone receptor family peroxisome proliferator-activated receptor gamma (PPARγ) and CCAAT/enhancer binding protein alpha, beta, and delta (C/EBPα, β, δ) (Cao et al., 1991). These transcription factors are highly expressed in WAT, and they regulate glucose, lipid metabolism, and adipokine secretion (Rosen and MacDougald, 2006). As a master regulator, PPARγ expressed in the middle stage of adipocyte differentiation is required for the terminal differentiation of preadipocytes toward adipocytes (Chandra et al., 2008). C/EBPβ requires binding C/EBPδ to promote the expression of PPARγ and C/EBPα (Steger et al., 2010). Indeed, PPARγ-deficient mice exhibit an increased expression of leptin, which is reduced in high fat diet–induced fatty liver, and were protected from adipocyte hypertrophy, obesity, and insulin resistance (Lowell, 1999; Yamauchi et al., 2001). Many reports have shown that adipogenic transcription factors play an important role in adipogenesis.

Post-translational modifications (PTM) of transcription factors can regulate protein stability, cellular localization, or function. Phosphorylations of PPARγ were

stimulated by UV, stress, cytokines, growth factor, and a high fat diet (HFD), and affect transcriptional activity. General transcription factor IIH phosphorylates PPARγ at Ser112, inhibits its recruitment of transcriptional coactivators, and stimulates its binding to the circadian regulator period homolog 2 (PER2), which reduces the binding of PPARγ to target gene promoters (Grimaldi et al., 2010). The phosphorylation of Ser273 via CDK5 decreases PPARγ target gene expression in adipocytes, but did not affect the regulation of adipocyte differentiation by PPARγ (Choi et al., 2010). Polypeptide modifiers such as ubiquitin and sumo also affect adipogenesis by regulating the function of adipogenic factors. PPARγ2 is also SUMOylated by PIAS or PIASx at Lys107, which negatively regulates PPARγ2's transcriptional activity (Ohshima et al., 2004). Interestingly, the relationship between polypeptide modifiers and obesity is supported by DNA microarray data. White adipose tissue from obese mice expressed ubiquitin less than that from lean control; conversely, NEDD8 expression is increased in fat tissues of obese mice (Nadler, et al., 2000). However, the reversal of the expression of these genes with adipocyte functions such as adipocyte differentiation and adipocyte fat storage was not clearly verified.

NEDD8 is ubiquitously expressed in mammalian tissues, and structurally similar to ubiquitin, NEDD8 is conjugated to substrates covalently though E1-E2-E3 enzyme cascades, which are called NEDDylation. Previously, our research group reported that hypoxia-inducible factor-1α (HIF-1α) stabilizes NEDD8 conjugation (Ryu et

al., 2011). NEDDylation regulates activity, stability, and localization of its substrates. For example, (1) NEDDylation of p53 inhibits its translation activity (Xirodimas et al., 2004). (2) NEDDylation of BCA3 promotes their interactions with SIRT1 and suppresses NF-κB-dependent transcription (Gao et al., 2006). (3) The NEDDylation of pVHL reduces its interaction with Cul2-containing complexes (Russell and Ohh, 2008). (4) The NEDDylation of pVHL leads to a proper fibronectin matrix assembly (Stickle et al., 2004). Yet, the physiological significance of NEDD8 as a posttranslational modifier remains to be elucidated in obesity.

In this study, I pursued the possibility that NEDDylation might play a role in regulating adipogenesis. To identify NEDDylated target proteins, proteomic approaches using over-expressed NEDD8 in 3T3-L1 cells were carried out to identify the substrates associated with adipogenesis. Intriguingly, PPARγ, a major transcriptional factor in adipogenesis, turned out to be a novel substrate of NEDDylation. Here, this study demonstrates that NEDDylation is essential for adipogenic differentiation, and PPARγ, one of the main transcriptional factors in adipogenesis, is stabilized by NEDDylation. Consistent with these observations, I propose that NEDDylation controls adipocyte differentiation and fat accumulation, and that NEDD8 is a new physiological regulator of PPARγ stability during adipogenesis. Furthermore, the results of this study implicate MLN4924 as a potential therapeutic target for obesity.

MATERIALS AND METHODS

Antibodies and Reagents

Antibodies against PPARγ (sc-7196, sc-1984), C/EBPα (sc-61), C/EBPβ (sc-150), C/EBPδ (sc-636), Tubulin (sc-9104), MDM2 (sc-965), SUMO (sc-9060) and Ub (sc-9133) were obtained from Santa Cruz Biotechnology (Santa Cruz, CA, USA). Antibodies against NEDD8 (2745) and perilipin (9349) were obtained from Cell signaling Technology (Beverly, MA, USA). Anti-HA was obtained from Roche (Basel, Switzerland). The antibody against APPBP1 (NBP1-92162) was obtained from NOVUS (St.Charles, MO, USA). Chemicals of 3-Isobutyl-1-methylxanthine: IBMX (I5879), dexamethasone (D4902), insulin (I1507), 1-(4-Chlorobenzoyl)-5-methoxy-2-methyl-3-indoleacetic acid: indomethacin (I7378), cycloheximide (C1988), HA-affinity bead (E6779), (D)-glucose (G7021), human insulin (I9278), Oil-red O (O0624) and EZview™RedAnti-HA AffinityGel (E6779) were obtained from Sigma-Aldrich (St. Louis, MO, USA). Nutlin-3 (10004372) was obtained from Cayman Chemical Company (Ann Arbor, MI, USA). MG132 (BML-PI102) was obtained from ENZO Life Sciences (Farmingdale, NY, USA). Ni-NTA Agarose beads were obtained from Qiagen (Hilden, Germany). MLN4924 was kindly gift from Lak Shin Jeong (Lee et al., 2011). Bovine serum, fetal bovine serum (FBS) and Dulbecco's modified eagle's medium (DMEM) were obtained from Thermo Fisher Scientific (Waltham, MA, USA).

Cell culture and adipocyte differentiation

HEK293 (human embryonic kidney, ATCC CRL-1573) was obtained from American Type Culture Collections (Manassas, VA, USA). 3T3-L1 and 3T3-F442A pre-adipocytes were kindly gift from Dr. Jae-Woo Kim (Yonsei University, Seoul, South Korea). Pre-adipocyte was maintained in DMEM supplemented with 10% bovine serum. Differentiation of 3T3-L1 cells were induced by the treatment of 1 μM dexamethasone, 500 μM IBMX, and 5 μg/ml insulin, which is designated DMI in DMEM supplemented with 10% FBS. Two days after starting differentiation cells were maintained in DMEM with 10% FBS and 1 μg/ml insulin up to 8 days with medium change every two day. Human adipose derived stem cells (H-ADSCs) were kindly gift from Dr. Seoung-Who Kim (Ulsan University, Seoul, South Korea). H-ADSCs were obtained from patients who provided informed consent, and the institutional review board of Asan Hospital (Seoul, Korea) approved the use of the clinical samples for this research (approve, #2012-0283). Human adipose tissue-derived stem cells (H-ADSCs) were isolated from 35–55 years old women undergoing liposuction and passage 3–5 cells were used in this study. The cells were isolated using ADSC markers under flow cytometry (BD Biosciences, Franklin Lakes, NJ). More than 95% of H-ADSCs were identified to express CD105, CD90, CD73, and HLA-abc. Adipocyte differentiation of H-ADSCs were induced with DMI and 200 μM indomethacin in α-MEM supplemented with 10% FBS. Cells were incubated in 5% CO_2 and 20% O_2 at 37°C.

Plasmid DNA, siRNA and transient transfection

The expression vectors for HA-tagged mouse PPARγ was kindly gift from Kyong-

Soo Park (Seoul National University, Seoul, South Korea). NEDD8 cDNA was obtained by reverse transcription-PCR was cloned into His_6-tagged pcDNA3. NEDD8-ΔGG mutant which is unable to conjugate target proteins was made by site-directed mutagenesis (Ryu et al., 2011). Ubiquitin, PPARγ-NT (1-140), PPAR γ-M (141-281) and PPAR γ-CT (282-505) amplified by PCR were constructed into HA-tagged pcDNA3 (Clontech Laboratories, Inc. Mountain View, CA, USA). pcMDM2 amplified by PCR was cloned into pcDNA (Clontech Laboratories). Myc-SENP8 amplified by PCR was constructed into Myc-tagged pcDNA (Clontech Laboratories). All siRNAs for each gene were synthesized from IDT Integrated DNA Technologies (Coralville, IA, USA) and were listed in Table1. Two different siRNAs were designed to target mouse NEDD8 and APPBP1. Plasmid and siRNA were transiently transfected into cells using Lipofectimine (Invitrogen, Carlsbad, CA, USA) according to the manufacturer's instructions.

Stable pre-adipocyte cell line

For stably knockdown to 3T3-L1 and 3T3-F442A cells, the shRNAs containing a hairpin loop were synthesized and inserted into pLKO.1-puro vector (Sigma-Aldrich). sh-NEDD8-I and -II, sh-APPBP1-I and -II, sh-Control were inserted into pLKO.1-puro vector and were listed in Table 2. Two different shRNAs were designed to target mouse NEDD8 and APPBP1. The viral vectors were co-transfected into HEK293 cells with pMD2-VSVG, pRSV-Rev and pMDLg/pRRE plasmids to make viral particles. To establish stable cell lines, lentiviruses were collected from the supernatant of HEK293 cells. 3T3-L1 or 3T3-F442A cells were

infected with viruses and then selected using puromycin (5 μg/ml). For generation of stable expression in 3T3-L1 cells, cDNA for His-NEDD8 and HA-PPARγ plasmids were subcloned into the lentiviral shuttle vector pLVX-IRES-puro (Clontech Laboratories). The viral vectors were co-transfected into HEK293 cells with pMD2-VSVG, pRSV-Rev and pMDLg/pRRE plasnids to make viral particles. To establish stable cell lines, lentiviruses were collected from the supernatant of HEK293 cells. 3T3-L1 cells were infected with viruses and then selected using puromycin (5 μg/ml).

RNA preparation and real-time PCR

Total RNAs were isolated from cultured cells or tissue using TRIzol (Invitrogen). For cDNA synthesis, we used Easy Script™ cDNA Synthesis Kit (Applied Biological Materials Inc, Richmond, BC, Canada). The cDNAs of pparg, c/ebpa, c/ebpb, c/ebpd, adiponectin, resistin, cd36, fabp4, scd1, perilipin, lpl, acs, fasn, nedd8, tnfa, il6, mcp1, f40/80, c11b, c11c, and 18S rRNA were amplified with EvaGreen qPCR master mix reagent (Applied Biological Materials) in StepOne™ Real-time PCR System (Applied Biosystems, BC, Foster City, CA, USA). The level of each cDNA was relatively quantified by being divided by the 18S rRNA level in the corresponding sample. The sequences of qPCR primers are listed in Table 3.

Adipogenesis induction and Oil-red O staining

3T3-L1 cells were grown to confluent and induced with adipogenesis media that include DMEM with 10% FBS, 1μM dexamethasone, 500 μM IBMX and 5 μg/ml

insulin (DMI). 3T3-F442A cells were grown to confluent and induced with adipogenesis media that include DMEM with 10% FBS and 5 μg/ml insulin. H-ADSCs were grown to confluent and induced with adipogenesis media that include αMEM with 10% FBS, 1 μM dexamethasone, 500 μM IBMX, 5 μg/ml insulin (DMI) and 0.2 μM indomethacin. Media were changed with DMEM or αMEM with 10% FBS and 5 μg/ml insulin after 2 days. After differentiation, cells were fixed in 0.5% formalin for 20 min at RT. Fixed cells were incubated 1h with 0.3% Oil-red O solution (Sigma-Aldrich) in 60% isopropanol.

Western blotting and immunoprecipitation analysis

Cell lysates in a 2 x SDS sample buffer were separated on SDS-polyacrylamide gels and transferred to Immobilon-P membranes (Millipore, Billerica, MA, USA). Membranes were blocked from nonspecific proteins with 5% skim milk in TTBS (Tris-buffered saline containing 0.1% Tween 20) for 30 min and incubated overnight with primary antibody diluted at 1:500 to 1:3000 in the blocking solution. The membranes were incubated with a horseradish peroxidase-conjugated secondary antibody for 1h with blocking solution and blots visualized using Pierce ECL Plus western blotting substrate kit. For immunoprecipitation assay, cells were lysed in 5 mM EDTA, 50 mM Tris-Cl, 100 mM NaCl, and 0.1% NP-40 buffer and freshly added protease inhibitor. Cell lysates (1 mg) were incubated with EZview™RedAnti-HA AffinityGel for 4 h at 4°C. Precipitates were eluted by 2 x SDS buffer and subjected to SDS-polyacrylamide gel electrophoresis, followed by western blotting analysis. 10 μg anti-PPARγ and anti-MDM2 antibody were

incubated with 1 mg protein for overnight at 4°C. After incubation, precipitates were bound with protein A/G-sepharose beads (GE Health care) for 4 h at 4°C. After beads washing, precipitates were eluted by 2 x SDS buffer and subjected to SDS-polyacrylamide gel electrophoresis, followed by western blotting analysis.

Identification of His_6-tagged NEDD8 conjugation

For NEDD8 conjugation, we modified protocol in Jaffray and Hay (2006, Methods). After transfection with His_6-tagged NEDD8 or NEDD8ΔGG plasmid, cells were divided into two dishes. One was lysed with 2 x SDS sample buffer and analyzed by western blotting to confirm the expression level of input proteins. The other was lysed by denaturing buffer (6 M guanidine hydrochloride, 0.1 M Na_2HPO_4/NaH_2PO_4, 0.01 M Tris-Cl (pH 8), 10 mM imidazole and 10 mM β-mercaptoethanol). The lysates were bound with Ni^{2+}-NTA-agarose bead (Qiagen) for 4 h at RT. The beads were washed for 5 min in each step with the washing solution: washing buffer 1 (pH 8: 8 M urea, 0.1 M Na_2HPO_4/NaH_2PO_4, 0.01 M Tris-Cl (pH 8), 20 mM imidazole and 10 mM β-mercaptoethanol), washing buffer 2 (pH 6.3: 8 M urea, 0.1 M Na_2HPO_4/NaH_2PO_4, 0.01 M Tris-Cl (pH 8), 20 mM imidazole and 10 mM β-mercaptoethanol) with 0.2% Triton-X100 and washing buffer 2 with 0.1% Triton-X100. Then, beads were eluted with 2 x SDS sample buffer and analyzed western blotting.

Enzymatic in-gel digestion

pLVX-IRES-His-NEDD8 expressed in 3T3-L1 stable cells were differentiated to

adipocytes. After 4 day adipocyte differentiation, cells were lysed. His-NEDD8-conjugated proteins were bound to Ni^{2+}-NTA-agarose beads under denaturing conditions and eluted with a SDS sample buffer and then the eluents were subjected to SDS-polyacrylamide gel electrophoresis. The SDS-polyacrylamide gel stained with PlusOne ™ Silver staining kit (GE Healthcare, Uppsala, Sweden) according to the manufacturer instructions. For in-gel digestion, the proteins separated by SDS-PAGE were excised from the gel and the gel pieces containing protein were destained with 50% acetonitrile (ACN) containing 50 mM NH_4HCO_3 and vortexed until CBB was completely removed. These gel pieces were then dehydrated in 100% acetonitrile and vacuum-dried for 20 min with speedVac. For the digestion, gel pieces were reduced using 10 mM DTT in 50 mM NH_4HCO_3 for 45 min at 56°C, followed by alkylation of cysteines with 55 mM iodoacetamide in 50 mM NH_4HCO_3 for 30 min in dark. Finally, each gel pieces were treated with 12.5 ng/μl sequencing grade modified trypsin (Promega, Madison, WI) in 50 mM NH_4HCO_3 buffer (pH 7.8) at 37°C for overnight. Following digestion, tryptic peptides were extracted with 5% formic acid in 50% ACN solution at RT for 20 min. The supernatants were collected and dried with SpeedVac. Re-suspended samples in 0.1% formic acid were purified and concentrated using C18 ZipTips (Millipore, MA) before MS analysis.

LC-MS/MS analysis

The tryptic peptides were loaded onto a fused silica microcapillary column (12 cm

x 75 μm) packed with C18 reversed phase resin (5 μm, 200 Å). LC separation was conducted under a linear gradient as follows: a 3-40% solvent B (ACN containing 0.1% formic acid) gradient (solvent A; DW containing 0.1% formic acid), with a flow rate of 250 nL/min, for 60 min. The column was directly connected to LTQ linear ion-trap mass spectrometer (Finnigan, CA) equipped with a nano-electrospray ion source. The electrospray voltage was set at 1.95 kV, and the threshold for switching from MS to MS/MS was 500. The normalized collision energy for MS/MS was 35% of main radio frequency amplitude (RF) and the duration of activation was 30 ms. All spectra were acquired in data-dependent scan mode. Each full MS scan was followed by five MS/MS scan corresponding from the most intense to the fifth intense peaks of full MS scan.

Database searching and validation

The acquired LC-ESI-MS/MS fragment spectrum was searched in the BioWorksBrowser™ (version Rev. 3.3.1 SP1, Thermo Fisher Scientific Inc., CA) with the SEQUEST search engines against National Center for Biotechnology Information (http://www.ncbi.nlm.nih.gov/) Mus musculus database. The searching conditions were trypsin enzyme specificity, a permissible level for two missed cleavages, peptide tolerance; ±2 amu, a mass error of ±1 amu on fragment ions and variable modifications of carbamidomethylation of cysteine (+57 Da) and oxidation of methionine (+16 Da) residues.

Chomatin Immunoprecipitation

Lysates from 1×10^7 cells were cross-linked with 1% formaldehyde for 10 min at RT, and glycine (final 125 mM) was added to quench the cross-linking reaction. Lysed cell extracts were subjected to sonication until the DNA fragments become less than 500 base pair. Chromatin complexes were precipitated with indicated antibodies overnight at 4°C. Protein G sepharose (Life technologies) beads were added and incubated 2 more hs. After washing with saline, DNA-protein complexes were eluted with 1% SDS and incubated overnight at 65°C to reverse crosslinking. The eluted DNAs were purified with Mega-quick spin DNA purification kit (Intron, Seoul, Korea). The precipitated DNAs were amplified and quantified on ABI StepOne^{TM} Real-Time PCR System using the Evagreen qPCR mastermix. PCR primer sequences used for ChIP are listed in Table 4.

Implantation of 3T3-L1 and 3T3-F442A preadipocytes and analysis of fat pads

All animals were maintained in compliance with the Guide for Experimental Animal Research from the Laboratory for Experimental Animal Research, Seoul National University Institutional Animal Care and Use Committee (SNUIACUC) (SNU-110718-1). 3T3-L1, 3T3-F442A cells were grown completely and infected with pLKO.1-puro-shControl and pLKO.1-puro-sh-NEDD8. Cells were trypsinized and suspended in DMEM with 10% bovine serum. 3×10^7 cells were injected into the subcutis of the abdomens of 9-wk-old BALB/c male nude mice (Orient Bio, Inc., Gyeonggi-Do, South Korea). After 5 wks, fat pads produced from the implanted

cells were fixed in formalin buffer and stained with hematoxylin and eosin (H&E) (Mandrup et al., 1997).

Immunofluorescence

Implanted fat fad was fixed in formalin solution and was cut into 4 μm slices. The fat slices were deparaffinized and hydrated, and then antigens were retrieved by in 10 mM sodium citrate buffer in a microwave for 20 min. After blocking, sections were incubated overnight with anti-perilipin (1:500). For visualizing specific protein, Alexa Fluor® 488 Goat Anti-Rabbit IgG (H+L) (Invitrogen) was used incubating sections and nucleus stained with DAPI (1:5000 in PBS, Sigma Aldrich).

Animals and animal care

Animal study was approved by the Seoul National University Animal Experiments Ethics Committee (SNU-130318-1-4). Mice were housed in pathogen free facility during 12 h light and 12 h dark cycle. We fed C57BL/6J mice (Central Lab. Animal Inc. Seoul Korea) HFD consisting of 60% of calories from fat (D12492 Research diets Inc. New Brunswick, NJ, USA) starting from 4 wks of age to 16 wks of age. MLN4924 30 mg/kg was injected intraperitoneally into mice once per 3 days. Daily food consumption and body weight provided food was measured every three day for singly housed mice. At the ends of MLN4924 treatments, blood was collected by eye and cardiac puncture. Fats and livers were rapidly excised and weighed and then frozen in liquid nitrogen. Samples were kept -80°C and portion of fats were fixed in 4% formalin for histology experiments.

Body composition

Computed tomography

128-slice multi-detector computed tomography multi-detector computed tomography (MDCT) was used (Ingenuity CT, Philips Healthcare, Cleveland, OH). The tube voltage was set at 120 kV with a constant 175 mA current. The slice-thickness was 0.7mm and the field of view (FOV) was set at 50×50 mm^2. Reconstruction in the axial, sagittal, and coronal planes was acquired for all CT scans.

Before CT scan, mice were anesthetized with a mixture of Zoletil (Virbac, Carros, France) (50 mg/kg) and xylazine (10 mg/kg) administered by intraperitoneal injection. They were placed prone in the appropriate holders. First, a scannogram of whole body was made to ensure proper placement in the holder and to set the scan area. Second, Whole-body scans of the entire mice were done. To avoid artificially including S leg fat in the abdominal area, mice' hind limbs were extended.

Measurement of intra-abdominal adipose tissue

Intra-abdominal adipose tissue *(IAAT)*

I selected the optimal single slice in which both renal hila were well observed around L3-L5. Cross-sectional abdominal contour was estimated by delineating the skin manually with a graph pen though the muscular structures and vertebral corpora. Hounsfield unit (HU) cut-off values of -250 to -50 were assigned for adipose tissue in the slice. The area between -250 HU and -50 HU pixels was

calculated automatically by the post-processing CT software (Rapidia 2.8, INFINITT, Seoul, Korea). IAAT inside the abdominal wall was measured. Abdominal fat was assessed by computed tomography (Dixon, 1983).

Blood chemistry analysis

Serum was isolated from the whole blood out of mice fasted for 12 h. The content of glucose in blood was measured by one touch glucometer Accu-Chek Active® system (Roche, Basel, Switzerland). The level of insulin and leptin was measured with ELISA kit (ALPCO Diagnostics, Salem, NH, USA) according to the manufacturer's instructions. The level of free fatty acid was quantified with the kit (Sigma-Aldrich, St. Louis, Missouri, USA) according to the manufacturer's instructions.

Glucose and insulin tolerance test

For glucose tolerance test (GTT), mouse was fasted for overnight and then intraperitoneally injected with D-glucose at a dose of 2 g per kg body weight. For insulin tolerance test (ITT), mouse was fasted 4 h and then intraperitoneally injected with insulin at a dose of 1 U per kg body weight. The level of glucose was measured at 0, 15, 30, 60, 90 and 120 min.

Statistical analysis

Mean and standard deviation (SD) were analyzed using Microsoft Excel software. Comparing two groups were determined statistical significance using Student's t

test P values < 0.05 were considered to be statistically significant.

Tables

Table 1. Targets and Nucleotide Sequences of siRNAs

Target Genes	GeneBank accession number	siRNA Sequences
hNEDD8	NM_006156.2	5’-CAGACAAGGUGGAGCGAAUCAAGGA-3’
mNEDD8-I	NM_008683.3	5’-UCCUUGAUUCGCUCCACCUUGUCUGUG-3’,
mNEDD8-II	NM_008683.3	5’-UUCACUUUAAUUAGCAUCUUCUUCCCA-3’
mAPPBP1-I	NM_144931.3	5’-GAGCAGAUUCCAAAGCUUCUUGUCCAU-3’
mAPPBP1-II	NM_144931.3	5’-AGGUAAAUUUCCUUGACCCUCCUUGGC-3’
hMDM2	NM_002392.5	5’-UUCCUGAAGCUCUUGUACAAGGUCCUU-3’
mMDM2	NM_010786.3	5’-GCAAUGAUCUACAGAAAUUUAGUGG-3’
Non-target		5’-UUGAGCAAUUCACGUUCAUTT-3’

Table 2. Targets and DNA Sequences for shRNAs

Target Genes	Sequences (5’ to 3’): Sense and Antisense strands
mNEDD8-I	Sense: CGGTTGATTCGCTCCACCTTGTCTCTCGAGAGACAAGGTGGAGCGAATCAATTTTT Antisence: ATTAAAAATTGATTCGCTCCACCTTGTCTCTCGAGAGACAAGGTGGAGCGAATCAA
mNEDD8-II	Sense: CCGGACTTTAATTAGCATCTTCTTCCTCGAGGAAGAAGATGCTAATTAAAGTTTTTT

	Antisence: ATTAAAAAACTTTAATTAGCATCTTCTTCCTCGAGGAAGAAGATGCTA ATTAAAGT
mAPPBP1-I	Sense: CGGCAGAATTCAAAGCTTCTTGTCCTCGAGGACAAGAAGCTTTGGAA TCTGTTTTT Antisence: ATTAAAAACAGATTCCAAAGCTTCTTGTCCTCGAGGACAAGAAGCTT TGGAATCTG
mAPPBP1- II	Sense: CGGTAAATTTCCTTGACCCTCCTTCTCGAGAAGGAGGGTCAAGGAAA TTTATTTTT Antisence: AATTAAAAATAAATTTCCTTGACCCTCCTTCTCGAGAAGGAGGGTCAA GGAAATTTA
Non-target (GFP)	Sense: CCGGCGTGATCTTCACCGACAAGATCTCGAGATCTTGTCGGTGAAGA TCACGTTTTT Antisence: AATTAAAAACGTGATCTTCACCGACAAGATCTCGAGATCTTGTCGGT GAAGATCACG

Table 3. Nucleotide Sequences of Primers used for RT-PCR

Mouse Genes	Primer sequence: forward (For) and reverse (Rev)
Pparg	For 5'- AGTGGAGACCGCCCAGGCTT -3' Rev 5'- CAGTTCCAGGGCCTGCAGCA-3'
Cebpa	For 5'-CTCGCCATGCCGGGAGAACTCTA-3' Rev 5'-GAGGTGACTGCTCATCGGGGGC-3'
Cebpb	For 5'- ACCACGACTTCCTCTCCGACCTCT -3' Rev 5'- CGTAGTCGGCCGGCTTCTTGC -3'
Cebpd	For 5'-ATCGACTTCAGCGCCTACA-3' Rev 5'-GCTTTGTGGTTGCTGTTGAA-3'
Adiponectin	For 5'-ATGACGGCAGCACTGGCA-3' Rev 5'-CGGCCTTGTCCTTCTTGA-3'

Resistin	For 5’-CGCTTCCTGATGTCGGTC-3’ Rev 5’-ATGCCCACTTCGCCATCC-3’
Cd36	For 5’- GCTTGCAACTGTCAGCACAT - 3’ Rev 5’- GCCTTGCTGTAGCCAAGAAC- 3’
Fabp4	For 5’- CATGGCCAAGCCCAACAT -3’ Rev 5’- CGCCCAGTTTGAAGGAAATC -3’
Scd1	For 5’-GCGATACACTCTGGTGCTCA-3’ Rev 5’-CCCAGGGAAACCAGGATATT-3’
Perilipin	For 5’-TGCTGGATGGAGACCTC-3’ Rev 5’-ACCGGCTCCATGCTCCA-3’
Lpl	For 5’-GCACTTTCCAGCCAGGATGC-3’ Rev 5’-GGCCTGGTTGTGTTGCTTGC-3’
Acs	For 5’-GCTGATCCAGAAGGGGTTCA-3’ Rev 5’-CCACCCCACACTTCTTGCCT-3’
Fasn	For 5’-CTGGCCCCGGAGTCGCTTGAGTATA-3’ Rev 5’-GGAGCCTCCGAAGCCAAATGA-3’
Nedd8	For 5’-AACCCACAGACAAGGTGGAG -3’ Rev 5’-CAAGGAGGTAAACGGAACCA -3’
Tnfa	For 5’- ACGGCATGGATCTCAAAGAC-3’ Rev 5’-AGATAGCAAATCGGCTGACG-3’
Il6	For 5’-TAGTCCTTCCTACCCCAATTTCC-3’ Rev 5’- TTGGTCCTTAGCCACTCCTTC-3’
Mcp1	For 5’-CCACTCACCTGCTGCTACTCAT-3’ Rev 5’-GGTGATCCTCTTGTAGCTCTCC-3’
F40/80	For 5’-CCCCAGTGTCCT TACAGAGTG-3' Rev 5’-GTGCCCAGAGTGGATGTCT-3'
C11b	For 5’- 5'-CCTTGT TCTCTT TGATGCAG-3' Rev 5’- 5'-GTGATGACAACTAGGATCTT-3'
C11c	For 5’-CCTGAGGGTGGGCTGGAT-3' Rev 5’-GCCAATTTCCTCCGGACAT-3'
18S RNA	For 5’- TTCGTATTGAGCCGCTAGA-3’ Rev 5’- CTTTCGCTCTGGTCCGTCTT-3’

Table 4.Chip-PCR primer sequences.

Purposes	Targets	Forward primers (5’ to 3’)	Reverse primers (5’ to 3’)
ChIP PCR	Mouse Fabp4	TTTGCTTCCACTTAATTCCT	GCTCAGGGTGTGCAAGCAGG
	Mouse C/ebpa	CTGAGCTACACCCTCGGCTC	TCCCCACCGGAGGGCATGAG
	Mouse Fabp4 (NS)	TTTCTCAGAGCATCCCGTGG	TTACAAGACAGCCAGAGAAA

RESULTS

NEDD8 was induced during adipocyte differentiation.

Adipocyte differentiation is temporally controlled through the hormonal stimulation of glucocorticoids, cAMP, and insulin, which are known to consistently induce C/EBPβ and δ, followed by PPARγ and C/EBPα expression (Rosen and Spiegelman, 2000). To examine whether NEDD8 was related to adipocyte differentiation, the differentiation of mouse 3T3-L1 pre-adipocyte cells were induced by dexamethasone, IBMX, and insulin (DMI): adipogenesis stimuling cocktail. NEDD8 expression gradually increased during adipogenesis and reached a peak at day 6, and other adipogenic transcription factors of PPARγ and C/EBPs were also induced (Fig 1A, B). To identify the NEDD8-conjugated substrates during adipogenesis, His-NEDD8 stable cell lines were established using lentivirus overexpression system in 3T3-L1 preadipocytes. After selection with puromycin, adiopogenesis was induced. His-NEDD8-conjugated proteins were isolated using Ni^{2+} affinity beads, electrophoresed, and identified by LC-MS analysis (Fig 2). Interestingly, PPARγ, the major adipogenic transcription factor, was identified as one of the NEDDylated proteins (Fig 2B). 3T3-L1 cell lines, which stably express His-NEDD8, were far more differentiated than that harboring control vector (Fig 3). Particularly, Oil-red O staining revealed that dexamethasone-treated His-NEDD8 cell lines were more differentiated than control cell lines. In addition, PPARγ protein levels were obviously increased by differentiation induction in His–NEDD8 stable cells compared with the control cell line. Thus NEDD8 enhances the actions

of glucocorticoid in adipogenesis. Collectively, these results suggest that NEDD8 is a positive regulator of adipogenesis.

The knockdown of NEDD8 reduced the expression of PPARγ and adipogenesis capacity of 3T3-L1 pre-adipocytes.

To understand the role of NEDD8 in the adipogenesis, I established stable knockdown cell lines using a lentiviral shRNA expression vector in 3T3-L1 pre-adipocytes. After selection with antibiotics, a control, NEDD8, and NEDD8-activating enzyme APPBP1 shRNA stable expressing cell lines were induced to differentiate into adipocytes. Two different shRNAs were designed to target mouse NEDD8 and APPBP1, and the efficiency of NEDD8 and APPBP1 knockdown were analyzed by western blotting (Fig 4A). Western blotting and Oil-red O staining revealed that the knockdown of both NEDD8 and APPBP1 significantly decreased adipogenesis; in particular, the knockdown of NEDD8 more dramatically inhibited adipogenesis and PPARγ protein expression. The differentiation of mouse 3T3-F442A pre-adipocyte cells was induced by insulin. Corresponding with this result, another preadipocyte, 3T3-F442A producing shRNAs against mouse NEDD8 and mouse APPBP1 was less differentiated compared with the control cells. In addition, the expression level of PPARγ was decreased, compared with the control cells (Fig 4B). In order to examine dose-dependent effect of the knockdown, I tried transient transfections of different doses of siRNA into 3T3-L1 cells. The efficient knockdown effects were confirmed by western blot analysis 8 days after transfection (Fig 5A). The knockdown of mouse NEDD8 and APPBP1 by siRNA

suppressed adipocyte differentiation dose-dependently in 3T3-L1 cells. Furthermore, kinetic expression analysis during adipogensis showed that NEDD8 expression paralleled with PPARγ, because both proteins were induced during the middle stage of adipogenesis. This induction of PPARγ was decreased by the knockdown of NEDD8 (Fig 5B). These results suggest that adipocyte differentiation might be associated with the NEDDylation process through the regulation of PPARγ protein levels.

The depletion of NEDD8 decreased adipogenic genes in 3T3-L1 pre-adipocytes.

To address the functional role of NEDD8 in adipogenesis, and which adipogenic factors are regulated by NEDD8, 3T3-L1 pre-adipocytes were transfected with control siRNA or anti-NEDD8 siRNA two days before adipogenesis. 3T3-L1 cells were induced for adipogenesis for eight days, and then were harvested on the indicated day. RT-qPCR analyses revealed that the NEDD8 knockdown significantly attenuated pparg and c/ebpa mRNA expression, and lipid deposition–related factors such as fatty acid binding protein 4 (fabp4), cluster of differentiation 36 (cd36), and fatty acid synthase (fasn). In addition, adipokines such as resistin and adiponectin were suppressed when PPARγ was inhibited by knockdown of NEDD8 (Fig 6), whereas c/ebpb and c/ebpd mRNA expression were not dependent on NEDD8 because the expression of c/ebpb and c/ebpd were induced prior to PPARγ expression. These results further demonstrate that NEDD8 is essential for adipogenesis.

NEDD8 was recruited to the peroxisome proliferator hormone response

elements (PPRE) of C/EBPα and FABP4 promoters during adipogenesis.

As PPARγ and NEDD8 were co-induced during adipogenesis, I examined whether NEDD8 regulates PPARγ. Western blot analysis showed a significant reduction of PPARγ protein in NEDD8 knockdown cell lines, compared to that in control cell lines. On the contrary, the PPARγ protein levels were dramatically increased in NEDD8-overexpressed cell lines (Fig 7). These results suggest that NEDD8 was required to induce PPARγ in 3T3-L1 cells was dependent on NEDD8 expression. As PPARγ is known to be transcriptional activator for the expression of C/EBPα and FABP4, the chromatin immunoprecipitation (ChIP) analysis with PPARγ antibodies was performed on the well-known PPRE sites for these proteins. The binding of PPARγ on the FABP4 and C/EBPα promoter was more enriched in 3T3-L1 cells after the adipogenesis stimuli, while was diminished in NEDD8 shRNA stable cell lines. (Fig 8A left and B left). On the contrary, the binding of PPARγ on the fabp4 and c/ebpa promoter was increased in NEDD8-overexpressed stable cell lines (Fig 8 A right and B right). These results suggest that enhanced expression of PPARγ by NEDD8 correlated with increased binding of PPARγ to downstream target promoters.

NEDD8 had an essential role in *in vivo* adipogenesis.

NEDD8 plays important role in *in vitro* adipocyte differentiation. To investigate the *in vivo* role of NEDD8, I established NEDD8-deficient 3T3-L1 (Fig 9) and 3T3-F442A cell lines (Fig 10), and implanted them into the subcutaneous tissue of mouse abdomen. Five wks after implantation, the grafted fat pads were examined

with the histology and the expression of anti-perilipin (a lipid droplet scaffold protein) via immunostaining. Upon comparison with the control fat pad, both NEDD8-deficient cell lines showed dramatic inhibition in adipose tissue formation. These results indicate that NEDD8 is necessary for *in vivo* adipocyte differentiation.

NEDDylation of PPARγ was required for its stability.

As shown above, proteomics analysis revealed that PPARγ was conjugated with NEDD8 during adipogenesis. Among the major adipogenic transcription factors, PPARγ turned out solely to be endogenously NEDDylated via Ni^{2+} pull-down assay (Fig 11). Ectopically expressed PPARγ in HEK293 cells was identified to be conjugated with NEDD8, but not with NEDD8ΔGG (conjugation-defective due to Gly-75/76 deletion) or SENP8 (deNEDDylase) overexpression (Fig 12 A). Moreover, since HIF-1α reported to be stabilized by NEDDylation (Ryu et al., 2011), I tested whether PPARγ is able to be stabilized with NEDD8. Ectopically expressed PPARγ was stabilized with NEDD8 dose dependently, but not with NEDD8ΔGG (Fig 12 B left). To solidify that NEDD8 increased the PPARγ stability, HEK293 cells were transfected either with PPARγ only or PPARγ and NEDD8 (Fig 12 B right). After 48 h incubation, the cells were treated with cycloheximide to inhibit de novo protein synthesis and PPARγ degradation was attenuated by NEDD8. To determine whether NEDDylation affects PPARγ ubiquitination, HEK293 cells were co-transfected with PPARγ and NEDD8 or Ub, which were incubated with or without MG132, an inhibitor of the proteasome (Fig 13 upper). In the presence of MG132, the combination of PPARγ and Ub, together with NEDD8 blocked the

PPARγ ubiquitination more strongly. NEDD8 siRNA was co-transfected with either PPARγ or PPARγ and Ub, and then the cells were incubated with or without MG132 (Fig 13 lower). In the presence of MG132, the co-express with PPARγ and Ub in NEDD8 siRNA knockdown cells up-regulated PPARγ ubiquitination. On the base of these results, NEDDylation is required for PPARγ stabilization by blocking its ubiquitination.

Identification of the PPARγ domain conjugated with NEDD8.

Next, to analyze which domain of PPARγ might be associated with NEDD8, HEK293 cells expressed with each domain of PPARγ were treated with MG132 or co-transfected with NEDD8 (Fig 14). Interestingly, western blot revealed that the expression levels of middle and C-term peptides increased with NEDD8 co-expression. To speculate the NEDDylated region of PPARγ, each of PPARγ fragments co-expressed with His-NEDD8 was subjected to Ni^{2+} pull-down assay. The middle and C-terminal regions turned out to be NEDDylated (Fig 15 upper), but abolished in His-NEDD8ΔGG co- expressed cells(Fig 15 lower). NEDD8 physically interacts with the PPARγ middle and C-terms.

MDM2 as an E3 ligase promoted PPARγ NEDDylation.

It was recently reported that murine double minute 2 (MDM2), the E3 ubiquitin ligase, has an important role in regulating the stability of p53 tumor suppressors and the expression level of MDM2 is amplified in 3T3-L1 preadipocytes (Berberich et al., 1999). A recent study showed that MDM2 is required for the cAMP-mediated

induction of C/EBPδ by the recruitment of cAMP regulatory element-binding protein (CREB), and promotes adipogenesis (Hallenborg et al., 2012). Yet, the reason for MDM2 amplification in adipogenesis was not clarified. On the base of previous reports, I expected that MDM2 has the role of E3 ligase for PPARγ NEDDylation. 3T3-L1 pre-adipocytes transfected with control siRNA or anti-MDM2 siRNA two days before adipogenesis were induced for adipogenesis for eight days, then harvested (Fig 16 A). Oil-red O staining revealed that MDM2 knockdown significantly decreased adipogenesis dose dependently. As expected, western blotting showed that the PPARγ protein level was significantly reduced, when MDM2 depleted. Furthermore, nutlin-3, an MDM2 inhibitor, also blocked adipocyte differentiation and reduced PPARγ protein levels dose dependently, suggesting that MDM2 has a crucial role in adipogenesis (Fig 16 B). As expected, MDM2 physically interacted with PPARγ in HEK293 cells (Fig 17). Ni^{2+} pull-down assay showed that ectopically expressed MDM2 mediated PPARγ NEDDylation. Conversely, PPARγ NEDDylation was down regulated by knockdown of MDM2 in HEK293 cells (Fig 18 left). Nutlin-3 also inhibited PPARγ NEDDylation (Fig 18 right). These results suggest that MDM2 physically interacts with PPARγ and specifically mediates PPARγ NEDDylation.

MLN4924 inhibited adipogenesis in 3T3-L1 and H-ADSC.

Searching for inhibitors that ubiquitin-proteasome system (UPS) and ubiquitin-like proteins (UBLs) may allow control over dynamic genes and be the key to find novel therapeutics for diseases; NEDDylation is activated by a NEDD8 activation enzyme

complex, which is a combination of APPBP1 and UBA3 during the first process (Rabut and Peter 2008). MLN4924, the adenosine sulfamate analog that targets NEDD8 E1 activating enzyme has a crucial therapeutic effect in the treatment of cancer (Soucy et al., 2009). Pharmaceutically, MLN4924 has possibility as a NEDDylation-targeting therapy that has a potential effect on other diseases. To address the effect on adipogenesis of NEDDylation, MLN4924 was treated in mouse and human pre-adipocytes, and then adipocyte differentiation was induced using adipogenic stimuli cocktails. Oil-red O staining showed that MLN4924 suppressed adipocyte differentiation. As assumed, western blotting showed that the PPARγ protein level was reduced in 3T3-L1 cells and human adipose tissue-derived mesenchymal stem cells (H-ADSCs) isolated from obese patients (Fig 19). I further checked the expression of adipogenic markers and lipid deposition-related genes in MLN4924 treatment (Fig 20). MLN4924 significantly reduced the expression of pparg, c/ebpa, and other adipogenic target genes such as fabp4, cd36, adiponectin, and resistin during adipogenesis. Furthermore, the expression of lipid metabolic genes such as fasn and scd1 were also suppressed, whereas c/ebpb and c/ebpd mRNA expression was not implicated in MNL4924. These data suggest that MLN4924 dramatically reduced adipogenesis in both mouse and human cell lines.

MLN4924 reduced fat accumulation.

To address whether MLN4924 reduces fat storage in 3T3-L1 and H-ADSCs, 3T3-L1 was treated with either 0.1 or 0.5 μM of MLN4924 daily from third or sixth day during 20 days-differentiation. After the daily treatment of MLN4924, the fat

accumulation was reduced by MLN4924 (Fig 21). The same results have shown in human cells (Fig 22). Furthermore, quantitative PCR showed that the expression of lipid metabolic genes such as perilipin, lpl, acs, scd1, cd36, and fabp4 was significantly reduced by MLN4924 in 3T3-L1 cells (Fig 23). The same results have been shown in human cells (Fig 24). These results indicate that MLN4924 can block fat accumulation.

MLN4924 effected on weight loss and improves glucose tolerance and insulin sensitivity in high fat diet–induced obesity mice.

MLN4924 diminished the number and size of lipid droplets in both 3T3-L1 cells and H-ADSCs dramatically. The above experiments lead to the question of whether MLN4924 can be an anti-obesity drug. As the early stages of adipogenesis are attenuated by the inhibition of NEDDylation, MLN4924 was expected to prevent childhood obesity. To systemically access weight gain, we fed young C57BL/6 mice with a 60% fat diet, injecting the mice intraperitoneally once every three days with vehicle or MLN4924 (30 mg/kg). Anti-obesity drugs should be less toxic than anticancer drugs, thus the drug treatment interval was increased for this study. Interestingly, MLN4924 prevented the high fat diet (HFD)-induced weight gain (Fig 25 A). Body weight was reduced by MLN4924 during 12 wks in HFD. As expected, MLN4924 did not reduce the body weight in normal chow diet (NCD) mice, suggesting that MLN4924 is not substantially toxic at the dose used in the experiment. Withdrawal of the drug after six wks of treatment restored weight gain, indicating that the action of MLN4924 is reversible (Fig 25 B). Food intake was not

influenced by the MLN4924 treatment, and the preventative effect of MLN4924 against weight gain was not dependent on the loss of appetite (Fig 25 C). Moreover, obesity is associated with type 2 diabetes (Kahn et al., 2006); to determine whether MLN4924 treatment could attenuate diabetic symptoms in HFD-fed mice, obesity was established 10 wks after, and then their metabolic parameters were examined. Consequently, the fasting serum glucose level was increased in HFD-fed mice, and HFD-induced hyperglycemia was reduced by MLN4924 treatment. Similarly, the fasting insulin level was significantly increased by HFD, and HFD–insulin overproduction was restored by MLN4924 (Fig 26 A). This result indicates that the insulin sensitivity in diet induced obesity (DIO) mice can be significantly improved by MLN4924. Following the confirmation that characterized HFD-induced hyperglycemia, I next employed a glucose tolerance test and insulin tolerance test, which revealed that MLN4924 relived HFD-induced glucose and insulin intolerance, while not affecting glucose tolerance and insulin sensitivity in NCD-fed mice (Fig 26 B). Moreover, MLN4924 reduced plasma leptin concentrations in the DIO mice model (Fig 26 C). These results indicate that MLN4924 significantly enhanced glucose homeostasis and insulin sensitivity in DIO mice.

MLN4924 reduced adipose tissue size in DIO mice.

As described above, this study observed that the body weight of HFD-fed mice was reduced via treatment with MLN4924. To analyze how obese HFD-fed mice were, the abdominal fat of mice was analyzed using Computed Tomography (CT). The analysis of the body fat composition revealed a remarkable reduction of adipose

deposition in HFD-fed MLN4924-treated mice compared with HFD-fed control mice (Fig 27 A). This CT-based analysis of the fat area and volume that were enormously reduced in HFD-fed mice treated with MLN4924 (Fig 27 B). As expected, the size of white adipose tissues (WAT), epididymal fat, subcutaneous fat, and visceral fat restored to normal in MLN4924-treated HFD-fed mice treated with MLN4924 (Fig 27 C). Next, I determined which genes were down regulated by MLN4924 in DIO mice. As shown in fig 11, PPARγ was NEDDylated at adipocyte differentiation and the expected target of MLN4924. These results indicate that the down regulation of PPARγ expression is a potential therapeutic effect of anti-obesity drugs. From western blotting, the MLN4924-treated HFD-fed mice showed reduced PPARγ expression in WAT (Fig 28). Furthermore, the patients with obesity had adipose tissue dysfunction, which leads to adipocyte hypertrophy and inflammatory processes in the adipose tissue (Ouchi et al., 2011). Interestingly, the expression of adipogenic genes, lipid metabolic genes, and inflammatory cytokines increased in the epididymal fat of HFD-fed mice, MLN4924 also prevents this response (Fig 29, 30). From the *in vivo* results, MLN4924 prevents obesity in HFD-fed mice by reducing the adipogenesis and fat accumulation; yet this mode of action did not disturb the development of normal fat tissue. Taken together, this study suggests that MLN4924 might have an advantageous effect for anti-obesity drugs.

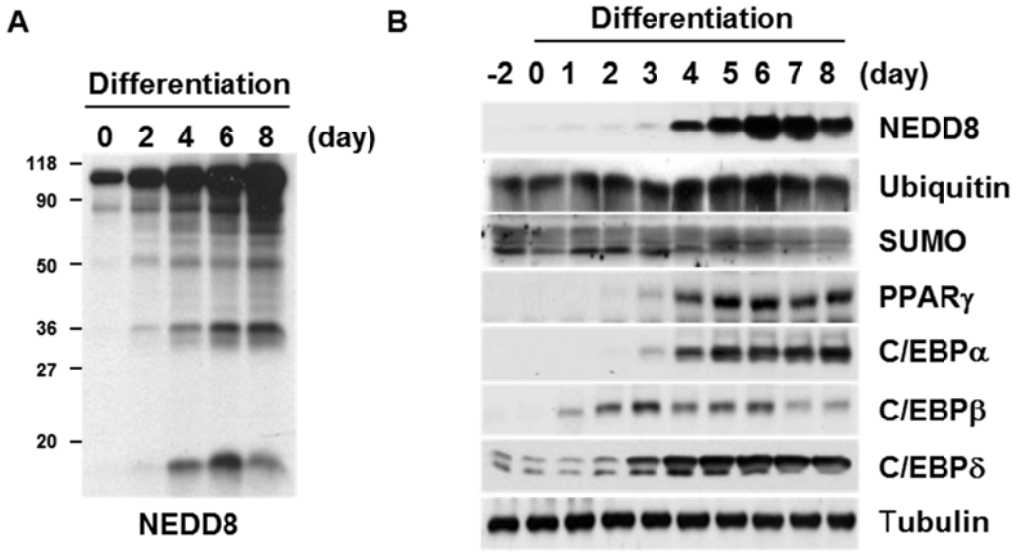

Figure 1. NEDD8 is induced during adipocyte differentiation.

(A) 3T3-L1 cells were incubated with adipogenesis stimuli cocktail (DMI) for the indicated lengths of time. The protein level of NEDD8 was determined by western blotting analysis during adipogenesis. (B) Before or after treatment of DMI for the indicated lengths of time, NEDD8, Sumo, Ubiquitin, PPARγ and C/EBPs protein levels were determined by western blotting analysis using indicated antibodies. Tubulin was used as a loading control with particular total protein samples.

A

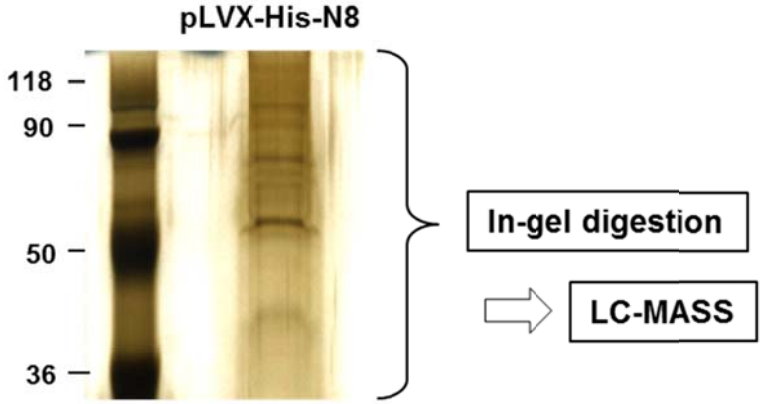

B

NEDDyated proteins by proteomics in the adipocytes

Non-POU domain-containing octamer-binding protein

Putative pre-mRNA-splicing factor ATP-dependent RNA helicase

Ataxin-2

Insulin-like growth factor 2 mRNA-binding protein 2

Mannosyl-oligosaccharide glucosidase

DNA topoisomerase 1

E3 ubiquitin-protein ligase CBL

GDH/6PGL endoplasmic bifunctional protein

1,4-alpha-glucan-branching enzyme

NADH-cytochrome b5 reductase 3

Serine/threonine-protein phosphatase 1 regulatory subunit 10

60S ribosomal protein L15

ATP-binding cassette sub-family D member 3

Constitutive coactivator of PPAR-gamma-like protein 2

60S ribosomal protein L27a

Trimethyllysine dioxygenase, mitochondrial

Peroxisome proliferator-activated receptor gamma

Figure 2. Proteomic analysis of NEDDylated protein that might play important roles in adipogenesis in 3T3-L1 cells.

(A) 3T3-L1 cells were infected with viral pLVX-His-NEDD8 vector. After selections with puromycin, stable cells were treated with DMI. After 4 days, cells were lysed. His-NEDD8-conjugated proteins were bound to Ni^{2+}-NTA-agarose beads under denaturing conditions and subjected to silver staining and then LC/MS analysis was performed after in-gel digestion. (B) LC/MS data for His-NEDD8-conjugated proteins.

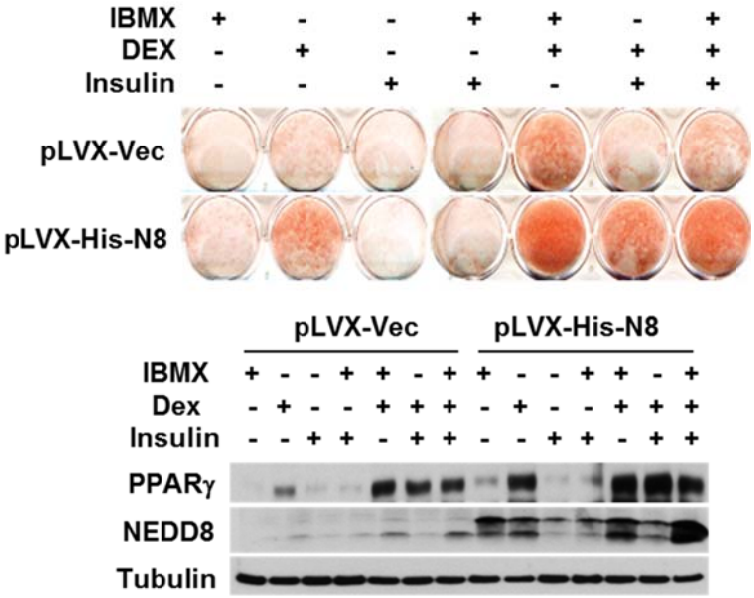

Figure 3. NEDD8 mediates actions of glucocorticoid in the adipogenesis.

Stably expressed pLVX-IRES-Control (pLVX-Vec) or pLVX-IRES-His-NEDD8 (pLVX-His-N8) 3T3-L1 cells were differentiated with indicating conditions (1 μM dexamethasone, 500 μM IBMX, 5 μg/ml insulin) and then at day 8, cells were stained with Oil-red-O staining (upper). Cell lysates were analyzed for PPARγ and NEDD8 protein levels by western blotting using anti-PPARγ and anti-NEDD8 antibodies. Tubulin was used as a loading control (lower).

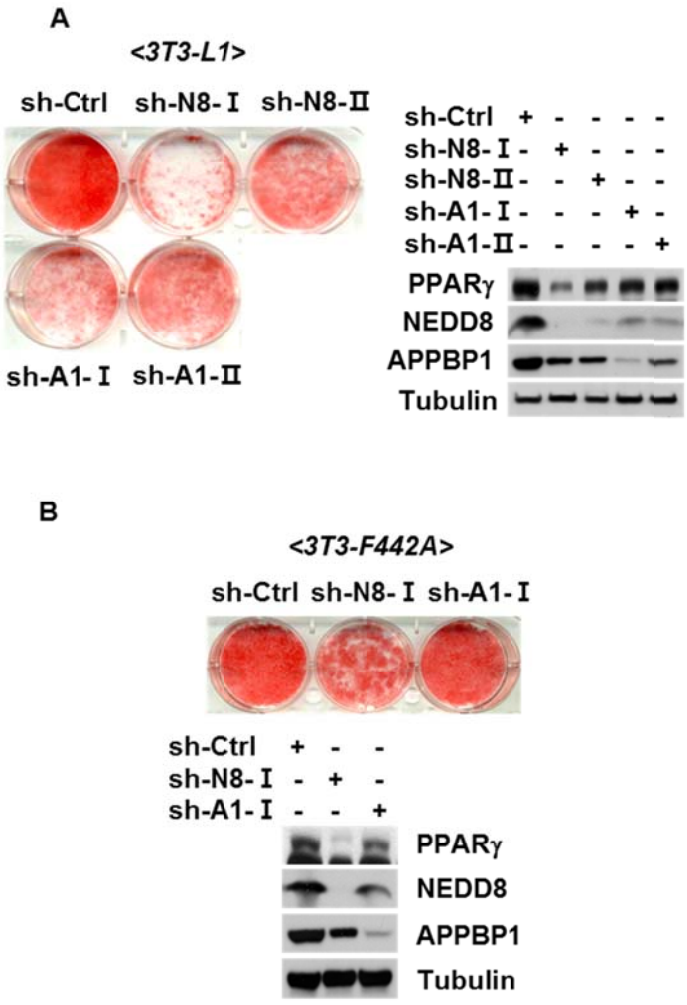
A
<3T3-L1>
sh-Ctrl
sh-N8-Ⅰ
sh-N8-Ⅱ
sh-A1-Ⅰ
sh-A1-Ⅱ
sh-Ctrl + - - - -
sh-N8-Ⅰ - + - - -
sh-N8-Ⅱ - - + - -
sh-A1-Ⅰ - - - + -
sh-A1-Ⅱ - - - - +
PPARγ
NEDD8
APPBP1
Tubulin
B
<3T3-F442A>
sh-Ctrl
sh-N8-Ⅰ
sh-A1-Ⅰ
sh-Ctrl + - -
sh-N8-Ⅰ - + -
sh-A1-Ⅰ - - +
PPARγ
NEDD8
APPBP1
Tubulin

Figure 4. NEDD8 knockdown reduced the adipogenesis capability of preadipocytes.

(A) 3T3-L1 cells were stably knock downed with each targeting shRNA viruses, pLKO.1-sh-Control (sh-Ctrl), two different NEDD8-targeting pLKO.1-sh-NEDD8 (sh-N8-I and -II）or pLKO.1-sh-APPBP1 (sh-A1-I and -II）and then stimulated with DMI. After adipogenesis cells were stained with Oil-red O at day 8. PPARγ, NEDD8 and APPBP1 protein levels were determined by western blotting analysis at 8 day. Tubulin was used as a loading control with particular total protein samples. (B) 3T3-F442A cells were stably knockdowned with pLKO.1-sh-Control (sh-Ctrl), pLKO.1-sh-NEDD8-I (sh-N8-I) and pLKO.1-sh-APPBP1-I (sh-A1-I) and then stimulated with DMI. Cells were stained with Oil-red O at day 8 (upper). PPARγ, NEDD8 and APPBP1 protein levels were determined by western blotting analysis. Tubulin was used as a loading control with particular total protein samples (lower).

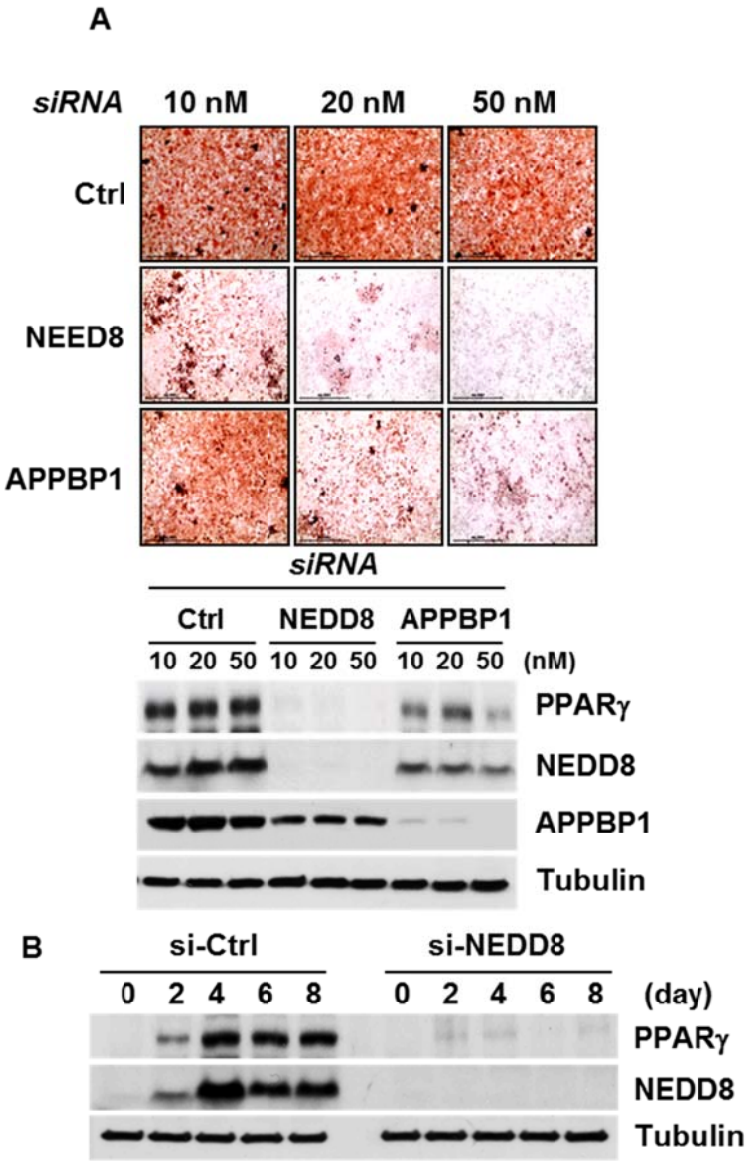
A
siRNA
10 nM
20 nM
50 nM
Ctrl
NEED8
APPBP1
siRNA
Ctrl
NEDD8
APPBP1
10 20 50 10 20 50 10 20 50 (nM)
PPARγ
NEDD8
APPBP1
Tubulin
B
si-Ctrl
si-NEDD8
0 2 4 6 8 0 2 4 6 8 (day)
PPARγ
NEDD8
Tubulin

Figure 5. Analysis of dose-dependency and kinetics of NEDD8 knockdown in 3T3-L1 cells.

(A) 3T3-L1 cells were transiently transfected with si-Control (si-Ctrl), si-NEDD8 or si-APPBP1 to 10, 20, 50 nM at 2 day before differentiation and then stimulated with DMI. After differentiation, cells were stained with Oil-red-O at day 8 (upper). Cell lysates were analyzed by western blotting using anti-PPARγ, anti-NEDD8 or anti-APPBP1 antibodies. Tubulin was used as a loading control with particular total protein samples (lower). (B) 3T3-L1 cells were transiently transfected with si-Control or si-NEDD8 (50 nM) at 2 days before differentiation. 3T3-L1 cells treated with DMI and then harvested at 0, 2, 4, 6 and 8 day. Cell lysates were analyzed by western blotting using anti-PPARγ, anti-NEDD8 or anti-APPBP1 antibodies. Tubulin was used as a loading control with particular total protein samples.

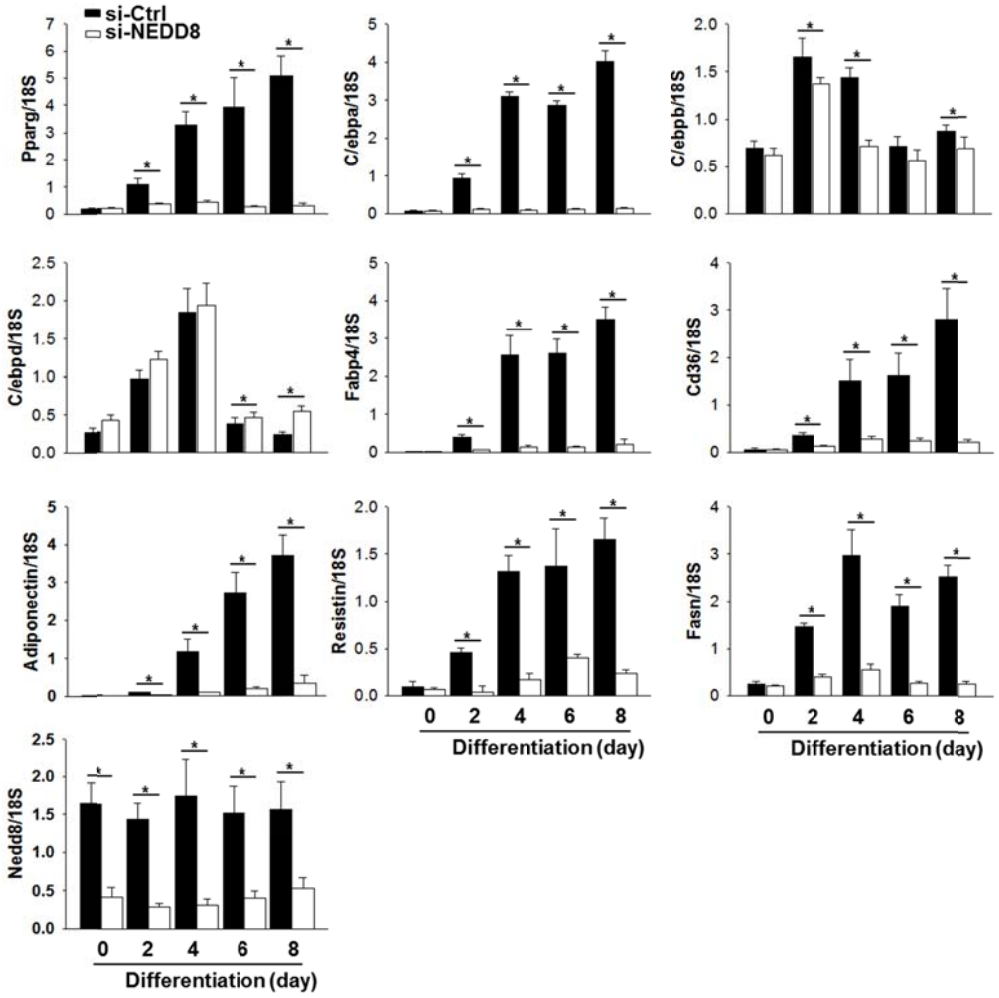
si-Ctrl
si-NEDD8
Pparg/18S
C/ebpa/18S
C/ebpb/18S
C/ebpd/18S
Fabp4/18S
Cd36/18S
Adiponectin/18S
Resistin/18S
Fasn/18S
Nedd8/18S
0 2 4 6 8
Differentiation (day)

Figure 6. NEDD8 knock down by si-NEDD8 down regulated the expression of adipogenic genes during adipogenesis.

3T3-L1 cells were transfected with si-Ctrl or si-NEDD8 (50 nM) at 2 days before differentiation and then stimulated with DMI for the indicated lengths of time. Total RNA was extracted from cells, and RT-qPCR was applied to measure the expression levels of pparg, c/ebpa, c/ebpb, c/ebpd, fabp4, cd36 resistin, adiponectin, fasn, and nedd8. Results were quantified as the relative levels versus 18S RNA level. Data shown represent the mean±SD (n=3) and * denotes $p < 0.05$.

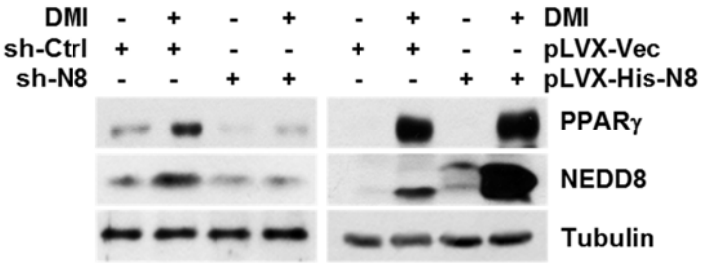

Figure 7. PPARγ induction in 3T3-L1 cells required NEDD8 during adipogenesis.

3T3-L1 stable cell lines expressing non-targeting sh-RNA (pLKO.1-sh-Ctrl) and NEDD8-targeting shRNA (pLKO.1-sh-N8) (left) and cells stably over-expressing each targeting vector viruses, pLVX-IRES-Control (pLVX-Vec) or pLVX-IRES-His-NEDD8 (pLVX-His-N8) (right) were treated with DMI. After 4 days cell lysates were analyzed by western blotting using anti-PPARγ and anti-NEDD8 antibodies. Tubulin was used as a loading control with particular total protein samples

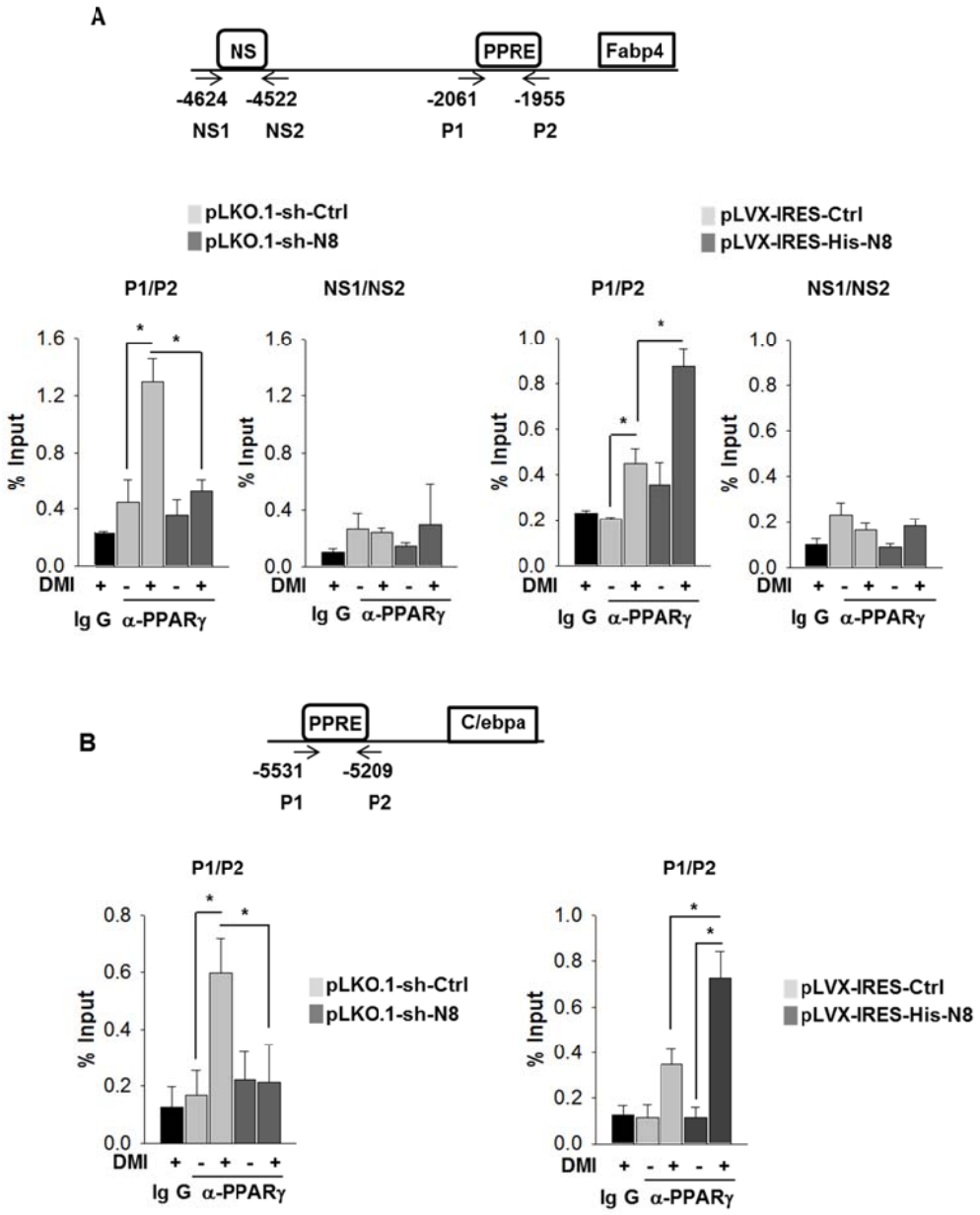
A
NS
PPRE
Fabp4
-4624
-4522
-2061
-1955
NS1
NS2
P1
P2
pLKO.1-sh-Ctrl
pLKO.1-sh-N8
pLVX-IRES-Ctrl
pLVX-IRES-His-N8
P1/P2
NS1/NS2
% Input
DMI
Ig G
α-PPARγ
B
PPRE
C/ebpa
-5531
-5209
P1
P2

Figure 8. Enhanced NEDD8 expression correlates with enhanced binding of PPARγ on PPRE.

(A) Chromatin immunoprecipitation (ChIP) was performed to reveal the binding of PPARγ to the promoter of its target genes. A schematic representation of fabp4 PPRE and segments amplified by PCR (upper). P1/P2 was fabp4 promoter sequence and NS1/NS2 was non-specific promotor sequence. 3T3-L1 stable cell lines expressing non-targeting sh-RNA (pLKO.1-sh-Ctrl) and NEDD8-targeting shRNA (pLKPO.1-sh-N8) or pLVX-IRES-Control and pLVX-IRES-His-NEDD8 vectors were treated with DMI and then after 4 days chromatin complexes were precipitated with anti-PPARγ antibody. The precipitated DNAs were amplified and quantified on RT-qPCR system using fabp4 primers. The results (mean±SD, n=3) are expressed as percentages of the input level (lower). (B) A schematic representation of c/ebpa PPRE and segments amplified by PCR (upper). P1/P2 was c/ebpa promoter sequence. 3T3-L1 stable cell lines expressing non-targeting sh-RNA (pLKO.1-sh-Ctrl) and NEDD8-targeting shRNA (pLKPO.1-sh-N8) or pLVX-IRES-Control and pLVX-IRES-His-NEDD8 vectors were treated with DMI and then after 4 days chomatin complexes were precipitated with indicated anti-PPARγ antibody. The precipitated DNAs were amplified and quantified on RT-qPCR system using c/ebpa primers. The results are expressed as percentages of the input level. Data shown represent the mean±SD (n=3) and * denotes $p < 0.05$.

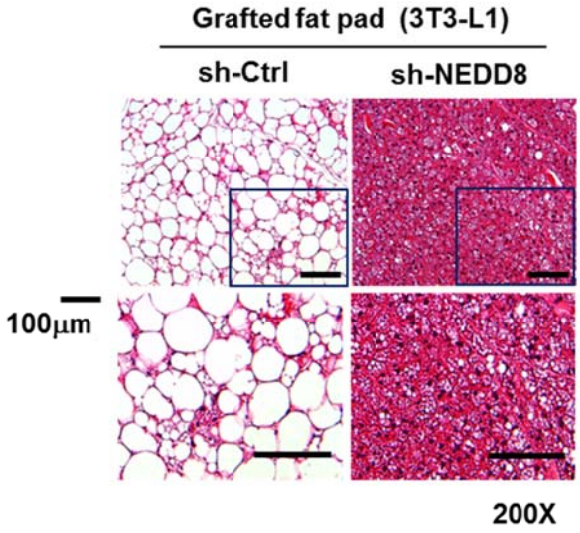
Grafted fat pad (3T3-L1)
sh-Ctrl
sh-NEDD8
100μm
200X

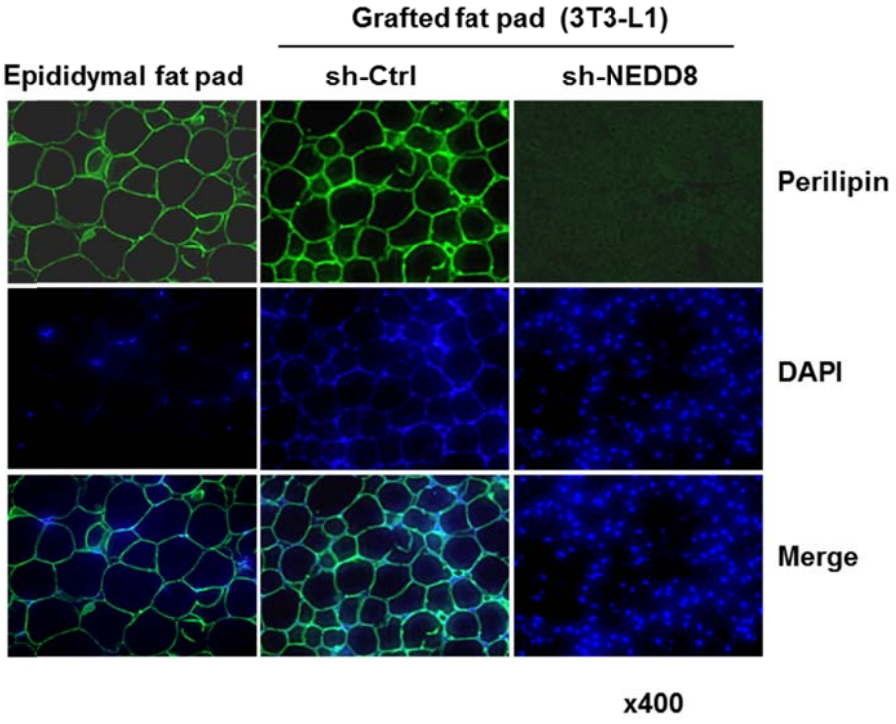
Grafted fat pad (3T3-L1)
Epididymal fat pad
sh-Ctrl
sh-NEDD8
Perilipin
DAPI
Merge
x400

Figure 9. NEDD8 is essential for the adipogenesis in implanted mouse fat pad. 3T3-L1 cells stably expressing by pLKO.1-sh-Control (sh-Ctrl) or pLKO.1-sh-NEDD8 (sh-NEDD8) were implanted into the subcutis of the abdomens of 9-wk-old male BALB/c nude mice. 5 wks after implantation, implanted fat pads were stained with hematoxylin and eosin (H&E, upper panel) or subjected to immunofluorescence analysis with anti-perilipin antibody (lower panel). Nuclei were stained with DAPI.

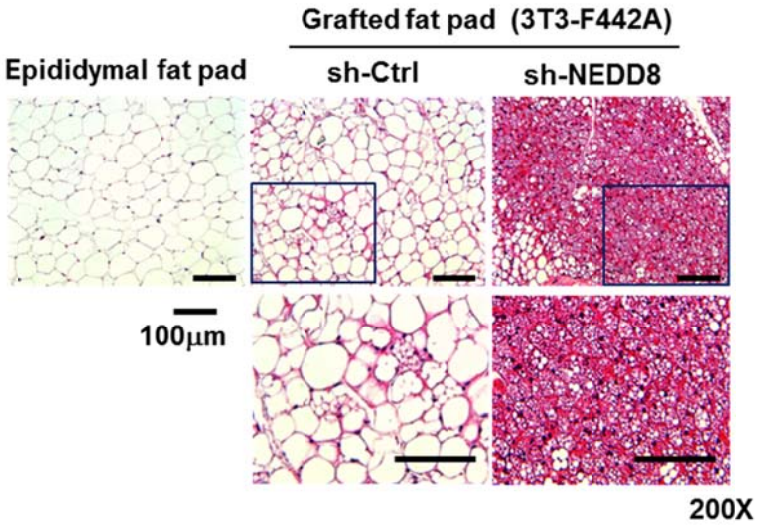
Grafted fat pad (3T3-F442A)
Epididymal fat pad
sh-Ctrl
sh-NEDD8
100μm
200X

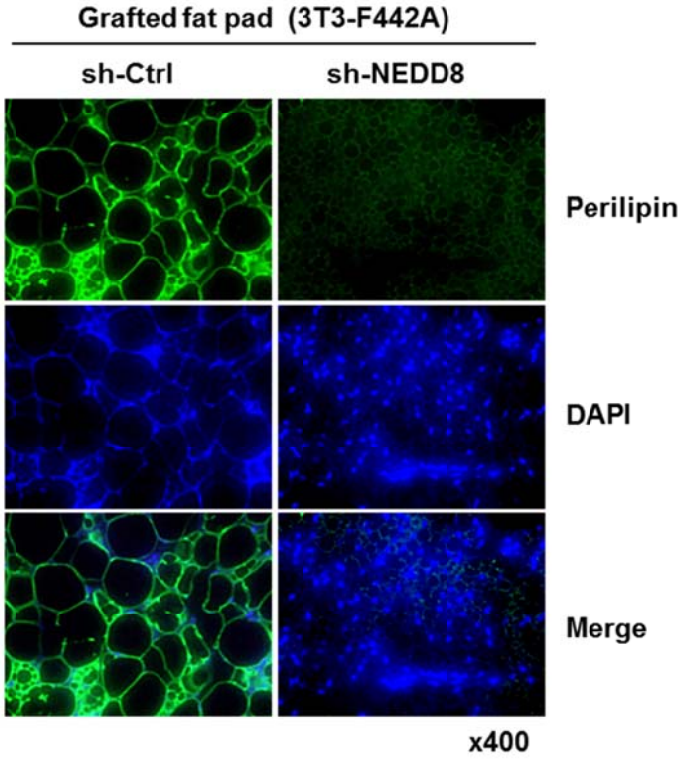
Grafted fat pad (3T3-F442A)
sh-Ctrl
sh-NEDD8
Perilipin
DAPI
Merge
x400

Figure 10. NEDD8 is essential for the adipogenesis in implanted mouse fat pad.

3T3-F442A cells stably expressing by pLKO.1-sh-Control (sh-Ctrl) or pLKO.1-sh-NEDD8 (sh-NEDD8) were implanted into the subcutis of the abdomens of 9-wk-old male BALB/c nude mice. 5 wks after implantation, implanted fat pads were stained with hematoxylin and eosin (H&E, upper panel)) or subjected to immunofluorescence analysis with anti-perilipin antibody (lower panel). Nuclei were stained with DAPI.

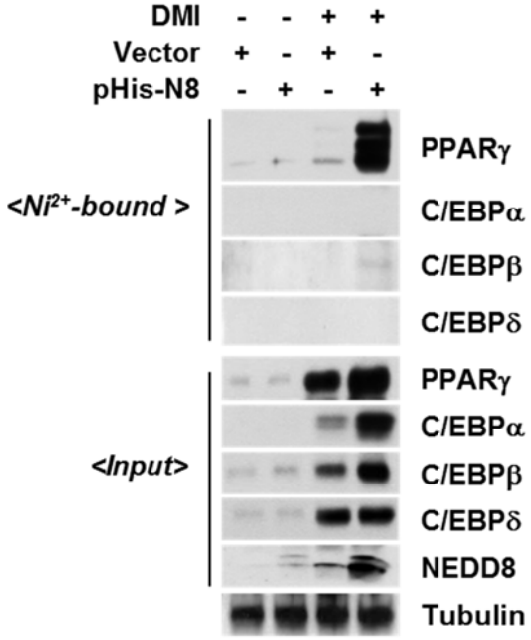

Figure 11. Endogenous PPARγ conjugates with NEDD8 during adipogenesis.

3T3-L1 cells stably expressing pLVX-IRES-vector or pLVX-IRES-His-NEDD8 cell lines were induced to adipogenesis using DMI. After 4 days, cells were lysed. His-NEDD8-conjugated proteins were bound to Ni^{2+}-NTA-agarose beads under denaturing conditions. His-NEDD8-conjugations were analyzed by western blotting analysis using the indicated antibodies. Tubulin was used as a loading control.

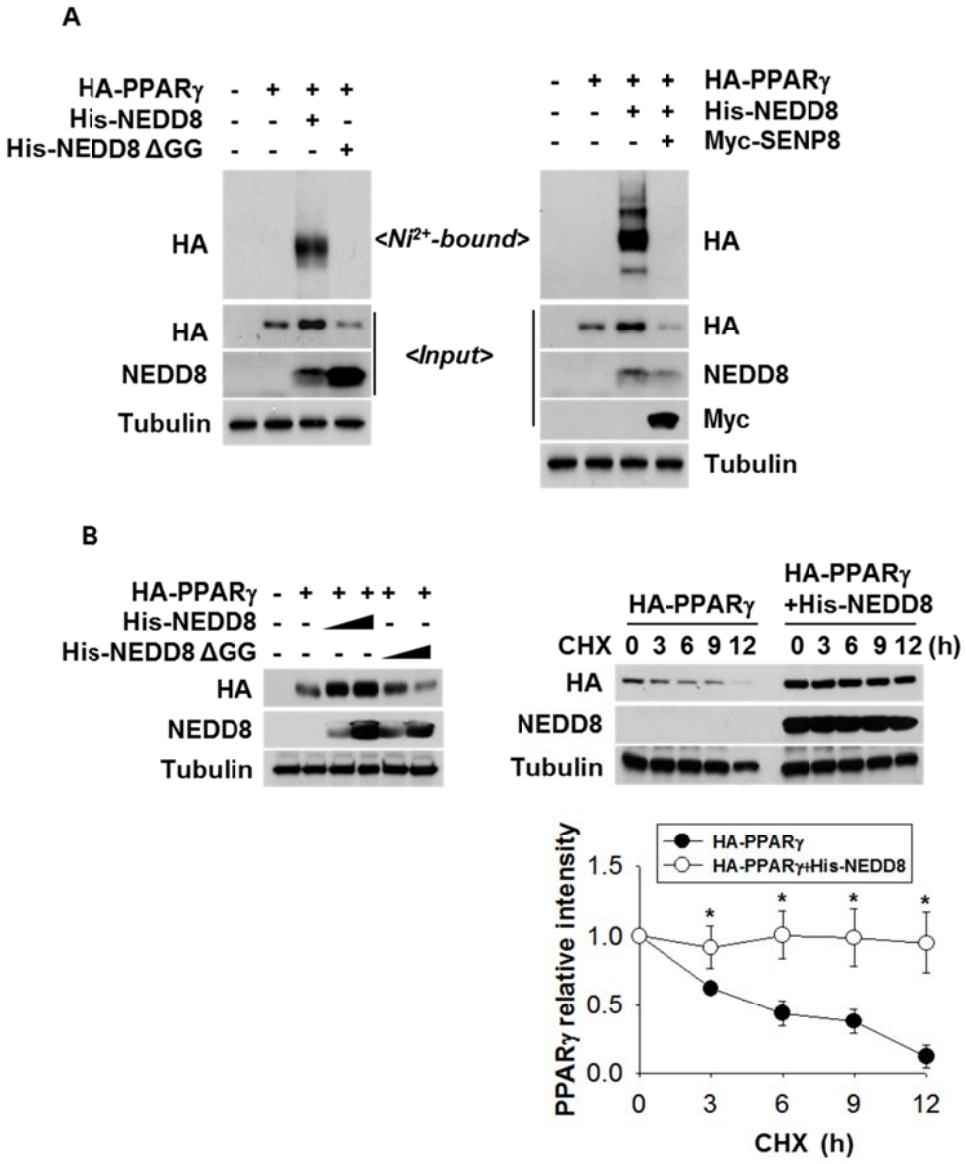
A
HA-PPARγ - + + +
His-NEDD8 - - + -
His-NEDD8 ΔGG - - - +
HA
<Ni2+-bound>
HA
NEDD8
Tubulin
<Input>
- + + + HA-PPARγ
- - + + His-NEDD8
- - - + Myc-SENP8
HA
HA
NEDD8
Myc
Tubulin
B
HA-PPARγ - + + + + +
His-NEDD8 - - - -
His-NEDD8 ΔGG - - - -
HA
NEDD8
Tubulin
HA-PPARγ
HA-PPARγ +His-NEDD8
CHX 0 3 6 9 12 0 3 6 9 12 (h)
HA
NEDD8
Tubulin
HA-PPARγ
HA-PPARγ+His-NEDD8
PPARγ relative intensity
1.5
1.0
0.5
0.0
0 3 6 9 12
CHX (h)

Figure 12. NEDDylation of PPARγ increased its stability.

(A) NEDDylation of PPARγ is blocked by mutant NEDD8 (NEDD8ΔGG) and deNEDDylating enzyme SENP8. HEK293 cells were transfected with HA-PPARγ, or co-transfected HA-PPARγ and His-NEDD8 or His-NEDD8ΔGG. After 48 h, cells were lysed. His-NEDD8-conjugated proteins were bound to Ni^{2+}-NTA-agarose beads under denaturing conditions. The His-NEDD8-conjugated PPARγ was purified and analyzed by western blotting using anti-HA or anti-NEDD8 antibodies. Tubulin was used as a loading control (left). HEK293 cells were transfected with HA-PPARγ, or co-transfected HA-PPARγ and His-NEDD8 or His-NEDD8 and Myc-SENP8. After 48 h, cells were lysed. His-NEDD8-conjugated proteins were bound to Ni^{2+}-NTA-agarose beads under denaturing conditions. The His-NEDD8-conjugated PPARγ was purified and analyzed western blotting using anti-HA anti-NEDD8 or anti-Myc antibodies. Tubulin was used as a loading control (right). (B) HA-PPARγ was co-transfected with His-NEDE8 or His-NEDD8ΔGG into HEK293 cells. After 48 h, cell lysates were analyzed by western blotting by using anti-HA or anti-NEDD8 antibodies. Tubulin was used as a loading control (left). HEK293 cells were transfected with HA-PPARγ only or HA-PPARγ and His-NEDD8 and then incubated 0, 3, 6, 9, 12 h with 50 μM cycloheximide. Proteins were analyzed by western blotting using anti-HA or anti-NEDD8 antibodies. Protein intensities form the western blottings were analyzed using ImageJ 1.36b software (NIH, Bethesda, MD, USA) and plotted. Tubulin was used as a loading control (right). Data shown

represent the mean±SD (n=3) and * denotes $p < 0.05$.

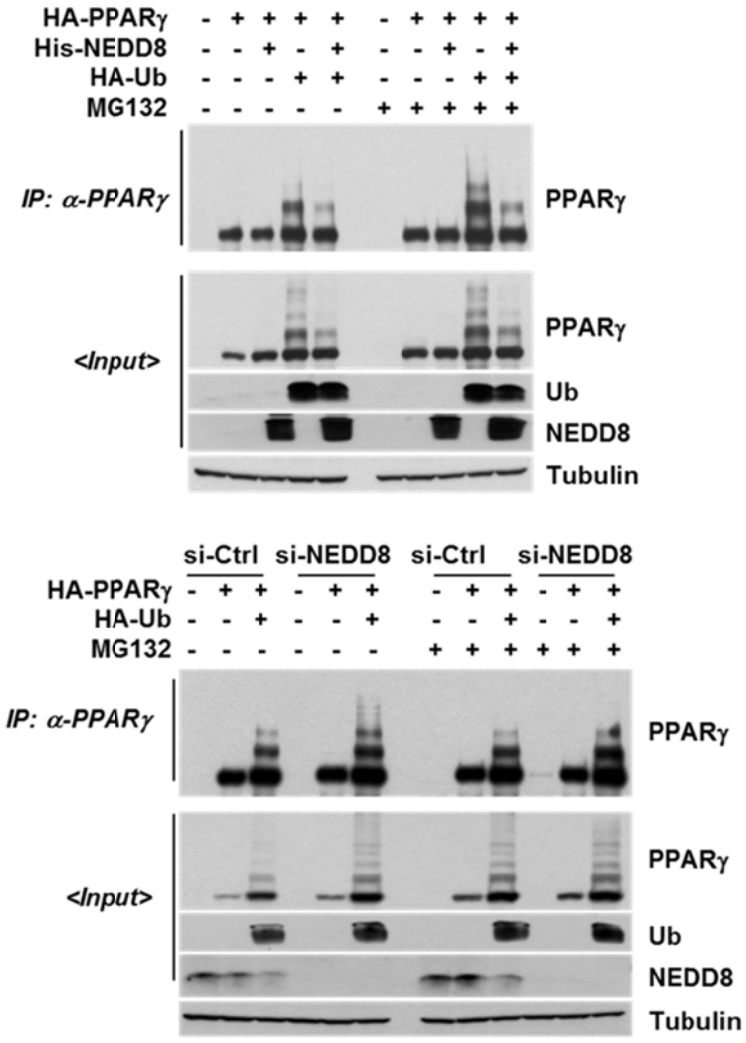
HA-PPARγ - + + + + - + + + +
His-NEDD8 - - + - + - - + - +
HA-Ub - - - + + - - - + +
MG132 - - - - - + + + + +
IP: α-PPARγ
PPARγ
<Input>
PPARγ
Ub
NEDD8
Tubulin
si-Ctrl si-NEDD8 si-Ctrl si-NEDD8
HA-PPARγ - + + - + + - + + - + +
HA-Ub - - + - - + - - + - - +
MG132 - - - - - - + + + + + +
IP: α-PPARγ
PPARγ
<Input>
PPARγ
Ub
NEDD8
Tubulin

Figure 13. NEDDylation of PPARγ attenuates its ubiquitination.

HEK293 cells were co-transfected with HA-PPARγ, His-NEDD8 or HA-Ub as indicated and then stabilized 48 h. After incubation with MG132 (10 μM) for 8 h, cell lysates were immunoprecipitated using anti-PPARγ antibody and analyzed by western blotting analysis using indicated antibodies. Tubulin was used as a loading control (upper). HEK293 cells were co-transfected with 50 nM Control si-RNA or anti-NEDD8 siRNA and indicated plasmids and then stabilized 48 h. After incubation with MG132 (10 μM) for 8 h, cell lysates were immunoprecipitated using anti-PPARγ antibody and analyzed by western blotting analysis using indicated antibodies. Tubulin was used as a loading control (lower).

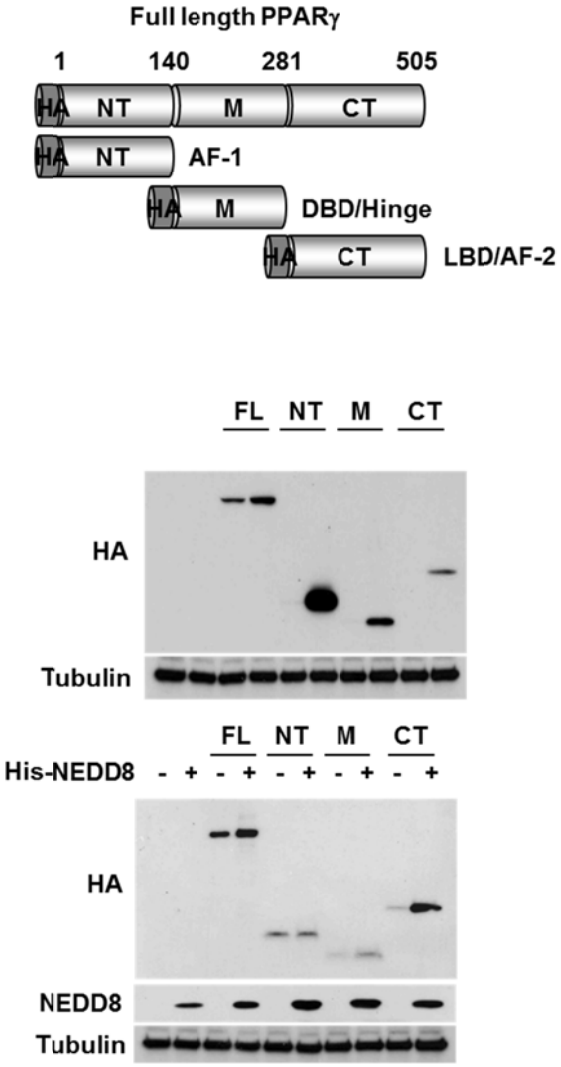
Full length PPARγ
1
140
281
505
HA
NT
M
CT
AF-1
DBD/Hinge
LBD/AF-2
FL
NT
M
CT
HA
Tubulin
His-NEDD8
NEDD8

Figure 14. PPARγ domains stabilize with NEDD8.

HEK293 cells were transfected with HA-PPARγ domains. After incubation with MG132 (10 μM) for 8 h, cell lysates were analyzed by western blotting analysis using anti-HA antibody. Tubulin was used as a loading control (upper). Ectopic PPARγ domains were stabilized by NEDD8. HA-PPARγ or PPARγ domains were co-transfected with His-NEDE8 into HEK293. After 48 h, cell lysates were analyzed by western blotting analysis using anti-HA and anti-NEDD8 antibodies. Tubulin was used as a loading control (lower).

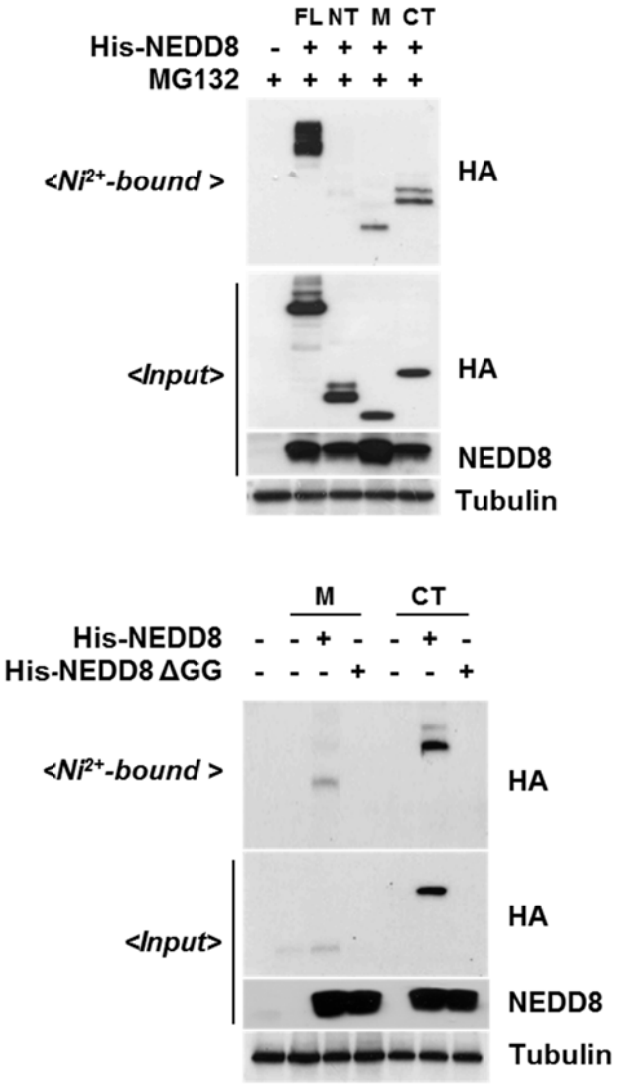
FL NT M CT
His-NEDD8 - + + + +
MG132 + + + + +
<Ni2+-bound >
HA
<Input>
HA
NEDD8
Tubulin
M CT
His-NEDD8 - - + - - + -
His-NEDD8 ΔGG - - - + - - +
<Ni2+-bound >
HA
<Input>
HA
NEDD8
Tubulin

Figure 15. Identification of the NEDDylated domains of PPARγ.

HEK293 cells were co-transfected with HA-PPARγ domains and His-NEDD8. PPARγ FL: full length (aa 1-505), NT: N-terminus (aa 1-140), M: middle (aa 141-281) and CT: C terminus (aa 281-505). After 48 h, 10 μM MG132 was treated with 8 h. HEK293 cells were lysed. His-NEDD8-conjugated proteins were bound to Ni^{2+}-NTA-agarose beads under denaturing conditions. His-NEDD8 conjugated PPAR-γ domains were isolated with Ni^{2+} affinity resin. Proteins were analyzed by western blotting using anti-HA and anti-NEDD8 antibodies. Tubulin was used as a loading control (upper). HA-PPARγ M and CT were co-transfected with His-NEDE8 or His-NEDD8ΔGG plasmids into HEK293 cells. After 48 h cells were lysed. His-NEDD8-conjugated proteins were bound to Ni^{2+}-NTA-agarose beads under denaturing conditions. His-NEDD8 conjugated PPARγ domains were isolated with Ni^{2+} affinity resin and eliminated by His-NEDD8ΔGG. Proteins were analyzed by western blotting using anti-HA and anti-NEDD8 antibodies. Tubulin was used as a loading control (lower).

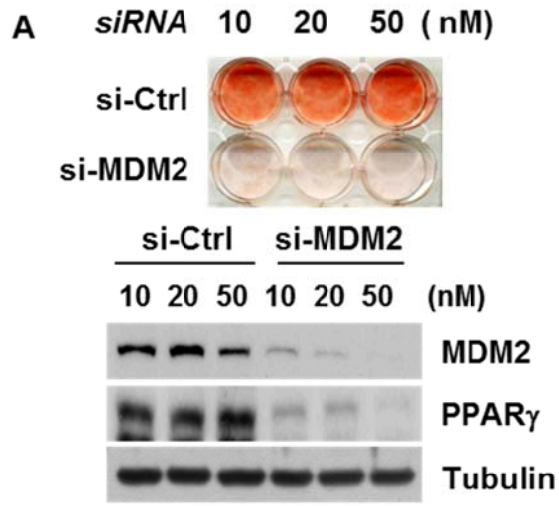
A
siRNA 10 20 50 (nM)
si-Ctrl
si-MDM2
si-Ctrl si-MDM2
10 20 50 10 20 50 (nM)
MDM2
PPARγ
Tubulin
B
Nutlin-3 - 10 20 (μM)
Nutlin-3 - 10 20 (μM)
MDM2
PPARγ
Tubulin

Figure 16. MDM2 is essential for the adipogenesis.

(A) Knockdown of MDM2 by si-Mdm2 blocked the adipogenesis and PPARγ expression. 3T3-L1 cells were transfected with control si-RNA or anti-MDM2 siRNA to 10, 20, 50 nM and then stimulated with DMI. After differentiation, cells were stained with Oil-red-O and cell lysates were analyzed by western blotting at 8 day using anti-MDM2 and anti-PPARγ antibodies. (B) 3T3-L1 cells were treated with nutlin-3 to 10, 20 μM for 48 h and then stimulated with DMI. After differentiation, Cells were stained with Oil-red O (upper) and cell lysates were analyzed by western blotting at 8 day using anti-MDM2 and anti-PPARγ antibodies. Tubulin was used as a loading control (lower).

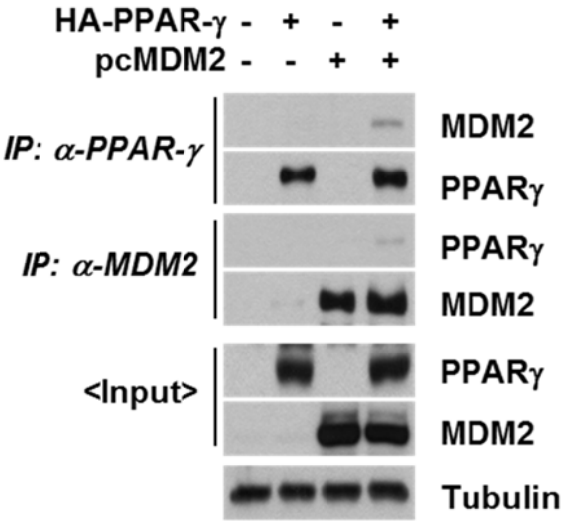

Figure 17. PPARγ physically interacts with MDM2.

HEK293 cells were co transfected with HA-PPARγ and pcMDM2. After stabilized 48 h, cell lysates were immunoprecipitated using anti-PPARγ antibody and analyzed by western blotting using indicated antibodies. Tubulin was used as a loading control.

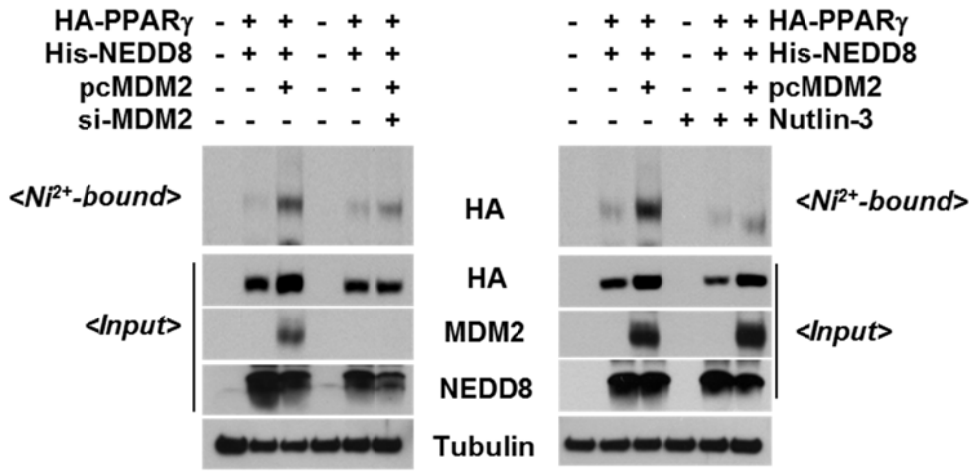

Figure 18. MDM2 is a specific E3 ligase for PPARγ NEDDylation.

Knockdown of MDM2 by si-MDM2 blocked PPARγ NEDDylation. HEK293 cells were co-transfected with indicated plasmids together with si-MDM2. After 48 h, cells were lysed in denaturing conditions. His-NEDD8 conjugated PPARγ was isolated with Ni^{2+} affinity resin. Proteins were analyzed by western blotting using anti-HA, anti-MDM2 and anti-NEDD8 antibodies. Tubulin was used as a loading control (left). Blocking of MDM2 by nutlin-3 diminished PPARγ NEDDylation. HEK293 cells were co-transfected with indicated plasmids. After 48 h, nutlin-3 treated to 20 μM for 8 h and then cells were lysed in denaturing conditions. His-NEDD8 conjugated PPARγ was isolated with Ni^{2+} affinity resin. Proteins were analyzed by western blotting using anti-HA, anti-MDM2 and anti-NEDD8 antibodies (right). Tubulin was used as a loading control.

<3T3-L1>

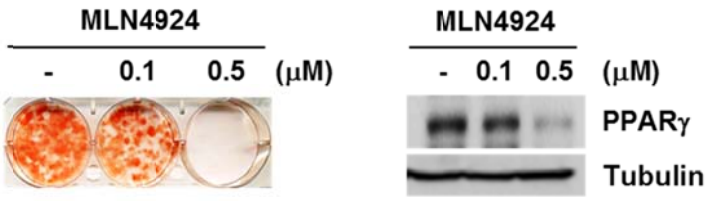

<H-ADSCs>

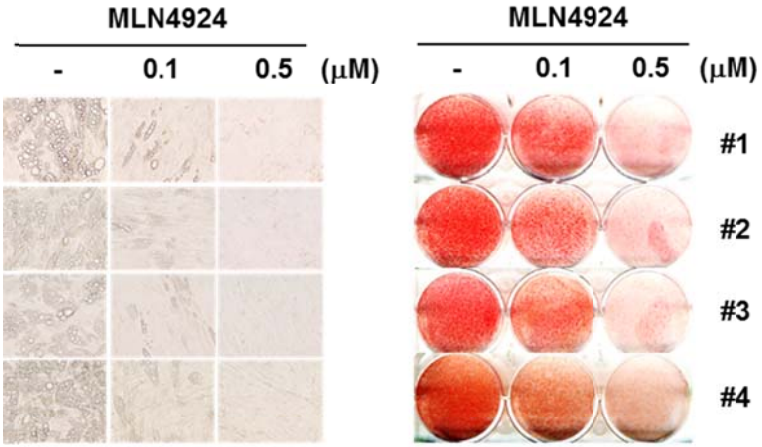

x400

<H-ADSCs#1>

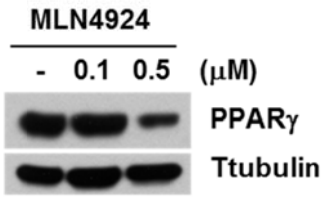

Figure 19. MLN4924, an E1 inhibitor of NEDDylation, inhibits adipogenesis in 3T3-L1 cells and H-ADSCs.

3T3-L1 cells were pre-incubated with MLN4924 (0.1 and 0.5 μM) for 2 days and then stimulated with DMI. After adipogenesis cells were stained with Oil-red-O at day 8 (upper). Cell lysates were analyzed by western blotting using anti-PPARγ antibody (lower). Tubulin was used as a loading control. H-ADSCs from four donors were pre-incubated with MLN4924 (0.1 and 0.5 μM) for 2 days and then stimulated with DMI+indomethacin (200 μM). After adipogenesis cells were stained with Oil-red-O at day 21 (upper). Cell lysates were analyzed by western blotting using anti-PPARγ antibody (lower). Tubulin was used as a loading control.

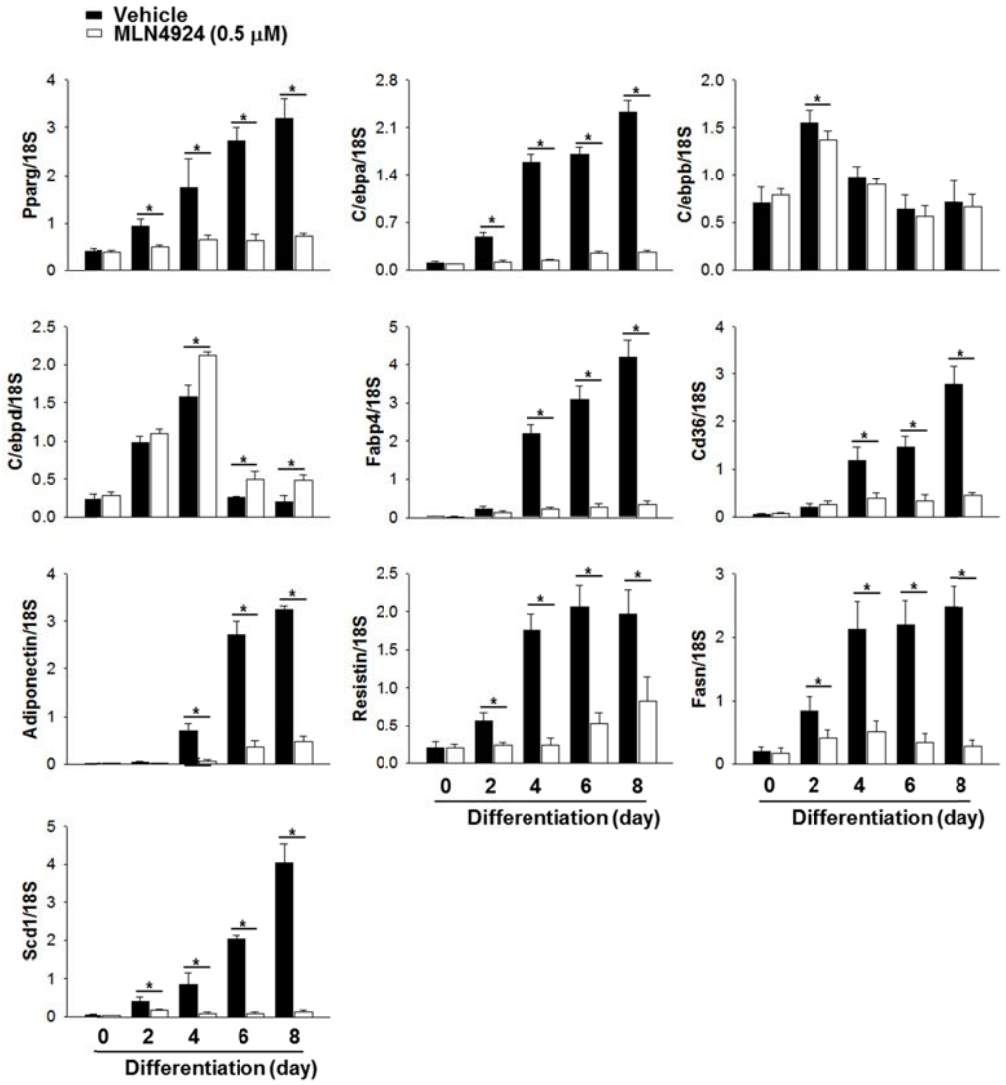
Vehicle
MLN4924 (0.5 μM)
Pparg/18S
C/ebpa/18S
C/ebpb/18S
C/ebpd/18S
Fabp4/18S
Cd36/18S
Adiponectin/18S
Resistin/18S
Fasn/18S
Scd1/18S
0 2 4 6 8
Differentiation (day)

Figure 20. MLN4924 down-regulates the expression level of adipogenic genes during adipogenesis.

3T3-L1 cells were pre incubated with MLN4924 to 0.5 μM at 2 days before differentiation and then stimulated with DMI for the indicated lengths of time. After differentiation total RNAs were prepared from cells and RT-qPCR was applied to measure the expression levels of pparg, c/ebpa, c/ebpb, c/ebpd, fabp4, resistin, adiponectin, fasn, cd36 and scd1. Results were quantified as the relative levels versus 18S RNA level. Data shown represent the mean±SD (n=3) and * denotes $p < 0.05$.

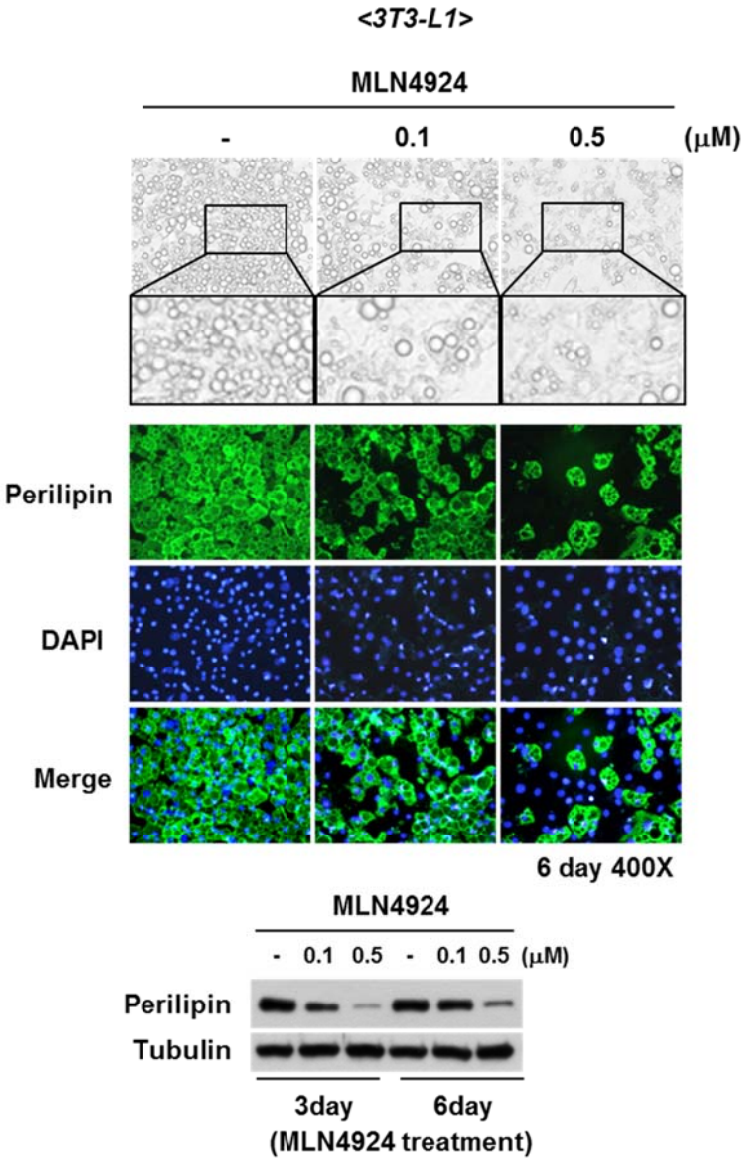
<3T3-L1>
MLN4924
-
0.1
0.5
(μM)
Perilipin
DAPI
Merge
6 day 400X
MLN4924
- 0.1 0.5 - 0.1 0.5 (μM)
Perilipin
Tubulin
3day
6day
(MLN4924 treatment)

Figure 21. MLN4924 reduces lipid accumulation in 3T3-L1.

3T3-L1 cells were differentiated with DMI and then treated with MLN4924 (0.1 and 0.5 μM) at 3 day and 6 day. After 20 day, cells were subjected to immunofluorescence analysis with anti-perilipin antibody and cell lysates were determined by western blotting analysis. Nuclei were stained with DAPI. Tubulin was used as a loading control.

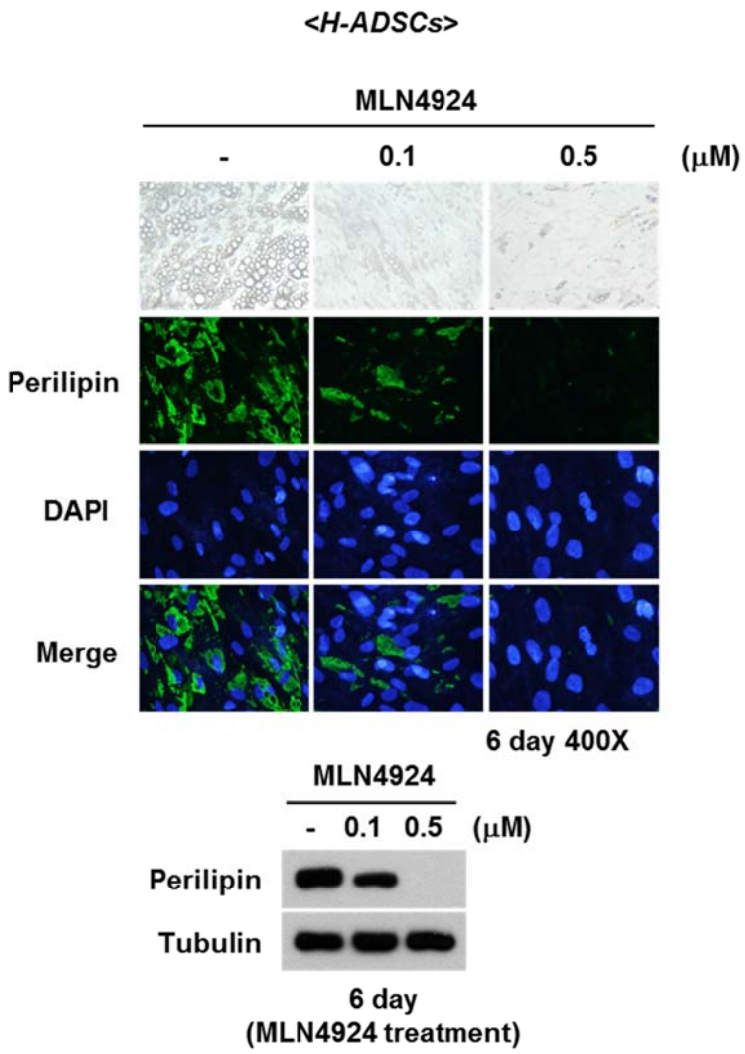
<H-ADSCs>
MLN4924
-
0.1
0.5
(μM)
Perilipin
DAPI
Merge
6 day 400X
MLN4924
- 0.1 0.5 (μM)
Perilipin
Tubulin
6 day
(MLN4924 treatment)

Figure 22. MLN4924 inhibits fat accumulation in H-ADSCs.

H-ADSCs were differentiated with DMI+ indomethacin (200 μM) and then treated with 0.1 and 0.5 μM MLN4924 at 6 day. After 30 day, cells were subjected to immunofluorescence analysis with anti-perilipin antibody and cell lysates were determined by western blotting analysis. Nuclei were stained with DAPI. Tubulin was used as a loading control.

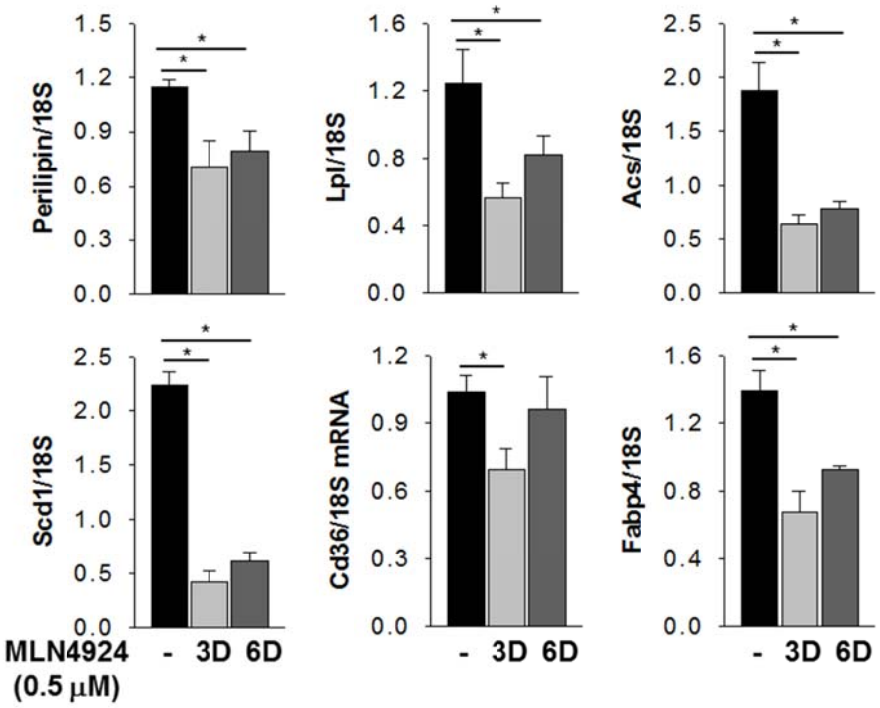
<3T3-L1>
Perilipin/18S
Lpl/18S
Acs/18S
Scd1/18S
Cd36/18S mRNA
Fabp4/18S
MLN4924 (0.5 μM)
- 3D 6D
- 3D 6D
- 3D 6D

Figure 23. Lipid metabolic genes are decreased by MLN4924 in 3T3-L1 cells.

3T3-L1 cells were differentiated with DMI and then treated with 0.5 μM MLN4924 at day 3 and 6. After 20 days, total RNAs were analyzed for genes involved in lipid metabolism. perilipin, lpl, acs, scd1, cd36 and fabp4 mRNA levels were quantified by RT-qPCR. Results were quantified as the relative levels versus 18S RNA level. Data shown represent the mean±SD (n=3) and * denotes $p < 0.05$.

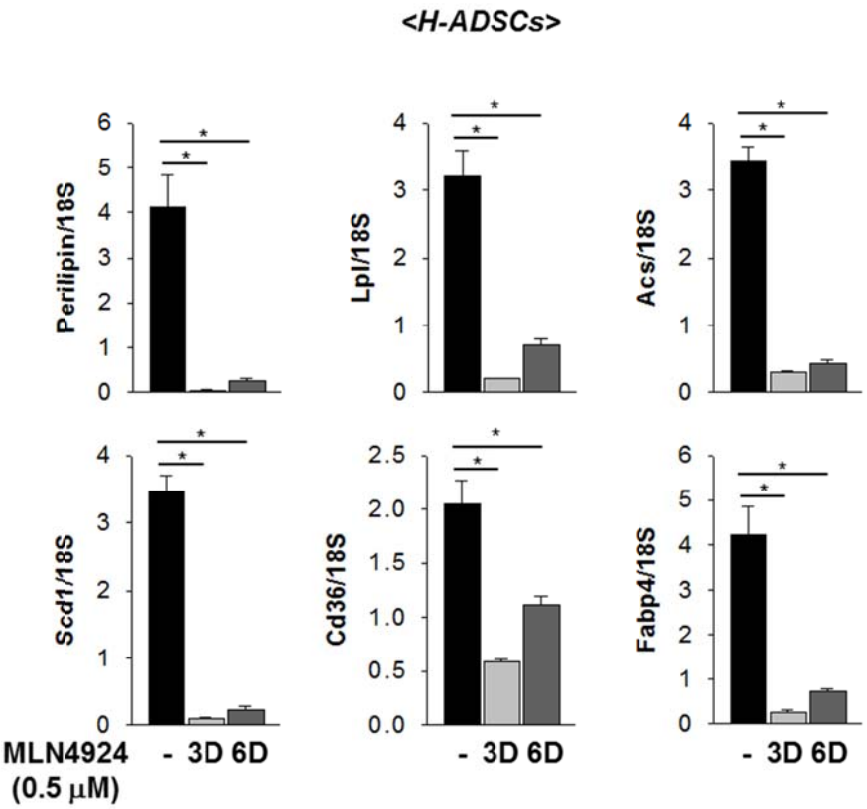
<H-ADSCs>
Perilipin/18S
Lpl/18S
Acs/18S
Scd1/18S
Cd36/18S
Fabp4/18S
MLN4924 - 3D 6D
(0.5 μM)
- 3D 6D
- 3D 6D

Figure 24. Lipid metabolic genes are decreased by MLN4924 in H-ADSCs.

H-ADSCs were differentiated with DMI+ indomethacin (200 μM) and then treated with MLN4924 (0.5 μM) at day 3 and 6. After 20 days, total RNAs were analyzed of lipid metabolic genes. perilipin, lpl, acs, scd1, cd36 and fabp4 mRNA levels were quantified by RT-qPCR. Results were quantified as the relative levels versus 18S RNA level. Data shown represent the mean±SD (n=3) and * denotes $p < 0.05$.

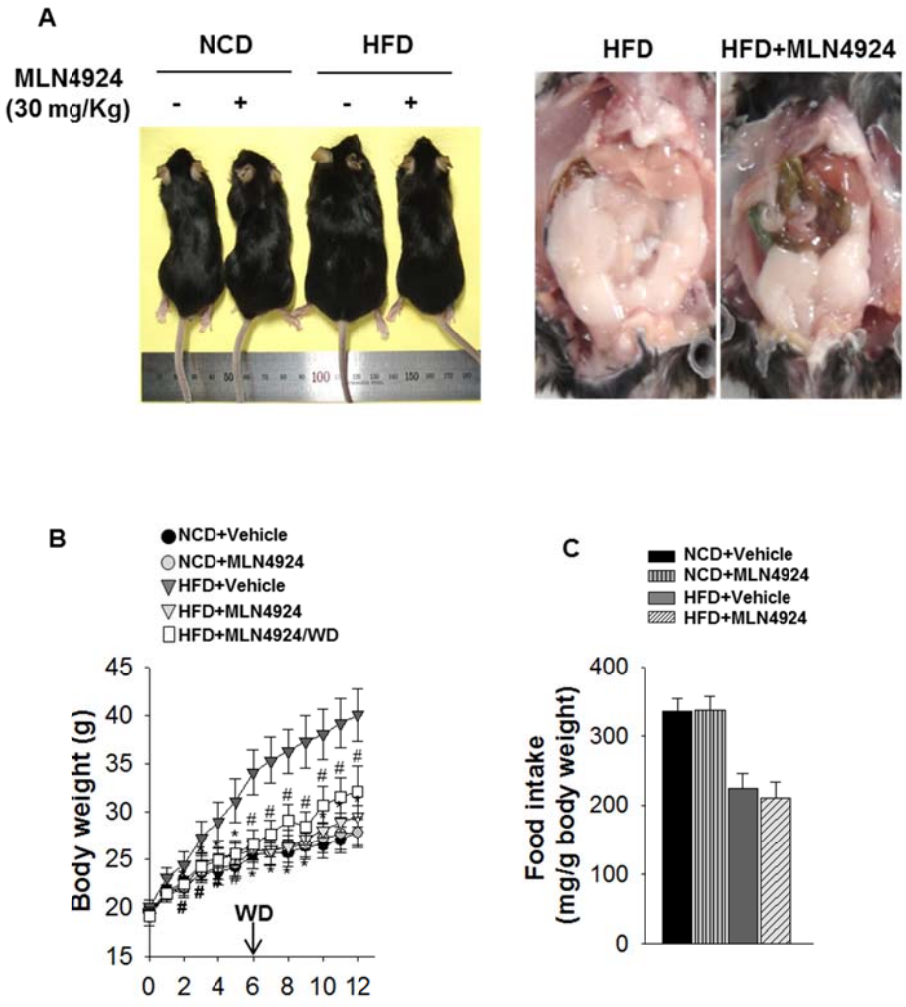
A
NCD
HFD
MLN4924
(30 mg/Kg)
- + - +
HFD
HFD+MLN4924
B
NCD+Vehicle
NCD+MLN4924
HFD+Vehicle
HFD+MLN4924
HFD+MLN4924/WD
Body weight (g)
WD
C
NCD+Vehicle
NCD+MLN4924
HFD+Vehicle
HFD+MLN4924
Food intake
(mg/g body weight)

Figure 25. MLN4924 prevents HFD-induced obesity in mice.

(A) Representative photographs of mice (left). Representative photographs of mice abdomen (right). (B) Weekly increases in the body weights of mice. Mice were divided into five groups: vehicle treatment in NCD-fed and HFD-fed mice, MLN4924 treatment (30 mg/Kg) in NCD-fed and HFD-fed mice and HFD with withdrawal of MLN4924 (30 mg/kg) after 6 wks treatment. (C) Weekly food intakes of mice. All data were presented as the mean±SD (n=8 per group) and * denotes $p < 0.05$ (HFD+vehicle vs HFD+MLN4924) and # denotes $p < 0.05$ (HFD+vehicle vs HFD+MLN4924 withdrawal)

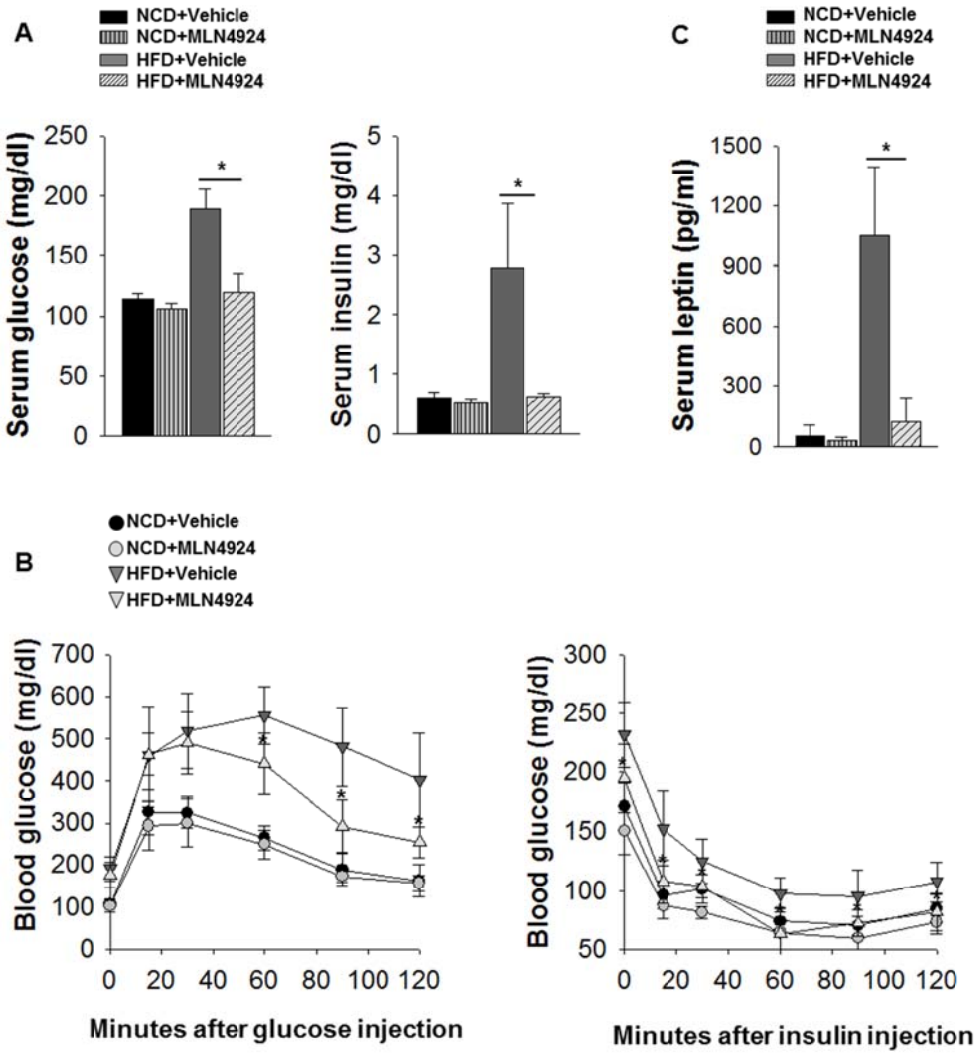
A
NCD+Vehicle
NCD+MLN4924
HFD+Vehicle
HFD+MLN4924
Serum glucose (mg/dl)
250
200
150
100
50
0
*
Serum insulin (mg/dl)
5
4
3
2
1
0
*
C
NCD+Vehicle
NCD+MLN4924
HFD+Vehicle
HFD+MLN4924
Serum leptin (pg/ml)
1500
1200
900
600
300
0
*
B
NCD+Vehicle
NCD+MLN4924
HFD+Vehicle
HFD+MLN4924
Blood glucose (mg/dl)
700
600
500
400
300
200
100
0
0 20 40 60 80 100 120
Minutes after glucose injection
Blood glucose (mg/dl)
300
250
200
150
100
50
0 20 40 60 80 100 120
Minutes after insulin injection

Figure 26. The effects of MLN4924 recover glucose, insulin homeostasis and physiological parameters.

(A) After 12 h fasting, insulin level was measured in serum. After 12 h fasting, glucose level was measured in serum (*n*=8 per group). (B) Glucose tolerance test (GTT) and insulin tolerance test (ITT) in mice (*n*=8 per group). Glucose was injected into intraperitoneal. Insulin tolerance test in mice (*n*=8 per group). Insulin was injected into intraperitoneal. (C) After 12 h fasting, leptin level was measured in serum (n=8 per group). All data were presented as the mean±SD (n=8 per group) and * denotes $p < 0.05$ (HFD+vehicle vs HFD+MLN4924).

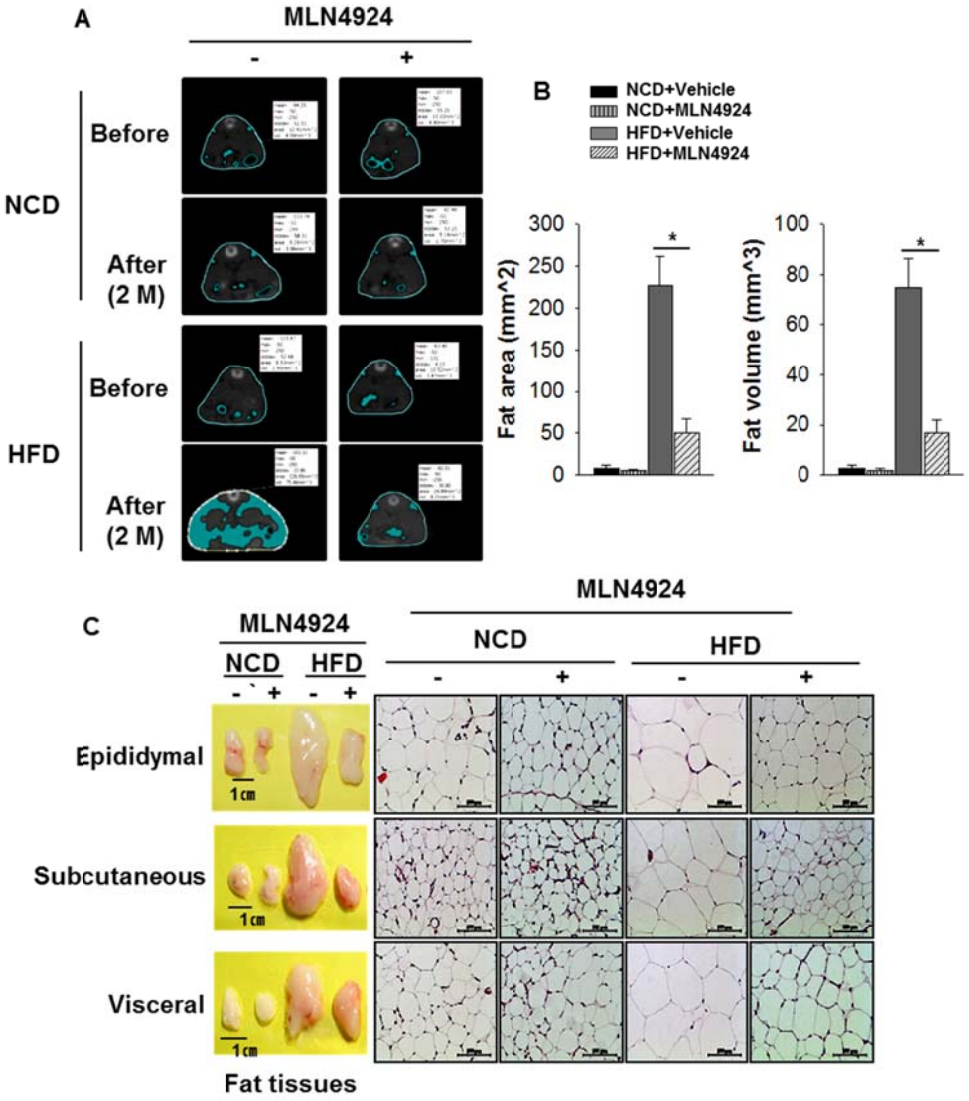
A
MLN4924
-
+
NCD
Before
After (2 M)
HFD
Before
After (2 M)
B
NCD+Vehicle
NCD+MLN4924
HFD+Vehicle
HFD+MLN4924
Fat area (mm^2)
300
250
200
150
100
50
0
*
Fat volume (mm^3)
100
80
60
40
20
0
*
C
MLN4924
NCD
HFD
- + - +
MLN4924
NCD
HFD
- + - +
Epididymal
Subcutaneous
Visceral
1 cm
Fat tissues

Figure 27. MLN4924 reduces fat size in HFD model.

(A) Representative CT image of mice abdomen. (B) Fat area and volume of mice. All data were presented as the mean±SD (n=8 per group) and * denotes $p < 0.05$ (HFD+vehicle vs HFD+MLN4924). (C) Representative photographs of mouse epididymal, subcutaneous, visceral fat (left). Representative H/E staining of mouse epididymal, subcutaneous, visceral fat (right).

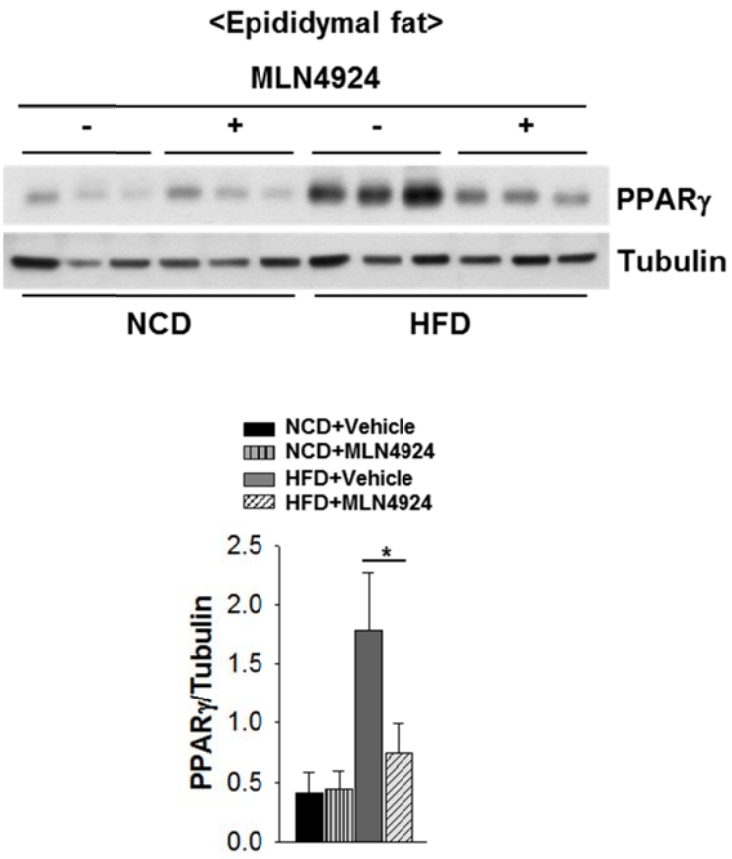

Figure 28. MLN4924 decreases PPARγ protein levels in HFD model.

In epididymal fat, protein expression of PPARγ was measured using 15 μg lysates from NCD-fed, NCD-fed+MLN4924, HFD and HFD-fed+MLN4924 and analyzed by western blotting. Tubulin was used as a loading control. Data shown represent the mean±SD (n=3 per group) and * denotes $p < 0.05$ (HFD+vehicle vs HFD+MLN4924).

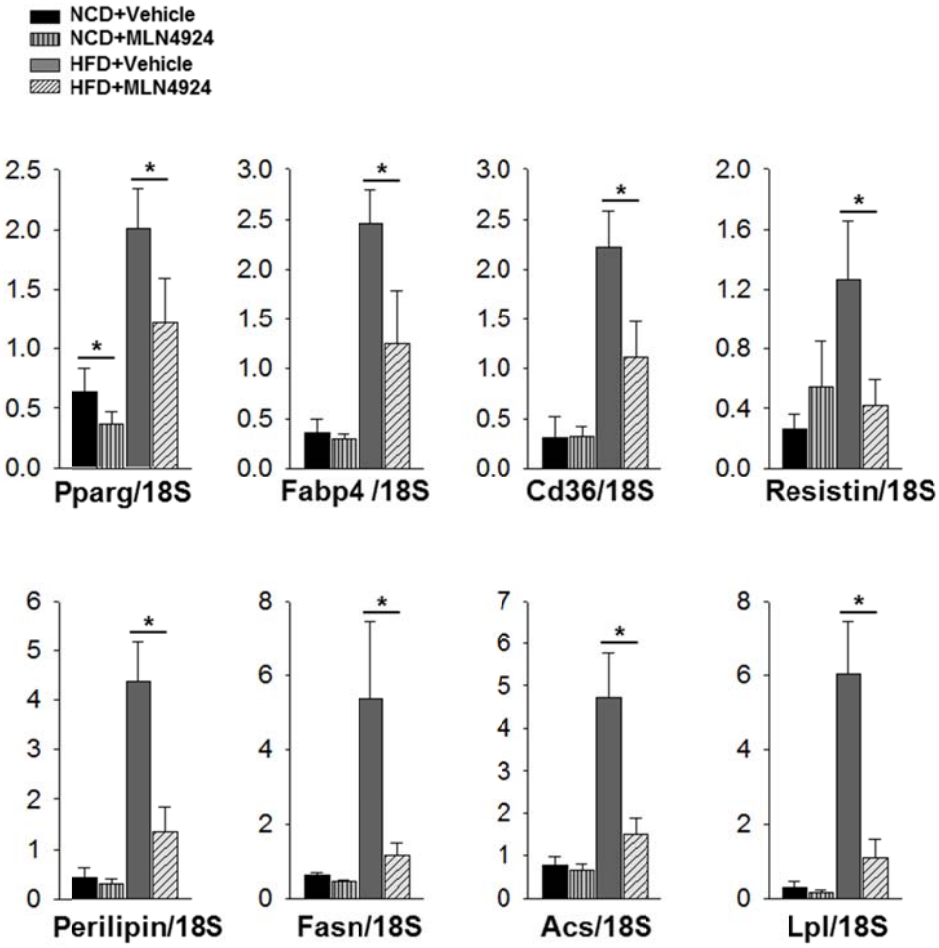

Figure 29. Lipid metabolism in HFD is recovered by MLN4924 treatment.

Total RNAs were prepared from WAT. pparg, fabp4, cd36, resistin, perilipin, fasn, acs and lpl, mRNA levels were quantified by RT-qPCR. Results were quantified as the relative levels versus 18S RNA level. All data were presented as the mean±SD (n=8 per group) and * denotes $p < 0.05$ (HFD+vehicle vs HFD+MLN4924).

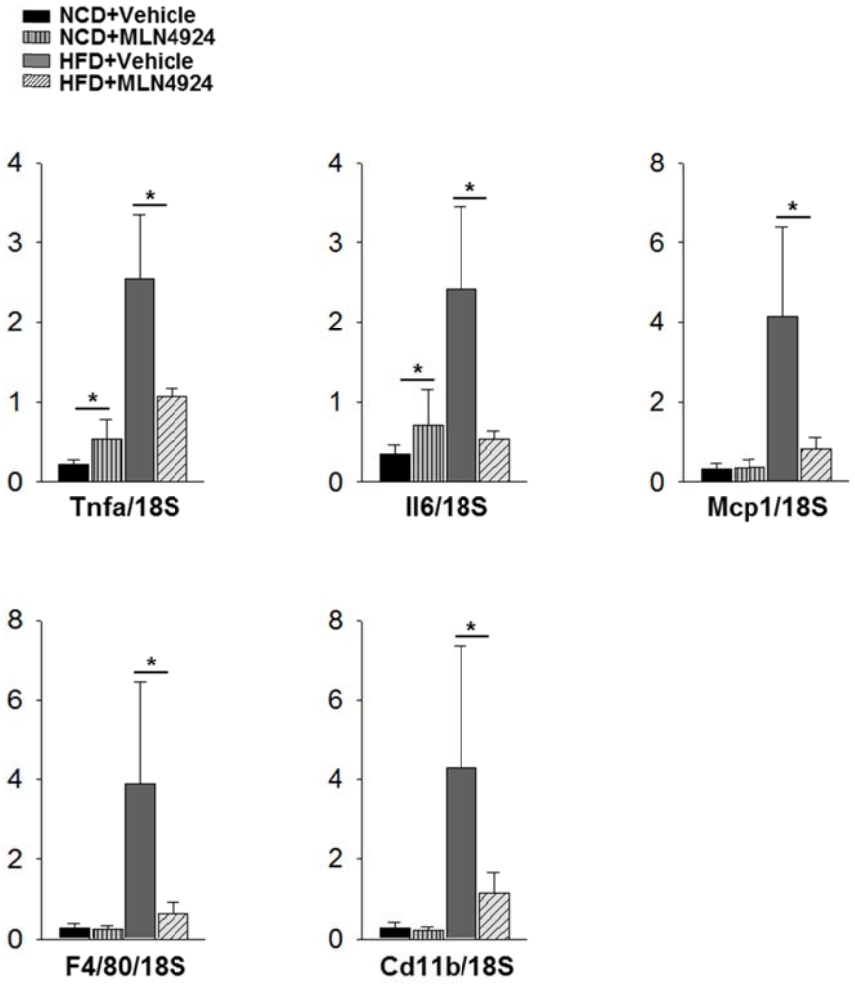

Figure 30. The expression of inflammatory cytokines in HFD is recovered by MLN4924 treatment.

Total RNAs were prepared from WAT. Tnfa, il6, mcp1, f4/80 and cd11b mRNA levels were quantified by RT-qPCR. Results were quantified as the relative levels versus 18S RNA level. All data were presented as the mean±SD (n=8 per group) and * denotes $p < 0.05$ (HFD+vehicle vs HFD+MLN4924).

DISCUSSION

Adipogenesis is controlled by a network of transcription factors that lead to the induction of the expression of the necessary adipogenic gene products for gaining the specialized function and morphology of adipocytes. The major question that motivates this study is: what is the role of NEDD8 in adipogenesis? In this study, I have demonstrated that NEDD8 plays an important role in adipogenesis and fat accumulation. PPARγ acts as a transcription factor in adipogenesis, and lipid sensor in metabolism. Endogenous NEDD8 turns out to be covalently conjugated to PPARγ during adipogenesis in 3T3-L1 cells (Fig 11). Prior studies have addressed that PPARγ is regulated by ubiquitination or SUMOylation, which is the down-regulating PPARγ activity or stability. NEDDylation has a crucial role in PPARγ stability, by interfering in its ubiquitination. Moreover, MDM2 is a specific E3 ligase that promotes PPARγ NEDDylation, and MLN4924, a NEDDylation E1 enzyme inhibitor was found to have a potential therapeutic effect on obesity by functioning as a negative regulator of adipogenesis and fat accumulation in both 3T3-L1 cells and H-ADSCs. Based on these results, I suggest that the NEDDylation of PPARγ plays an important role in adipogenesis and fat accumulation.

The molecular mechanism that governs increasing the number of fat cells (hyperplasia) in obesity is unclear, and the function of NEDD8 during adipogenesis has not yet been elucidated, but that of SUMO and Ub have been uncovered for other adipogenic transcription factors such as C/EBPα, β, δ, and PPARγ. In this

study, we first reported that NEDD8 expression was up regulated during adipocyte differentiation (Fig 1). Similar to PPARγ, NEDD8 expression is also increased in the middle stage of adipogenesis. Further studies of the upstream signaling for NEDD8 regulation in adipogenesis remain to be done.

PPARγ was activated by various fatty acids, eicosanoids, and linoleic acid. In lipid metabolism, PPARγ regulates the expression of targets that participate in fatty acid release, transport, and storage such as lipoprotein lipase (LPL), fatty acid binding proteins (FABP4), and fatty acid transporters or cluster of differentiation 36 (CD36). PPARγ was shown to stimulate adipogenesis alone in mouse fibroblasts (Tontonoz et al., 1994). Previous studies have shown that C/EBPβ is capable of inducing PPARγ in Ppar-γ+/- MEFs, which leads to the activation of adipogenesis, involving C/EBPα expression, which follows exposure to a PPARγ ligand. Constantly, C/EBPβ was unable to induce C/EBPα expression or adipogenesis in Pparγ-/- MEFs. (Zuo et al., 2006). C/EBPβ and C/EBPδ stimulate PPARγ expression, and PPARγ activates C/EBPα expression. Helix-loop-helix (HLH) transcription factor SREBP-1c, another up regulatory factor of PPARγ, has been found to play an important role in stimulating adipogenesis using insulin-induced 3T3-L1 cells (Kim et al., 1998). In NEDD8-overexpressed 3T3-L1 cells, dexamethasone, a synthetic member of the glucocorticoids, accelerates adipocyte differentiation (Fig 3). NEDD8 probably participates in the regulation of hormone signaling, yet this remains to be clarified. Currently, the NEDD8 regulatory mechanism remains unknown in adipogenesis. The knockdown of NEDD8 in 3T3-L1 cells down

regulates PPARγ expression, and blocks several PPARγ downstream genes and adipogenic target genes in 3T3-L1 cells (Fig 6). Furthermore, mice that are implanted with NEDD8-stably-knockeddown 3T3-L1 and 3T3-F442A cells failed to form a fat pad (Fig 9, 10). Our ChIP data clearly shows that NEDD8 is a key modulator of PPARγ promoter binding capability. The NEDDylation of PPARγ dynamically changed the assembly of transcriptional regulatory chromatin structure, and enhanced expression of PPARγ by NEDD8 correlated with increased binding of PPARγ to downstream target promoters (Fig 8).

PPARγ proteins have a short half-life (t½=2 h), and were degraded by a poly-ubiquitination proteasome system (Kilroy et al., 2009). Paradoxically, PPARγ protein levels were sustained during adipogenesis, while the molecular mechanism by which PPARγ stability was maintained is still unclear. From previous studies, in adipocytes, ubiquitination or SUMOylation do not increase PPARγ protein levels. In addition, PPARγ targets the proteasome via ubiquitin-independent or dependent manners. The ligand-binding domain (LBD) occurred in the ubiquitin-dependent degradation of PPARγ (Gail et al., 2009). Interestingly, our data suggests that PPARγ NEDDylation dominantly occurred in LBD (Fig 15) and blocked ubiquitination (Fig 13). In this study, that the claim is made that PPARγ NEDDylation inhibits ubiquitination and stabilizes the protein. Another important finding of this study is that MDM2 mediates the NEDDylation of PPARγ (Figure 18). A RING finger-type E3 ligase MDM2 has been reported for which p53, the tumor suppressor protein, was NEDDylated by MDM2, leading to an increase in its

transactivation activity (Xirodamas et al., 2004). MDM2 has reported self-NEDDylation, which regulates its stability (Watson et al., 2010). TAp73 is also NEDDylated though MDM2, and suppresses its transactivity and reduces its cytoplasmic localization (Watson et al., 2006). In addition, the MDM2 gene was up regulated in 3T3-L1 cells (Berberich et al., 1999).

The current therapies for obesity are based on exercise, diet, surgery, and pharmacological drugs. The available anti-obesity drugs can be divided into two modes of action: Central actors (central nervous system: CNS) and peripheral actors (muscle, fat, kidneys, and gastrointestinal tract) (Schwartz et al., 2000). To reduce the appetite and induce a sensation of satiation, anti-obesity drugs may act on serotoninergic, noradrenergic, dopaminergic, cannabinoid, and hormone receptor mechanisms in the brain (Dietrich and Horvath, 2012). Anti-obesity drugs should also increase energy expenditure and fat oxidation via activating the catecholaminergic system in the CNS and peripheral tissues. Lipase inhibition in the gastrointestinal tract reduces fat absorption (Hainer and Hainerová, 2012). In the past, available pharmacological therapies have been thyroid hormones, dinitrophenol, and amphetamines. Thyroid hormones activate the basal metabolic rate (BMR) and induce energy expenditure, which may lead to side effects such as sleep problems and heart failure. Dinitrophenol, a well-known anti-obesity agent, is reported to cause rapid weight loss by increasing the energy expenditure. The biological process of dinitrophenol results in heat instead of APT, by uncoupling the oxidative phosphorylation in mitochondria. Overheating, sweating, and fatal

hyperthermia are attributable side effects (Harper 2001). Amphetamines decrease food intake and increase locomotors activity by releasing noradrenaline (NA) from the presynaptic vesicles in the lateral hypothalamus. Increasing NA leads to the stimulation of β2-adreneric receptors and inhibition of appetite (Valentino et al., 2010). Since the 1930s, amphetamines have been discarded as a treatment, due to the occurrence of cardiovascular diseases and their addictive properties. The next generation of obesity drugs includes Sibutramine, a noradrenalin and serotonin reuptake inhibitor utilized by the hepatic cytochome P450 system that affects both food intake and energy expenditure. Rimonabant, a cannabinoid 1(CB1) receptor antagonist that acts by blocking the CB1 receptor in the nervous system and inhibiting food intake (Colombo 1998). Orlistat, a gastric and pancreatic lipase inhibitor that blocks enzyme activity. Unfortunately, these drugs come with side effects. Sibutramine has cardiovascular side effects, and was withdrawn in 2010. Rimonabant lost tis approval in 2008, when an association with anxiety and depression was discovered. Orlistat may cause hypoglycemia, headaches, and respiratory infections. Recently, Qsymia and locaserin have been approved by the FDA, but they also have side effects. Lorcaserin, a serotonin 2C agonist, acts in the CNS and reduces food intake. It may cause headaches, dizziness, insomnia, and carcinogenesis. Qsymia, a noradrenalin releaser and phentermine/topiramate combination has side effects including increased dizziness, headaches, insomnia, and heart rate. The market for obesity drugs is potentially huge, but the drugs' safety levels do not allow the realization of the market. From the limitations of drug

responses, anti-obesity drug research requires a more effective approach and developing the new therapy target. Fundamentally, obesity drugs should be developed to reduce the fat size or fat cell numbers, and controlling these factors is crucial for obesity drugs. New therapeutic insights have been made into the molecular regulation of adipogenesis and the reduction of fat storage. PPARγ adipose knockout mice had reduced fat formation and were protected from HFD-induced obesity and insulin resistance in mice (Jones et al., 2005). Thiazolidinediones (TZDs) activated PPARγ, and led to altered adipocytes, skeletal muscle, and liver metabolism, by regulating insulin sensitivity (Way et al., 2001). However, few reports have described the PPARγ antagonist. Bisphenol A diglycidyl ether (BADGE) was reported as a PPARγ antagonist that negatively regulated PPARγ activity and adipogenesis in 3T3-L1 and 3T3-FF2A cells (Wright et al, 2000). Dimethyl a-(dimethoxyphophinyl)-p-chlorobenzyl phosphate (SR-202) blocks PPARγ transcriptional activity and improves insulin sensitivity in ob/ob mice (Rieusset et al., 2002). In the present study, MLN4924, a PPARγ NEDDylation inhibitor, is therapeutically beneficial for obesity and insulin sensitivity, MLN4924 has an effect on highly proliferating cancers in *in vivo* xenograft models (Soucy et al., 2009). Another study has verified that MLN4924 also affected acute myeloid leukemia (AML) by inducing apoptosis (Swords et al., 2010). MLN4924 also reduced the outgrowth of liver cancer cells both *in vivo* and *in vitro* via induced autophagy (Luo Z et al., 2012). Preclinical models of solid tumors and acute lymphoblastic leukemia xenografts were tested from the pediatric preclinical testing

program (Smith et al., 2012). Furthermore, searching for inhibitors of the ubiquitin-proteasome system (UPS) and ubiquitin-like proteins (UBLs) may control dynamic genes and be the key to novel disease therapies.

Visceral fat surrounds the internal organs and is associated with peripheral and hepatic insulin resistance (Cases and Barzilai, 2000). From the *in vivo* experiments, MLN4924 reduced subcutaneous, visceral, and epididymal fats in DIO mice (Figure 13). The abnormal accumulation of fatty acyl-CoA and triglycerides in muscles and the liver lead to insulin resistance by inhibiting insulin receptor signaling (liver: IRS-1 and muscle: IRS-2) (Kim et al., 2001; Yu et al., 2002). My findings support that MLN4924 can inhibit adipocyte differentiation and fat accumulation by decreasing the genes involved in adipogenesis and lipid metabolism *in vitro*. In the treatment of MLN4924 in DIO mice, abnormal fat accumulation is reduced and lipid metabolism is normalized by decreasing the expression of lipid metabolic genes. PPARγ can modulate both adipocyte function and endothelial cells by regulating inflammation and atherosclerosis (Marx et al., 1999). MLN4924 treatment in DIO mice can also recover glucose tolerance, insulin sensitivity, body weight, leptin level, and the expression of inflammatory cytokine genes.

In conclusion, taken together with these data, I suggest that NEDD8 is a novel posttranslational modification that can regulate the stability of PPARγ in adipogenic differentiation. MLN4924 recovered lipid metabolism via normalizing the glucose tolerance, insulin sensitivity, lipid metabolic target genes, and

inflammatory cytokine target genes in DIO mice. Based on these results, MLN4924 can be suggested as a therapeutic target for obesity.

REFERENCES

Berberich SJ, Litteral V, Mayo LD, Tabesh D, Morris D. Mdm-2 gene amplification in 3T3-L1 preadipocytes. Differentiation. 1999;64:205-212.

Bourlier V, Zakaroff-Girard A, Miranville A, De Barros S, Maumus M, Sengenes C, Galitzky J, Lafontan M, Karpe F, Frayn KN, Bouloumié A. Remodeling phenotype of human subcutaneous adipose tissue macrophages. Circulation. 2008;117:806-815.

Cao Z, Umek RM, McKnight SL. Regulated expression of thee C/EBP isoforms during adipose conversion of 3T3-L1 cells. Genes Dev. 1991;5:1538-1552.

Cases JA, Barzilai N. The regulation of body fat distribution and the modulation of insulin action. Int T Obes Relat Metrab Disord. 2000;24:S63-S66.

Chandra V, Huang P, Hamuro Y, Raghuram S, Wang Y, Burris TP, Rastinejad F. Structure of the intact PPAR-gamma-RXR- nuclear receptor complex on DNA. Nature. 2008;456:350–356.

Choi JH, Banks AS, Estall JL, Kajimura S, Boström P, Laznik D, Ruas JL, Chalmers MJ, Kamenecka TM., Blüher M. Griffin PR, Spiegelman BM. Anti-diabetic drugs inhibit obesity-linked phosphorylation of PPARγ by Cdk5. Nature. 2010;466: 451-456.

Colombo G, Agabio R, Diaz G, Lobina C, Reali R, Gessa GL. Appetite suppression and weight loss after the cannabinoid antagonist SR 141716. Life Sci. 1998;63:PL113-PL117.

Dietrich MO, Horvath TL. Limitations in anti-obesity drug development: the critical role of hunger-promoting neurons. Nat Rev Drug Discov. 2012 ;11:675-691

Dixon, A.K. Abdominal fat assessed by computed tomography: sex difference in distribution. Clin. Radiol. 1983;34:189-191.

Drolet R, Richard C, Sniderman AD, Mailloux J, Fortier M, Huot C, Rhéaume C, Tchernof A. Hypertrophy and hyperplasia of abdominal adipose tissues in women. Int J Obes (Lond). 2008;32:283–291.

Fabbrini E, Sullivan S, Klein S. Obesity and nonalcoholic fatty liver disease: biochemical, metabolic, and clinical implications. Hepatology. 2010;51:679-689

Gail E. Kilroy, Xiaoying Zhan, Elizabeth Floyd. PPAR-g AF-2 domain functions as a cmponent of a Ubuiquitin-dependent degradation signal. Obesity. 2009;17:665-673.

Gao F, Cheng J, Shi T, Yeh ET. NEDDylation of a breast cancer-associated protein recruits a class III histone deacetylase that represses NFkappaB-dependent transcription. Nat Cell Biol. 2006;8:1171-1177.

Grimaldi B, Bellet MM., Katada S, Astarita G, Hirayama J, Amin RH, Grannema JG, Piomelli D, Leff T, Sassone-Corsi P. PER2 controls lipid metabolism by direct regulation of PPARg. Cell Metab. 2010;12:509-520.

Hainer V, Hainerová IA. Do we need anti-obesity drugs? Diabetes Metab Res Rev. 2012;28:Suppl 2:8-20.

Hallenborg P, Feddersen S, Francoz S, Murano I, Sundekilde U, Petersen RK, Akimov V, Olson MV, Lozano G, Cinti S, Gjertsen BT, Madsen L, Marine JC, Blagoev B, Kristiansen K. Mdm2 controls CREB-dependent transactivation and initiation of adipocyte differentiation. Cell death and diffrentiation. 2012;19:1381–1389.

Harper JA, Dickinson K, Brand MD. Mitochondrial uncoupling as a target for drug development for the treatment of obesity. Obes Rev. 2001; 2:255-265.

Henegar C, Tordjman J, Achard V, Lacasa D, Cremer I, Guerre-Millo M, Poitou C, Basdevant A, Stich V, Viguerie N, Langin D, Bedossa P, Zucker JD, Clement K. Adipose tissue transcriptomic signature highlights the pathological relevance of extracellular matrix in human obesity. Genome Biol. 2008;9:R14.

Hirsch J, Batchelor B. Adipose tissue cellularity in human obesity. Clin Endocrinol Metab. 1976;5:299-311.

Hofbauer KG, Nicholson JR. Pharmacotherapy of obesity. Exp Clin Endocrinol Diabetes 2006;114:475–484

Jaffray, E.G., and Hay, R.T. Detection of modification by ubiquitin-like proteins. Methods. 2006;38:35-38.

Jones JR, Barrick C, Kim KA, Lindner J, Blondeau B, Fujimoto Y, Shiota M, Kesterson RA, Kahn BB, Magnuson MA. Deletion of PPARgamma in adipose

tissues of mice protects against high fat diet-induced obesity and insulin resistance. Proc Natl Acad Sci U S A. 2005;102:6207-6212.

Kahn SE, Hull RL, Utzschneider KM. Mechanisms linking obesity to insulin resistance and type 2 diabetes. Nature. 2006;444:840-846.

Kilroy GE, Zhang X, Floyd ZE. PPAR-gamma AF-2 domain functions as a component of a ubiquitin-dependent degradation signal. Obesity. 2009;17:665-673.

Kim JB, Sarraf P, Wright M, Yao KM, Mueller E, Solanes G, Lowell BB, Spiegelman BM. Nutritional and insulin regulation of fatty acid synthetase and leptin gene expression though ADD1/SREBP1. J. Clin.Invest. 1998;101:1–9.

Kim JK, Fillmore JJ, Chen Y, Yu C, Moore IK, Pypaert M, Lutz EP, Kako Y, Velez-Carrasco W, Goldberg IJ, Breslow JL, Shulman GI. Tissue-specific overexpression of lipoprotein lipase causes tissue-specific insulin resistance. Proc. Natl. Acad. Sci. USA. 2001;98:7522-7527.

Lee HW, Nam SK, Choi WJ, Kim HO, Jeong LS. Stereoselective synthesis of MLN4924, an inhibitor of NEDD8-activating enzyme. J Org Chem. 2011;76:3557-3361.

LeRoith D, Novosyadlyy R, Gallagher EJ, Lann D, Vijayakumar A, Yakar S. Obesity and type 2 diabetes are associated with an increased risk of developing cancer and a worse prognosis; epidemiological and mechanistic evidence. Exp Clin Endocrinol Diabetes. 2008;116:S4-6.

Lowell BB. PPARgamma: an essential regulator of adipogenesis and modulator of fat cell function. Cell. 1999;99:239-242.

Luo Z, Yu G, Lee HW, Li L, Wang L, Yang D, Pan Y, Ding C, Qian J, Wu L, Chu Y, Yi J, Wang X, Sun Y, Jeong LS, Liu J, Jia L. The NEDD8-activationg enzyme inhibitor MLN4924 induces autophagy and apoptosis to suppress liver cancer cell growth. Cancer res. 2012;72:3360-3371.

Mandrup S, Loftus TM, MacDougald OA, Kuhajda FP, Lane MD. Obese gene expression at in vivo levels by fat pads derived from s.c. implanted 3T3-F442A preadipocytes. Proc Natl Acad Sci U S A. 1997;94:4300-4305.

Marx N, Brourcier T, Sukhova GK, Libby P, Plutzky J. PPARgamma activation in human endothelial cells increases plasminogen activator inhibitor type 1 expression: PPAR gamma as a potential mediator in vascular disease. Arterioscler Thomb Vasc Biol. 1999;19:546-551.

Nadler ST, Stoeh JP, Schueler KL, Tanimoto G, Yandell BS, Attie AD. The expression of adipogenic genes is decreased in obesity and diabetes mellitus. Proc Natl Acad Sci U S A. 2000;97:11371-11376.

Ohshima T, Koga H, Shimotohno K. Transcriptional activity of peroxisome proliferator-activated receptor gamma is modulated by SUMO-1 modification. J Biol Chem. 2004;279:29551-29557.

Ouchi N, Parker JL, Lugus JJ, Walsh K. Adipokines in inflammation and metabolic disease. Nat Rev Immunol. 2011;11:85-97

Rabut G, Peter M. Function and regulation of protein neddylation. 'Protein modifications: beyond the usual suspects' review series. EMBO Rep. 2008;9:969-976.

Rieusset J, Touri F, Michalik L, Escher P, Desvergne B, Niesor E, Wahli W. A new selective peroxisome proliferator-activated receptor-g antagonist with antiobesity and antidiabetic acitivity. Mol Endocrinol. 2002;11:2628-2644 .

Rosen ED, MacDougald OA. Adipocyte differentiation from the inside out. Nat. Rev. Mol. Cell Biol. 2006;7:885-896.

Rosen ED, Spiegelman BM. Molecular regulation of adipogenesis. Annu Rev Cell Dev Biol. 2000;16:145-171.

Russell RC, Ohh M. NEDD8 acts as a 'molecular switch' defining the functional selectivity of VHL. EMBO Rep. 2008;9:486-491.

Ryu JH, Li SH, Park HS, Park JW, Lee B, Chun YS. Hypoxia-inducible factor α subunit stabilization by NEDD8 conjugation is reactive oxygen species-dependent. J Biol Chem. 2011;28:6963-6970.

Salans LB, Horton ES, Sims EA. Experimental obesity in man: cellular character of the adipose tissue. J Clin Invest. 1971;50:1005-1011.

Schwartz MW, Woods SC, Porte D Jr, Seeley RJ, Baskin DG. Central nervous system control of food intake. Nature. 2000;404:661-671.

Smith MA, Maris JM, Gorlick R, Kolb EA, Lock R, Carol H, Keir ST, Reynolds CP, Kang MH, Morton CL, Wu J, Smith PG, Yu J, Houghton PJ. Initial testing of the investigational NEDD8-activating enzyme inhibitor MLN4924MLN4924 by the pediatric preclinical testing program. Pediatr Blood Cancer. 2012;59:246-253.

Soucy TA, Smith PG, Milhollen MA, Berger AJ, Gavin JM, Adhikari S, Brownell JE, Burke KE, Cardin DP, Critchley S, Cullis CA, Doucette A, Garnsey JJ, Gaulin JL, Gershman RE, Lublinsky AR, McDonald A, Mizutani H, Narayanan U, Olhava EJ, Peluso S, Rezaei M, Sintchak MD, Talreja T, Thomas MP, Traore T, Vyskocil S, Weatherhead GS, Yu J, Zhang J, Dick LR, Claiborne CF, Rolfe M, Bolen JB, Langston SP. An inhibitor of NEDD8-activating enzyme as a new approach to treat cancer. Nature. 2009;458:732-736.

Spalding KL, Arner E, Westermark PO, Bernard S, Buchholz BA, Bergmann O, Blomqvist L, Hoffstedt J, Näslund E, Britton T, Concha H, Hassan M, Rydén M, Frisén J, Arner P. Dynamics of fat cell turnover in humans. Nature. 2008;453:783-787.

Steger DJ, Grant GR., Schupp M., Tomaru T, Lefterova MI, Schug J, Manduchi E, Stoeckert CJ, Lazar MA. Propagation of adipogenic signals though an epigenomic transition state. Genes Dev. 2010;24:1035-1044.

Stickle NH, Chung J, Klco JM, Hill RP, Kaelin WG Jr, Ohh M. pVHL modification by NEDD8 is required for fibronectin matrix assembly and suppression of tumor development. Mol Cell Biol. 2004 ;24:3251-3261.

Swords RT, Kelly KR, Smith PG, Garnsey JJ, Mahalingam D, Medina E, Oberheu K, Padmanabhan S, O'Dwyer M, Nawrocki ST, Giles FJ, Carew JS. Inhibition of NEDD8-activating enzyme: a novel approach for the treatment of acute myeloid leukemia. Blood. 2010;115:3796-3800.

Tontonoz P, Hu E, Spiegelman BM. Stimulation of adipogenesis in fibroblasts by PPARγ, a lipid-activated transcription factor. Cell. 1994;79:1147–1156.

Valentino MA, Lin JE, Waldman SA. Central and peripheral molecular targets for antiobesity pharmacotherapy. Clin Pharmacol Ther. 2010;87:652-662.

Van Gaal LF, Mertens IL, De Block CE.Mechanisms linking obesity with cardiovascular disease. Nature. 2006;7121:875-880.

Watson IR, Blanch A, Lin DC, Ohh M, Irwin MS. Mdm2-mediated NEDDylation of RAp73 regulates its transacivation function. J Biol Chem. 2006;281:34096-34103.

Watson IR, Li BK, Roche O, Blanch A, Ohh M, Irwin MS. Chemotherapy induces NEDP1-mediated destabilization of MDM2. Oncogene. 2010;29:297-304.

Way JM, Harrington WW, Brown KK, Gottschalk WK, Sundseth SS, Mansfield TA, Ramachandran RK, Willson TM, Kliewer SA. Comprehensive messenger

ribonucleic acid profiling reveals that peroxisome proliferator-activated receptor-g activation has coordinate effects on gene expression in multiple insulin sensitive tissue. Endocinology. 2001;6:763-774.

Wright HM, Clish CB, Mikami T, Hauser S, Yanagi K, Hiramatsu R, Serhan CN, Spiegelman BM. A synthetic antagonist for the peroxisome proliferator-activated receptor-g inhibits adipocyte differentiation. J Biol Chem. 2000;3:1873-1877.

Xirodimas DP, Saville MK, Bourdon JC, Hay RT, Lane DP. Mdm2-mediated NEDD8 conjugation of p53 inhibits its transcriptional activity. Cell. 2004;118:83-97.

Yamauchi T, Kamon J, Waki H, Murakami K, Motojima K, Komeda K, Ide T, Kubota N, Terauchi Y, Tobe K, Miki H, Tsuchida A, Akanuma Y, Nagai R, Kimura S, Kadowaki T. The mechanisms by which both heterozygous peroxisome proliferator-activated receptor gamma (PPARgamma) deficiency and PPARgamma agonist improve insulin resistance. J Biol Chem. 2001;276:41245-41254.

Yu C, Chen Y, Cline GW, Zhang D, Zong H, Wang Y, Bergeron R, Kim JK, Cushman SW, Cooney GJ, Atcheson B, White MF, Kraegen EW, Shulman GI. Mechanism by which fatty acids inhibit insulin acitivation of insulin receptor substrate-1 (IRS-1)- associated phosphatidylinositol 3-Kinase activity in muscle. J Biol. Chem. 2002;277:50230-50236.

Zuo Y, Qiang L, Farmer SR. Activation of C/EBPalpha expression by C/EBPbeta during adipogenesis requires a PPARgamma-associated repression of HDAC1 at the C/EBPalpha gene promoter. J. Biol. Chem. 2006;281:7960–7967.

국 문 초 록

비만은 과잉 섭취된 음식과 에너지 소비의 불균형에 의해 생기는 대사성 질환으로써 지방세포 수와 크기를 증가시켜 에너지 대사에 이상을 유발시킬 뿐만 아니라 다른 대사성 질환에 원인이 된다. 비만연구에 있어 지방세포의 분화 연구와 기능 연구는 필수적이다. 특히 분자 수준에서 가장 중요한 인자라고 알려진 PPARγ는 핵 수용체일 뿐만 아니라 전사인자로써 retinoid X receptor (RXR)와 heterodimer를 이루며 타깃 유전자의 promoter의 peroxisome proliferator hormone response elements (PPREs) 위치에 결합하여 타깃 유전자 발현을 유도한다고 알려져 있다. PPARγ의 주된 기능은 지방세포 분화를 유도하고 당과 지질 대사에 관여하며, 염증유발 인자를 조절한다고 알려져 있다. 본 연구에서는 PPARγ 안정화를 증가시키는 새로운 post-translation modification인 NEDDylation을 소개하고, 이는 PPARγ의 분해를 매개하는 ubiquitination을 억제 함으로써 PPARγ 안정화 시킨다. 또한 PPARγ의 NEDDylation을 매개하는 E3 ligase가 MDM2임을 밝히고 이 또한 지방세포 분화에 중요한 역할을 하고 있음을 연구하였다. 나아가 NEDDylation의 E1 효소의 inhibitor라고 알려진 MLN4924가 지방분화 억제 효과가 있을 뿐만 아니라, 지방축적을 감소시키며, 비만 쥐에서 몸무게와 지방 대사가 정상적으로 회복됨으로써 비만 치료제로의 효과가

있음을 확인하였다. 이러한 결과는 새로운 PPARγ의 NEDDylation을 통해 지방세포 기능이 조절 될 수 있으며, 지방세포 분화 자체를 조절함으로써 새로운 비만 치료 메커니즘을 제시하고자 한다.

주요어: 지방세포 분화, PPARγ, NEDDylation, MDM2, MLN4924, 비만

학번: 2010-30610